NASA Technical Paper 1905

Description and Calibration of the Langley Unitary Plan Wind Tunnel

Charlie M. Jackson, Jr., William A. Corlett,
and William J. Monta
Langley Research Center
Hampton, Virginia

National Aeronautics
and Space Administration

**Scientific and Technical
Information Branch**

1981

CONTENTS

SUMMARY

The two test sections of the Langley Unitary Plan Wind Tunnel have been calibrated over the operating Mach number range from 1.47 to 4.63, and the results are presented along with a description of the facility and its operational capability. The calibrations include Mach number and flow-angularity distributions in both test sections at selected Mach numbers and tunnel stagnation pressures, as well as measurements of turbulence, test-section boundary-layer characteristics, moisture effects, blockage, and stagnation-temperature distributions.

The test-section calibrations indicated that the Mach number variation throughout the test region associated with smaller models is ±0.01; whereas at the higher Mach numbers and for longer models at angle of attack, the variation can reach ±0.04. Both test sections have a positive or upflow angle generally within 0.5° except at the higher Mach numbers of test section 1 where the upflow angle can reach 1.5°.

The facility is described in detail including dimensions and capacities where appropriate, and examples of special test capabilities are presented. The operating parameters are fully defined and the power-consumption characteristics are discussed.

INTRODUCTION

Immediately following World War II the need was recognized for wind-tunnel equipment to develop advanced airplanes and missiles. The military and the National Advisory Committee for Aeronautics (NACA) developed a plan for a series of facilities which was approved by the U.S. Congress in the Unitary Wind Tunnel Plan Act of 1949. This plan included five wind-tunnel facilities, three at NACA laboratories and two along with an engine test facility at the Arnold Engineering Development Center (AEDC). These facilities were built to provide experimental aerodynamic support to the industry, the military services, and other government agencies.

The facility of interest in the present report is the Unitary Plan Wind Tunnel which is located at the Langley Research Center. It is a closed-circuit pressure tunnel with two 4- by 4- by 7-ft (1.22- by 1.22- by 2.13-m) test sections which cover a Mach number range from 1.47 to 4.63 and a nominal Reynolds number range from 0.5×10^6 per ft (1.64×10^6 per m) to 8.0×10^6 per ft (26.23×10^6 per m). Construction of this facility was completed in 1955 and it has been in continuous operation since that time except for periodic maintenance. In the operational history of the Langley Unitary Plan Wind Tunnel are developmental tests of virtually every supersonic military airplane, missile, and spacecraft to have become operational in the United States inventory. Most of the many aircraft configurations proposed in the National Supersonic Transport (SST) Program as well as many of their progenitors were extensively tested in this facility. Considerable experimental investigations in support of the Space Shuttle Program were conducted; and continuing throughout the operational life of the facility has been the basic experimental fluid-mechanics research which has given rise to the development of methods for predicting supersonic aerodynamic performance.

Brief descriptions of the Langley Unitary Plan Wind Tunnel are presented in the facility compilations of references 1, 2, and 3. The present paper offers a description of the wind tunnel with revised specifications.

The purpose of this report is to present a description of the Langley Unitary Plan Wind Tunnel (UPWT) and its auxiliary equipment and operational capability. Also included is a description of the calibration procedures and a summary of the flow-calibration data obtained over the life of the facility.

SYMBOLS

The units for the physical quantities in this paper are given both in U.S. Customary Units and in the International System of Units (SI). Measurements and calculations were made in U.S. Customary Units. Factors relating the two systems are given in reference 4. The authors did not adhere to the NASA policy of expressing dimensional quantities with the International System of Units (SI) as the primary system. This requirement has been waived, and U.S. Customary Units are given first with equivalent SI units in parentheses.

b	tunnel nozzle block position
M	test-section stream Mach number
$\bar{M}$	weighted average test-section Mach number (taken between $0 \leqq x \leqq 48$ in. (1.22 m) and -10 in. (-0.254 m) $\leqq z \leqq 10$ in. (0.254 m))
N	profile exponent for a turbulent boundary layer
p_p	probe pitot pressure, psf (Pa)
p_{st}	probe static pressure, psf (Pa)
p_t	tunnel total pressure, psf (Pa)
q	test-section dynamic pressure, psf (Pa)
R	unit Reynolds number per ft (per m)
$R_{x,tr}$	transition Reynolds number based on boundary-layer laminar run
$T_{dp,atm}$	dew-point temperatures corrected to standard atmospheric pressure, ^{o}F (^{o}C)
T_t	tunnel stagnation temperature, ^{o}F (^{o}C)
$T_{t,CL}$	tunnel center-line stagnation temperature, ^{o}F (^{o}C)
t	time from initiation of heat pulse, sec
$\sqrt{\overline{u'^2}}$	root-mean-square turbulent fluctuation velocity in the x-direction, ft/sec (m/sec)
u/u_∞	ratio of local boundary-layer velocity to free-stream velocity
V	mean velocity along X-axis, ft/sec (m/sec)
X,Y,Z	tunnel coordinate system (fig. 12)

x,y,z dimensions in tunnel coordinate system, in. (m)

x_1,z_1 nozzle contour coordinates for test section 1, in. (m)

x_2,z_2 nozzle contour coordinates for test section 2, in. (m)

α angle of attack (fig. 15), deg

β angle of sideslip (fig. 15), deg

δ boundary-layer thickness, in. (cm)

δ^* boundary-layer displacement thickness, in. (cm)

θ boundary-layer momentum thickness, in. (cm)

θ_H flow angle measured in the horizontal plane (positive for flow toward the left facing upstream), deg

θ_V flow angle measured in the vertical plane (positive up), deg

WIND TUNNEL AND EQUIPMENT

Wind Tunnel

Arrangement.- The Langley Unitary Plan Wind Tunnel is a closed-circuit pressure tunnel with two 4- by 4- by 7-ft (1.22- by 1.22- by 2.13-m) test sections. An exterior view of the facility is shown in figure 1, a schematic drawing of the arrangement of the major elements is shown in figure 2, and a detailed planform of the tunnel circuit arrangement is shown in figure 3. The major elements of the facility are the 100 000-hp (74.6-MW) drive system, a dry air supply and evacuating system, a cooling system, and the interconnecting ducting to produce the proper airflow through either of the two test sections. The tunnel overall volume is 163 922 ft^3 (4642 m^3), and the tunnel duct circuit can be circumscribed by a rectangle 263 ft (80.2 m) by 210 ft (64.0 m). The tunnel circuit is designed to operate at pressures from near-vacuum to 10 atm (1 atm = 101.3 kPa). The axial locations and dimensions of the components of the high and low Mach number circuits and compressor circuits (as defined in fig. 3) of the wind tunnel are presented in tables I and II, respectively. The duct juncture and turning vanes just downstream of configuration valve I are shown in figure 4 to illustrate typical internal duct configurations. Figure 5 shows a typical tunnel-duct-configuration valve (number IV, downstream of cooler 1) in the open position. These valves are used to configure the tunnel ducts for different compressor staging modes.

Settling chambers.- The settling chambers provide a large volume which results in low-velocity flow and smooth transition from the circular tunnel duct work to the rectangular nozzles and test section. The settling chamber for the low Mach number test section is a cylindrical duct 15 ft (4.57 m) in diameter and 25 ft (7.62 m) long followed by a 7-ft-long (2.13-m) transition section from circular to 4- by 11.51-ft (1.22- by 3.51-m) rectangular. The settling chamber for the high Mach number test section is a cylindrical duct 12 ft (3.66 m) in diameter and 24.5 ft (7.47 m) long followed by a 3.5-ft-long (1.07-m) transition section from circular to 4- by 8.75-ft (1.22- by 2.67-m) rectangular. A photograph of the settling chamber and transition section of the low Mach number test section is shown in figure 6.

Nozzles, test sections, and second minimums.- The low and high Mach number nozzles are of the asymmetric sliding-block type such that the nozzle throat-to-test-section area ratio can be varied to provide continuous variation of Mach number. A schematic drawing of the low Mach number nozzle is shown in figure 7 which illustrates the asymmetric nozzle contours and sliding block and drive mechanism. The low and high Mach number test sections (referred to as test sections 1 and 2, respectively) are formed by the downstream contours of the nozzle and are nominally 4 by 4 ft (1.22 by 1.22 m) in cross section by 7 ft (2.13 m) in length. The variable-area second-minimum sections of the facility are formed downstream of test sections 1 and 2. The second-minimum area is controlled by moving the hinged sidewalls to provide the proper constriction to stabilize the normal shock downstream of the test section at the various operating Mach numbers. These components are described in detail in a subsequent section of this report.

Diffuser.- The overall diffuser sections for test sections 1 and 2 are circular in cross section and extend downstream 85.5 ft (26.06 m). Transition sections from the rectangular second minimums form the entrance into the diffusers. The overall diffuser cross sections vary from 5.665 ft (1.73 m) in diameter at the entrance to 12 ft (3.66 m) in diameter at the exit. The initial included conical angle of the diffusers for both tunnel circuits is 2.93° and remains constant for 45.8 ft (13.96 m) when it changes to 4.77° for the low Mach number circuit and to 6.4° for the high Mach number circuit.

Drive section and compressors.- The configuration of the starting and main-drive motors and compressors is shown in figure 2. The schematic drawing of the tunnel shows the location of the drive section and compressors within the facility, and the arrangement of the starting motor, main-drive motor, and six compressors is illustrate in the insert of figure 2. The main-drive motor is located in line with three compressors on each end forming a continuous driveline 120 ft (36.58 m) long. The starting motor is located offset from this driveline and transmits power to the driveline through a speed-increase gear. Figure 8 is a photograph showing the main-drive motor and six compressors.

The main-drive motor is of the synchronous type and is rated for continuous operation at 63 333 hp (47.2 MW) at a rotational speed of 3600 rpm with a 76 000-hp (56.7-MW) overload rating for 1/2 hour. The starting motor is a wound-rotor, liquid rheostat-controlled machine and is used to bring the driveline up to synchronous speed. At a synchronous speed of 720 rpm, this machine delivers continuous power to the driveline at a rating of 20 000 hp (14.9 MW) with a 24 000-hp (17.9-MW) overload rating for 1/2 hour. A combined overload rating of the drive motors gives a maximum power rating for the facility of 100 000 hp (74.6 MW). The starting motor is mechanically connected to the compressor driveline through a speed-increase gear of 685:3600 ratio such that the compressor speed is constant at 3600 rpm for all tunnel operating conditions.

The compression ratio and airflow required to establish stable flow conditions i either of the test sections is supplied by six centrifugal compressors. These compressors are designated by the letters C, D, E, F, G, and I and are located as shown in figure 2. Compressors C, D, E, F, and I are single-stage machines manufactured by the Roots-Connerville Blower Company with each having a design compression ratio of 1.95. Compressors C, D, and E have a design inlet volume flow of 298 000 ft^3/min (8438.41 m^3/min), and compressors F and I have a design inlet volume flow of 149 000 ft^3/min (4219.2 m^3/min). Compressor G is a three-stage machine manufactured by the Clark Compressor Company and has a design inlet volume flow of 60 000 ft^3/min (1699 m^3/min) and a design compression ratio of 2.25. These machines are used in fiv

different combinations or modes as shown in the following table to provide the required compression ratio and airflow to operate either test section over the indicated Mach number range.

Test section	Mode	Mach number range (a)	Stage of compression of compressor -					
			I	C	D	E	F	G
1	1-IA	1.469 to 2.160	1	1	1			
1	1-II	2.354 to 2.869	1	1	1	2		
2	2-II	2.287 to 2.973	1	1	1	2		
2	2-III	2.973 to 3.750	1	1	1	2	3	
2	2-IV	3.835 to 4.640		1	1	2	3	4

[a]Mach number corresponds to $R = 3 \times 10^6$ per ft (9.84×10^6 per m).

The tunnel duct configurations for operation, staging, and bypass for each of these modes as well as start-up and mode-changing procedures will be described in a subsequent section.

A detailed presentation and analysis of the measured compressor operating characteristics is presented in reference 5. Reference 5 also includes a study of the overall operating performance, power characteristics, and efficiency of the tunnel drive system at each of the operating modes.

Heat exchangers.- The facility is equipped with six crossflow heat exchangers located within the tunnel duct circuits as shown in figure 3. A photograph of heat exchangers downstream of compressors I, C, D, and E (coolers 6, 1, and 2) is shown in figure 9. The energy expended by the main-drive system is removed by the water flowing through these coolers and transmitted to the atmosphere through a cooling tower located outside the facility. The heat exchangers (coolers 1 to 6) within the tunnel circuit have the overall design operating characteristics presented in the following table:

Condition	Cooler					
	1	2	3	4	5	6
Design inlet-air temperature, ^{o}F (^{o}C)	285 (141)	273 (134)	273 (134)	242 (117)	400 (204)	286 (141)
Design outlet-air temperature, ^{o}F (^{o}C)	130 (54)	120 (49)	120 (49)	120 (49)	220 (104)	120 (49)
Design inlet-water temperature, ^{o}F (^{o}C)	85 (29)	85 (29)	85 (29)	85 (29)	85 (29)	85 (29)
Airflow, lb/sec (kg/sec) . . .	1895 (860)	945 (429)	630 (286)	470 (213)	1630 (739)	380 (172)
Coolant pump capacity, gal/min (m^3/min)	17 000 (64.35)	8320 (31.49)	5500 (20.82)	3400 (12.87)	12 200 (46.18)	3400 (12.87)

Cooler 5 acts as a precooler to compressors C, D, and I and, consequently, has higher design inlet and design outlet temperatures. These coolers are generally capable of maintaining the tunnel stagnation temperature at 100°F (37.7°C). However, as a result of the unique cooler design, the airflow can be rapidly bypassed around the cooling elements resulting in an airstream stagnation temperature of up to 400°F (204°C) for heat-transfer tests.

The cooling tower is located outside of the facility as shown in the schematic drawing of figure 2. The tower is composed of eight cells with each having a 17-ft-diameter (5.18-m) fan. The capacity of the tower is 20 000 gal/min (75.71 m^3/min) with design inlet-water temperature of 115°F (46.1°C) and design discharge-water temperature of 85°F (29.44°C). A photograph of the cooling tower is shown in figure 10.

Operating modes.- In order to cover the entire Mach number range for each test section, not only must the nozzle blocks be moved to provide the proper expansion ratio but the tunnel duct configurations must also be altered to provide the proper compression ratio. As previously mentioned, the six compressors are used in five tunnel configurations or modes to provide the required overall compression ratio. Figure 11 shows the tunnel duct configurations and airflow path for each of the five modes. It should be noted that the compressors not in use in these modes are not uncoupled from the driveline and, therefore, operate in a bypass condition. In order to reduce the power consumption for this condition, the pressure in the bypass ducts is reduced as much as possible.

Since the tunnel operating modes are available for only one test section at a time, maximum utilization of the facility is obtained by isolating the unused test section for installation and model changes. To reduce model transient loads during tunnel start-up or shutdown, the pressure in the tunnel circuit is reduced below 2 psia (13.79 kPa) until supersonic flow is established in the test section. Once supersonic flow is established, the tunnel pressure required for the tests is controlled by inbleeding or outbleeding dry air. A description of the makeup air equipment including capacities is provided in a subsequent section of this report.

Test Sections

General description.- The two test sections of the Unitary Plan Wind Tunnel provide test capability over a Mach number range from 1.46 to 4.63. The low Mach number test section (test section 1) covers the Mach number range from 1.46 to 2.86 and the high Mach number test section (test section 2) is capable of providing supersonic flow from a Mach number of 2.30 to 4.63. The test sections are formed by the downstream portion of the nozzles, nominally 4 by 4 ft (1.22 by 1.22 m) in cross section by 7 ft (2.13 m) in length. Figure 12 shows the details of the transition sections, nozzles, and test sections for both tunnel circuits. The superstructure is shown for both test sections as well as the drive mechanism for the movable lower nozzle blocks. A typical research model is shown in test section 1 in figure 13.

Nozzles and second minimums.- The nozzle contours for both tunnel circuits are asymmetric, and the lower walls of both nozzles move longitudinally to provide the necessary variation in area ratio of throat to test section. Figure 12 shows the lower walls of the nozzles in the minimum Mach number position (contraction ratio of 12.96 for test section 1 and of 15.41 for test section 2) with the maximum Mach number position indicated by the dashed line (contraction ratio of 43.07 for test section 1 and of 143.59 for test section 2). The movable nozzle blocks are powered by

150-hp (111.9-kW) motors which produce a drive rate of 2 ft/min (0.6 m/min). The nozzle sidewalls are parallel and 4 ft (1.22 m) apart. The coordinates of the contoured upper and lower nozzle walls are presented in table III for test section 1 and in table IV for test section 2. These coordinates are referenced to the coordinate systems defined in figure 12 for each test section. Contour coordinates are given for the lower nozzle block in the most upstream test position. Table V gives the lower nozzle-block position as a function of test-section Mach number for test section 1 and as a function of Mach number and Reynolds number for test section 2.

For determination of the nozzle coordinates in inches at any given Mach number and Reynolds number for the lower block only, x coordinates are defined for test section 1 by the equation

$$x = x_1 + \left(115.5 - \frac{b}{10}\right) \tag{1}$$

and for test section 2 by the equation

$$x = x_2 + \left(219.5 - \frac{b}{100}\right) \tag{2}$$

The high and low Mach number tunnel circuits have variable cross-sectional area second-minimum sections downstream of the test section. Elevation and plan-view drawings of these sections are shown in figure 14. Figure 14 also shows the details of the superstructure, movable sidewalls, and downstream transition section from rectangular to circular cross section. The second-minimum contraction ratio can be varied to a maximum of 2.66 for the low Mach number tunnel circuit and to 4 for the high Mach number tunnel circuit.

Operating second-minimum contraction ratios have been established to provide maximum supersonic-flow stability over a wide range of test-section blockage conditions. For the low Mach number tunnel circuit, the second minimum operates at a contraction ratio of 1.01 over all test conditions. The high Mach number tunnel circuit requires the variation of the second-minimum contraction ratio with nozzle-block position as presented in table VI.

Model support struts.- Many methods have been used to support models and probes depending on the objective of the test. The mounting mechanism most commonly used in both test sections to provide force and moment data on airplane and missile models is shown in figure 15. The basic mechanism is the horizontal wall-mounted strut which is capable of forward and aft travel of 36.25 in. (0.921 m) in the x-direction. To this strut is attached a sting support which has traverse (y) and sideslip (β) motion of ± 20 in. (± 0.508 m) and $\pm 14^{\circ}$, respectively. Forward of the sting support is the angle-of-attack (α) mechanism which provides pitch motion from -12° to 22°. Just upstream of the pitch mechanism is the roll mechanism which provides continuous roll motion through 310°. The model is mounted on the roll mechanism by means of a sting. A wide assortment of sting sizes and lengths are available to provide specific model position and load requirements. In addition to several alternate pitch mechanisms, one of which can provide up to 90° angle of attack, there are assorted angular couplings and "dog-leg" and offset stings.

Windows and access doors.- Access to each test section is provided by two doors which form the sidewalls of the test sections from station 0.625 in. (0.0159 m) to station 69.375 in. (1.762 m). Each of the test-section doors has nine 5.5-in. (0.140-m) by 48-in. (1.22-m) windows, separated by 1.25-in. (3.18-cm) webs, which form a field of view 59.5 in. (1.51 m) long by 48 in. (1.22 m) high through the test section. The windows are 1.5-in.-thick (0.038-m) glass of optical quality to provide minimum distortion for schlieren and flow visualization. Details of the test-section access doors and windows are shown in figure 12. An alternate set of solid-steel doors is available for sidewall model mounts and heat-transfer tests. In addition, each test section is provided with an access hatch in the region of the diffuser.

Instrumentation

Wind-tunnel stagnation temperature and pressure measurement.- The test-section Mach number is determined by the position of the movable lower nozzle block. The relation of the physical position of the block to the calibration Mach number is presented in table V. The tunnel stagnation pressure is measured in the settling chambers by using a system of sonar manometers up to 5000 psf (239.4 kPa) and pressure transducers in the higher range up to the maximum duct pressure of 10 atm. The accuracy of this measurement is ±0.5 psf (±23.94 Pa) in the lower range and ±21.6 psf (±1.034 kPa) in the higher range. Tunnel stagnation temperature is measured by an array of thermocouples mounted on the turning vanes upstream of the settling chambers.

Schlieren system.- Each test section is equipped with a schlieren system having a 49-in.-diameter (1.24-m) field of view. The complete system shown in schematic form in figure 16 is supported from a beam as a unit and can be positioned along the longitudinal axis of the test section. The system uses a silvered knife edge at the focal point to provide simultaneous viewing and recording of the image. The schlieren photographs are taken with an automatic 9- by 9-in. (0.229- by 0.229-m) aerial camera. A typical schlieren photograph is shown in figure 17.

Vapor-screen system.- A flow-visualization system can be set up in either test section to provide photographs of vapor-screen images of flow phenomena. Figure 18 shows a schematic drawing of the setup of lights and cameras both inside and outside of the test section. The appropriate vapor density is established by increasing the tunnel operating dew point to a value ranging from $20^{\circ}F$ ($-6.7^{\circ}C$) to $30^{\circ}F$ ($-1.1^{\circ}C$), depending upon Mach number. Figure 19 shows typical vapor-screen results obtained with the cameras located both inside and outside the tunnel.

Data acquisition.- The heart of the on-line data-acquisition system is a 48K word memory computer which is coupled to a data-acquisition system with 100 analog and 40 digital recording channels. This system provides on-line data reduction and displays in real time as well as calibration capability for the two test sections. Force and moment data are measured by strain-gage balances which are temperature compensated and calibrated to account for first- and second-order interactions such that the system is generally accurate to within ±1/2 percent of the design balance load. Each point of force data is computed on line from an average of 60 samples recorded at 30 samples per second. From 1 to 12 plots can be displayed on a cathode-ray tube at a time. Pressure data are taken with pressure transducers of appropriate sizes used with scanning valves. The data-acquisition system can accommodate up to six 48-port scanning valves. These are automatically calibrated at each data point to provide accuracy generally within ±1.0 psf (±47.88 Pa).

Air Systems

General description.- The equipment required to maintain the tunnel air supply is located in the general area of the compressor drive section as shown in the schematic drawing of figure 2. The air system consists of the following: a makeup air compressor, storage spheres, air dryers, a seal air compressor, and evacuation pumps. Air from the central 5000 psi (34 477 kPa) pumping station is used at reduced pressure as a backup for the facility air systems.

Makeup air equipment.- Air for the tunnel is supplied by three 31-ft (9.4-m) storage spheres charged with 150 psi (1034 kPa) dry air. A 12 500 ft^3/min (353.9 m^3/min) two-stage compressor powered with a 3500-hp (2610-kW) drive motor supplies air to the spheres. This air is dried with an activated-alumina air dryer having a capacity of 1140 lb/min (517.10 kg/min) at 150 psi (1034 kPa) with air-outlet dew point of $-90^{\circ}F$ ($-67.8^{\circ}C$).

Seal air system.- The seal air system consists of a 140 ft^3/min (3.96 m^3/min) compressor used to supply 300 psi (2068.42 kPa) air to pressurize the tunnel valve seals. Air for the labyrinth seals of the main-drive compressors is supplied from the storage spheres.

Vacuum system.- The tunnel is evacuated for start-up and purge by means of four vacuum pumps with a total capacity of 9100 ft^3/min (257.68 m^3/min). These vacuum pumps are also used to maintain stagnation pressure below atmospheric conditions. The vacuum system also has a 1000 ft^3/min (28.32 m^3/min) vacuum pump for maintaining low pressures in the main-drive bypass circuit and a 1000 ft^3/min (28.32 m^3/min) vacuum pump to evacuate the volume below the test-section sliding blocks.

CALIBRATION AND TUNNEL OPERATING CHARACTERISTICS

Calibration

Before the construction of the Langley Unitary Plan Wind Tunnel was initiated, the concept of asymmetric movable nozzle blocks was explored and evaluated for the Mach number range of the low Mach number circuit and was presented in reference 6. The results of reference 6 indicated that low values of flow angularity and Mach number variation through the test section could be obtained with the sliding asymmetric nozzle concept. The actual flow angularities measured in the full-scale facility were found to be somewhat higher than expected. An investigation into the source of the flow angularity was made on a 1/16-scale tunnel model in reference 7. It was found that the angularity was generally the same in both facilities and was due to nozzle contour. The limited flow-angle data for the full-scale tunnel which were presented in reference 7 were part of an extensive flow-angle calibration. This section presents the flow-angle calibration obtained in 1957 and a Mach number calibration obtained in 1966-67 for both test sections for the range of facility operating parameters of general interest. Periodic check calibrations made since these initial calibrations indicate no significant change in Mach number or flow angle.

Procedure.- The calibration tests of both test sections of the Unitary Plan Wind Tunnel have been obtained by presetting the lower nozzle block, stabilizing stagnation pressure and temperature, and using static or pitot-probe measurements to survey Mach number. Flow angularity was determined by six two-dimensional balance wedge probes mounted either vertically or horizontally. The details of the survey rake and the probes are presented in figure 20. Six static and/or six pitot probes were mounted

on the survey rake as shown and the rake was mounted vertically in the test section. Mach number calibration data were taken with both probes in test section 1 and with only the pitot probes in test section 2 at a series of longitudinal and lateral stations. However, to obtain the best accuracy and most repeatable data, the Mach numbers below $M = 2$ were computed from the static pressures and tunnel stagnation pressure according to the equation

$$M = \sqrt{5\left[\left(\frac{p_t}{p_{st}}\right)^{2/7} - 1\right]} \tag{3}$$

For Mach numbers greater than 2 the pitot pressure and tunnel stagnation pressure were used to define Mach number according to the equation

$$\frac{p_p}{p_t} = \left(\frac{6M^2}{M^2 + 5}\right)^{7/2}\left(\frac{6}{7M^2 - 1}\right)^{5/2} \tag{4}$$

The calibration Mach number $\bar{M}$ was determined for each test condition from results at the five longitudinal center-line survey stations between $x = 0$ in. (0 cm) and 48 in. (122 cm). At each survey station an average Mach number was determined from the four vertical probe positions closest to the center line (omitting the top and bottom) by weighing the two probes closest to the center line in full and the other two probes ($z = \pm 10.8$ in. (± 27.4 cm)) by one-half. For test section 2, the calibration Mach number $\bar{M}$ weighed all five longitudinal stations equally; whereas, for test section 1 one-half weight was given to longitudinal stations 0 in. and 48 in. (0 cm and 122 cm) and full weight was applied to the intermediate stations. The flow-angle probe configuration consisted of a double-wedge segment mounted on a one-component strain-gage balance as shown in figure 20. The balance output measured normal load on the wedge surfaces and was calibrated to measure flow angle.

Presentation of data.- Calibration data on the distribution of Mach number are presented in figures 21 and 22 for test sections 1 and 2, respectively. Calibration data on the distribution of flow angularity are presented in figures 23 and 24 for test sections 1 and 2, respectively. Since the geometry of the test sections and nozzles of the Unitary Plan Wind Tunnel is asymmetric, the large variations of flow parameters might be expected to exist in the xz-plane. For this reason the Mach number calibration data are presented primarily as contour plots in the xz-plane with additional information to indicate lateral, longitudinal, and Reynolds number sensitivity. The longitudinal variation of Mach number can be used to correct test results for buoyancy effects. The variation of nominal test-section Mach number with Reynolds number is accounted for in test section 2 by adjusting the nozzle block position according to table V(b). The calibration data of figures 21 and 22 indicate generally a variation in Mach number of ± 0.01 in the region of the test sections most used when testing smaller models (10 in. $< x <$ 30 in. (0.254 m $< x <$ 0.762 m) with $z = \pm 10$ in. (± 0.254 m)). At the higher Mach numbers and for longer models at angles of attack, the variation of test-section Mach number from the nominal can be as much as ± 0.04 over the test section. The flow-angle calibrations are presented primarily as contour plots of vertical angles in the xz-plane. Vertical and horizontal flow-angle variations are also presented for center line and lateral positions. Figures 23 and 24 indicate that the flow in both test sections has an upflow angle generally within 0.5°. At the higher Mach numbers in test section 1 the upflow angle can be as large as 1.5° within the test region occupied by typical models. The

accuracy of the calibration data is estimated to be within ±0.01 for Mach number in test section 1, ±0.004 for Mach number in test section 2, and flow angularity to within $\pm 0.1^{\circ}$. These estimates are based on individual accuracies of static, pitot, and total-pressure measurements as well as on wedge probe-balance and optical angular-measurement accuracies.

Test-section boundary layer.- Boundary-layer profiles have been measured on the tunnel test-section sidewalls over the range of test conditions. The measurements were obtained by using a rake with 22 tubes (0.050-in. (0.00127-m) outside diameter) spanning a distance of 6.5 in. (0.1651 m) perpendicular to the sidewall. The location of the tubes is indicated in figure 25 which shows typical velocity profiles for each test section at common conditions. The different lengths and pressure gradients of the nozzles are reflected in the shape of the sidewall profiles. In figure 26 a summary of the boundary-layer profile characteristics, including profile exponent for a turbulent boundary layer N, thickness δ, displacement thickness δ^*, and momentum thickness θ, is presented for several Reynolds numbers and Mach numbers. The velocities were calculated by assuming the static pressure across the boundary layer to be constant and equal to free-stream static pressure. The boundary-layer thickness corresponds to the value of u/u_{∞} of 0.996; and δ^*, θ, and N were calculated from equations (6) and (21) of reference 8.

Tunnel moisture effects.- Although the Unitary Plan Wind Tunnel is a closed-circuit pressure tunnel with sufficient makeup air capacity to provide dry air as the test medium, efficient utilization of the facility requires that the effects of moisture on test conditions be evaluated. A measurement of the static pressure was made at $x = 48.12$ in. (122.22 cm) in test section 1 and at $x = 44.12$ in. (112.06 cm) in test section 2, with $y = 0$ in. (0 cm) and $z = -1.11$ in. (-2.82 cm), for several Mach numbers and Reynolds numbers over a range of tunnel dew-point values. These results are presented in figure 27 in terms of the ratio of static pressure to total pressure or Mach number as computed by equation (3). These results indicate that, in general, tunnel moisture effects become significant above values of tunnel dew point (corrected to standard atmospheric pressure) ranging from -20°F (-28.9°C) at the lower Mach numbers to 20°F (-6.7°C) at the higher Mach numbers.

Tunnel turbulence level.- Measurements have been made to indicate the turbulence level of the Unitary Plan Wind Tunnel by using a hot-wire anemometer to determine the velocity fluctuation in the settling chambers and by measuring the transition Reynolds number on a smooth 10° cone in both test sections. The level of settling-chamber velocities and fluctuation velocities is shown in figure 28 for different values of unit Reynolds number and Mach number. These measurements were obtained at tunnel station 561.33 ft (171.09 m) for test section 1 and at tunnel station 774.65 ft (236.11 m) for test section 2 on the tunnel center line. These turbulence measurements shown in figure 28 provide some insight into the high-frequency turbulence which would be carried downstream into the test sections. Another indication of test-section turbulence is obtained by examining the transition Reynolds number measured on a smooth 10° cone. The cone and measurement system used is that of reference 9 and a photograph of the system is shown in figure 29. The measured transition Reynolds numbers are presented for both test sections in figure 30 and are compared with other facilities in figure 31.

Tunnel blockage.- Since the operation of a supersonic duct is dependent on the overall area ratio, the cross section of the model is critical for a fixed-size test-section cross-sectional area. Figure 32 gives the theoretical maximum model cross-sectional area determined from a one-dimensional flow analysis as a function of Mach number for the Unitary Plan Wind Tunnel. In reality, the theoretical maximum model

cross-sectional area indicates successful tunnel operation at a much larger model size than is possible. The size of some of the larger models tested at the UPWT is shown as experimental maximum model cross-sectional area over the Mach number range. The large width of the band of experimental maximum model sizes indicates the uncertainty of model shape, mounting, and attitude effects on blockage.

Tunnel temperature calibration.- The facility can be operated in such a way as to provide a heat pulse for heat-transfer tests. This mode of operation is described in detail in a subsequent section. A calibration of the total temperature variation across test section 2 at station $x = 30$ in. (0.762 m) is presented in figure 33 as a function of time from initiation of the heat pulse for several Mach numbers. The total-temperature measurements were obtained by using double-shielded probes containing a 30-gage iron-constantan thermocouple. The probes were 2 in. (0.0508 m) in length, and the diameter of the outside shield was 0.4 in. (0.0102 m). The calculated response time of the probes for a step increase in stagnation temperature at nominal test conditions is less than 1 sec. The results of figure 33 indicate that the time required for temperature stabilization after the heat pulse increases with Mach number to a maximum of approximately 15 sec at a Mach number of 4.44.

Tunnel Operating Characteristics

Operating parameters.- The operating range of test Mach number and Reynolds number for each of the test sections is presented in figure 34. For any specific Mach number the upper limit of Reynolds number is established by drive power and stagnation-pressure limits. The operating range is separated into five areas which correspond to the five compressor configurations or modes described earlier in this report. The upper limit of operational Reynolds numbers is established by the overload capability of the main-drive system, and the lower limit is an indication of the supersonic-flow stability characteristics at reduced pressure over the Mach number range. It should be noted that between compressor modes 1-IA and 1-II ($M \approx 2.16$ to 2.36) and between modes 2-II and 2-IV ($M \approx 3.75$ to 3.83) the compressor configurations are not capable of producing the required tunnel pressure ratio to assure stable supersonic test conditions in the test section. The tunnel operating regions shown in figure 34 represent constant temperature operations at $150^{\circ}F$ ($65.5^{\circ}C$) in all compressor modes except mode 2-IV which is for $175^{\circ}F$ ($79.44^{\circ}C$).

Although most of the tests made in the Langley Unitary Plan Wind Tunnel require constant temperature operation, the facility has a unique heat-transfer capability. Because of the tunnel duct configurations and the bypass feature of the heat exchangers, the facility can be operated in such a way as to provide a heat pulse or total temperature rise during a finite time interval. The magnitude of the available total temperature rise and time to stabilize is shown in figure 35 as a function of Mach number for test section 2. This capability is essentially independent of tunnel total pressure.

Power characteristics.- Total operating power requirements are presented in figure 36 for nominal operating temperatures and test Reynolds numbers of 2×10^6 per ft (6.56×10^6 per m) and 4×10^6 per ft (13.12×10^6 per m). The power values of figure 36 are average measurements for the conditions shown and include the main drive and auxiliary equipment. In general, the power range required for the auxiliary equipment ranges from 3 to 5 MW throughout the test range available. Because of the flexibility of the operational procedures of the facility, the power requirements can vary from these average numbers. For example, a total temperature reduction of $25^{\circ}F$ ($13.89^{\circ}C$) over the nominal test conditions at $R = 2 \times 10^6$ per ft (6.56×10^6 per m)

results in a 6-percent reduction in power required. Further power-reduction operating techniques are discussed in detail in reference 5 along with an analysis of power requirements of individual compressors at various operating conditions.

CONCLUDING REMARKS

The Langley Unitary Plan Wind Tunnel is a closed-circuit pressure tunnel with two 4- by 4- by 7-ft (1.22- by 1.22- by 2.13-m) test sections which cover a Mach number range M from 1.47 to 4.63 and a nominal Reynolds number range from 0.5×10^6 per ft (1.64×10^6 per m) to 8.0×10^6 per ft (26.25×10^6 per m). The facility has the flexibility to provide continuous variation of Mach number and tunnel stagnation pressure and temperatures. The Mach number variation is controlled by asymmetric sliding nozzle blocks and a combination of compressor staging modes. There exists two regions in the total Mach number range ($2.16 < M < 2.36$ and $3.75 < M < 3.83$) for which stable test conditions cannot be assured. The tunnel stagnation temperature and pressure are controlled by heat exchangers and auxiliary pumps and air dryers. The heat-exchanger capability to bypass tunnel air can provide a stagnation-temperature pulse at constant Mach number and stagnation pressure which results in a unique heat-transfer test capability for the facility.

The calibration of the test-section flow parameters over the operating range of the facility indicated that a variation in Mach number of ±0.01 occurred in the area of the test sections most used when testing smaller models. At the higher Mach numbers and for longer models at angle of attack, the variation of test-section Mach number from the nominal can be as much as ±0.04 over the test region. Both test sections have a positive or upflow angle generally within $\pm 0.5^{\circ}$. At the higher Mach numbers for test section 1 the upflow angle can be as large as 1.5° within the test region occupied by typical models. Tunnel moisture effects become significant above values of tunnel dew point (corrected to standard atmospheric pressure) ranging from $-20^{\circ}F$ ($-28.9^{\circ}C$) at the lower test Mach numbers to $20^{\circ}F$ ($-6.7^{\circ}C$) at the higher Mach numbers.

Langley Research Center
National Aeronautics and Space Administration
Hampton, VA 23665
August 17, 1981

REFERENCES

1. Schaefer, William T., Jr.: Characteristics of Major Active Wind Tunnels at the Langley Research Center. NASA TM X-1130, 1965.

2. National Wind-Tunnel Summary. NASA and Dept. Defense, July 1961. (Available from Clearinghouse, U.S. Dept. Com.)

3. Manual for Users of the Unitary Plan Wind Tunnel Facilities of the National Advisory Committee for Aeronautics. NACA, 1956.

4. Mechtly, E. A.: The International System of Units - Physical Constants and Conversion Factors. NASA SP-7012, 1964.

5. Hasel, Lowell E.; and Stallings, Robert L., Jr.: Analysis of the Performance of the Drive System and Diffuser of the Langley Unitary Plan Wind Tunnel. NASA TM-83168, 1981.

6. Burbank, Paige B.; and Byrne, Robert W.: The Aerodynamic Design and Calibration of an Asymmetric Variable Mach Number Nozzle With a Sliding Block for the Mach Number Range 1.27 to 2.75. NACA TN 2921, 1953. (Supersedes NACA RM L50L15.)

7. Matthews, George B.; and Shirley, John A.: A Comparison of Flow Inclination in the U. Va. Supersonic Wind Tunnel and the NASA Unitary Plan Wind Tunnel, Test Section No. 1. Rep. No. AST-4026-101-65U (Contract No. NAS1-4326), Res. Lab. Eng. Sci., Univ. of Virginia, June 1965.

8. Allen, Jerry M.: A Simple Method of Calculating Power-Law Velocity Profile Exponents From Experimental Data. NASA TM X-72000, 1974.

9. Dougherty, N. S., Jr.: Prepared Comment on the Cone Transition Reynolds Number Data Correlation Study. Flight/Ground Testing Facilities Correlation, AGARD-CP-187, 1976, pp. 3A-1 - 3A-7.

TABLE I.- MAJOR DIMENSIONS OF THE LANGLEY UNITARY PLAN WIND TUNNEL

(a) High Mach number circuit

Component	Axial station		Equivalent circular diameter		Shape
	Feet	Meters	Feet	Meters	
Test section begins	0	0	4.51	1.37	Square
Test section ends and model support section begins	7.00	2.13	4.51	1.37	Square
Model support section ends and second minimum begins	15.44	4.71	4.51	1.37	Square
Second minimum ends and transition section begins	50.69	15.45	5.27	1.61	Rectangular
Transition section ends and diffuser begins	60.22	18.36	5.66	1.73	Circular
Isolation valve II	108.03	32.93	8.00	2.44	Circular
Diffuser ends	145.72	44.42	12.00	3.66	Circular
Turning vanes	169.72	51.73	12.00	3.66	Elliptical
Turning vanes	311.72	95.01	14.00	4.27	Elliptical
Cooler 5 transition inlet	321.22	97.91	14.00	4.27	Circular
Cooler 5 transition exit	356.22	108.58	12.00	3.66	Circular
Compressors C and D	415.22	126.56			
Compressor F	415.22	126.56			
Cooler 3 transition inlet	474.72	144.69	6.00	1.83	Circular
Cooler 3 transition exit	504.72	153.84	6.00	1.83	Circular
Compressor G ducting	509.30	155.23			
Isolation valve IX	515.55	157.14	6.00	1.83	Circular
Turning vanes	546.80	166.66	8.00	2.44	Elliptical
Isolation valve V	678.80	206.90	8.00	2.44	Circular
Ducting turn 7.7^{o}	694.55	211.70	8.03	2.45	Elliptical
Turning vanes	762.15	232.30	12.00	3.66	Elliptical
Settling chamber begins	762.15	232.30	12.00	3.66	Elliptical
Settling chamber ends and transition cone begins	786.65	239.77	12.00	3.66	Circular
Transition cone ends and nozzle contour begins	790.15	240.84	6.67	2.03	Rectangular
Nozzle contour ends and test section begins	836.00	254.81	4.51	1.37	Square

TABLE I.- Continued

(b) Compressor I circuit

Component	Axial station		Equivalent circular diameter		Shape
	Feet	Meters	Feet	Meters	
Cooler 5	0	0			
Isolation valve XX	18.73	5.71	6.00	1.83	Circular
Turning vanes	35.73	10.89	7.14	2.18	Elliptical
Compressor I	84.04	25.62			
Cooler 6 inlet	107.96	32.91	6.00	1.83	Circular
Cooler 6 exit	139.91	42.64	7.00	2.13	Circular
Isolation valve VII	192.04	58.53	7.00	2.13	Circular
Turning vanes	200.09	60.99	7.00	2.13	Elliptical
Low Mach number circuit	225.35	68.69			

(c) Compressor E exit air to compressor F

Component	Axial station		Equivalent circular diameter		Shape
	Feet	Meters	Feet	Meters	
Compressor E duct	0	0			
Turning corner, 15°	4.38	1.34	6.03	1.84	Elliptical
Isolation valve XII	7.21	2.20	6.00	1.83	Circular
Compressor F	72.30	22.04			

TABLE I.- Concluded

(d) Compressor E circuit

Component	Axial station		Equivalent circular diameter		Shape
	Feet	Meters	Feet	Meters	
Low Mach number circuit	0	0			
Turning corner, 32.9°	17.75	5.41	7.64	2.33	Elliptical
Isolation valve XIII	57.02	17.38	7.00	2.13	Circular
Compressor E	99.02	30.18			
Turning corner center line, 9.8°	124.57	37.97	6.82	2.08	Elliptical
Cooler 2 inlet	126.45	38.54	7.00	2.13	Circular
Cooler 2 exit	162.57	49.55	7.00	2.13	Circular
Turning corner, 9.8°	162.90	49.65	7.05	2.15	Elliptical
Isolation valve XIV	191.15	58.26	7.00	2.13	Circular
High Mach number exit duct and isolation valve VIII	205.32	62.58	7.00	2.13	Circular
Turning vanes	215.57	65.71	7.00	2.13	Elliptical
Low Mach number circuit	253.24	77.19			

(e) Compressor G circuit

Component	Axial station		Equivalent circular diameter		Shape
	Feet	Meters	Feet	Meters	
Compressor G exit duct	0	0			
Cooler 4 inlet	28.25	8.61	5.00	1.52	Circular
Cooler 4 exit	58.25	17.75	4.00	1.22	Circular
Isolation valve X	75.00	22.86	4.00	1.22	Circular
Turning corner, 46°	105.63	32.20	4.17	1.27	Elliptical
High Mach number circuit	127.97	39.01			

(f) Compressor F exit air to compressor G

Component	Axial station		Equivalent circular diameter		Shape
	Feet	Meters	Feet	Meters	
Compressor F duct	0	0			
Isolation valve XI	14.75	4.50	4.00	1.22	Circular
Turning corner, 30°	70.96	21.63	4.07	1.24	Elliptical
Compressor G	98.43	30.00			

TABLE II.- MAJOR DIMENSIONS OF THE LOW MACH NUMBER CIRCUIT OF THE LANGLEY UNITARY PLAN WIND TUNNEL

Component	Axial station		Equivalent circular diameter		Shape
	Feet	Meters	Feet	Meters	
Test section begins	0	0	4.51	1.37	Rectangular
Test section ends and model support section begins	7.00	2.13	4.51	1.37	Rectangular
Model support section ends and second minimum begins	15.45	4.71	4.70	1.43	Rectangular
Second minimum ends and transition section begins	50.70	15.45	5.27	1.61	Rectangular
Transition section ends and diffuser begins	59.45	18.12	5.66	1.73	Circular
Diffuser ends	144.95	44.18	12.00	3.66	Circular
Isolation valve I	147.33	44.91	12.00	3.66	Circular
Turning vanes	155.95	47.53	12.00	3.66	Elliptical
Main tunnel intersection	174.33	53.14	12.00	3.66	Elliptical
Turning vanes	236.33	72.03	14.00	4.27	Circular
Cooler 5 transition inlet	245.83	74.93	14.00	4.27	Circular
Cooler 5 transition exit	280.83	85.60	12.00	3.66	Circular
Compressors C and D	339.83	103.58			
Cooler 1 transition inlet	346.65	105.66	4.00	1.22	Circular
Cooler 1 transition exit	408.08	124.38	10.00	3.05	Circular
Compressor E inlet ducting	425.83	129.79	10.00	3.05	Circular
Isolation valve IV	434.21	132.35	10.00	3.05	Circular
Compressor E outlet ducting	455.83	138.94	11.67	3.56	Circular
Turning vanes	473.33	144.27	12.50	3.81	Elliptical
Turning vanes	548.33	167.13	15.00	4.57	Elliptical
Settling chamber begins	548.33	167.13	15.00	4.57	Elliptical
Settling chamber ends and transition cone begins	573.33	174.75	15.00	4.57	Circular
Transition cone ends and nozzle contour begins	580.33	176.88	4.51	1.37	Rectangular
Nozzle contour ends and test section begins	616.38	187.87	4.51	1.37	Rectangular

TABLE III.- CONTOURED-NOZZLE WALL COORDINATES FOR TEST SECTION 1

(a) Lower block

x_l, in.	z_l, in.	x_l, cm	z_l, cm	x_l, in.	z_l, in.	x_l, cm	z_l, cm
-375.415	-142.500	-953.554	-361.950	-189.891	-29.667	-482.323	-75.354
-317.580	-78.789	-806.653	-200.124	-187.891	-29.363	-477.243	-74.582
-316.915	-78.081	-804.964	-198.326	-185.891	-29.070	-472.163	-73.838
-312.915	-74.321	-794.804	-188.775	-183.891	-28.787	-467.083	-73.119
-308.915	-71.148	-784.644	-180.716	-181.891	-28.514	-462.003	-72.426
-304.915	-68.356	-774.484	-173.624	-179.891	-28.251	-456.923	-71.758
-300.915	-65.852	-764.324	-167.264	-177.891	-27.996	-451.843	-71.110
-296.915	-63.568	-754.164	-161.463	-175.891	-27.750	-446.763	-70.485
-292.915	-61.476	-744.004	-156.149	-173.891	-27.514	-441.683	-69.886
-288.915	-59.556	-733.844	-151.272	-171.891	-27.288	-436.603	-69.312
-284.915	-57.796	-723.684	-146.802	-169.891	-27.071	-431.523	-68.760
-280.915	-56.177	-713.524	-142.690	-167.891	-26.863	-426.443	-68.232
-276.915	-54.673	-703.364	-138.869	-165.891	-26.665	-421.363	-67.729
-272.915	-53.262	-693.204	-135.285	-163.891	-26.474	-416.283	-67.244
-268.915	-51.915	-683.044	-131.864	-161.891	-26.292	-411.203	-66.782
-264.915	-50.583	-672.884	-128.481	-159.891	-26.118	-406.123	-66.340
-260.915	-49.268	-662.724	-125.141	-157.891	-25.952	-401.043	-65.918
-256.915	-47.944	-652.564	-121.778	-155.891	-25.794	-395.963	-65.517
-256.186	-47.705	-650.712	-121.171	-153.891	-25.643	-390.883	-65.133
-241.160	-42.770	-612.546	-108.636	-151.891	-25.500	-385.803	-64.770
-240.160	-42.442	-610.006	-107.803	-149.891	-25.364	-380.723	-64.425
-239.160	-42.115	-607.466	-106.972	-147.891	-25.235	-375.643	-64.097
-238.160	-41.789	-604.926	-106.144	-145.891	-25.113	-370.563	-63.787
-237.160	-41.464	-602.386	-105.319	-143.891	-25.000	-365.483	-63.500
-231.447	-39.608	-587.875	-100.604	-141.891	-24.894	-360.403	-63.231
-229.891	-39.105	-583.923	-99.327	-139.891	-24.795	-355.323	-62.979
-227.891	-38.463	-578.843	-97.696	-137.891	-24.702	-350.243	-62.743
-225.891	-37.834	-573.763	-96.098	-135.891	-24.614	-345.163	-62.520
-223.891	-37.216	-568.683	-94.529	-133.891	-24.533	-340.083	-62.314
-221.891	-36.612	-563.603	-92.994	-131.891	-24.456	-335.003	-62.118
-219.891	-36.024	-558.523	-91.501	-129.891	-24.387	-329.923	-61.943
-217.891	-35.454	-553.443	-90.053	-127.891	-24.325	-324.843	-61.785
-215.891	-34.906	-548.363	-88.661	-125.891	-24.271	-319.763	-61.648
-213.891	-34.379	-543.283	-87.323	-123.891	-24.223	-314.683	-61.526
-211.891	-33.877	-538.203	-86.048	-121.891	-24.180	-309.603	-61.417
-209.891	-33.401	-533.123	-84.839	-119.891	-24.142	-304.523	-61.321
-207.891	-32.949	-528.043	-83.690	-117.891	-24.109	-299.443	-61.237
-205.891	-32.520	-522.963	-82.601	-115.891	-24.079	-294.363	-61.161
-203.891	-32.112	-517.883	-81.564	-113.891	-24.054	-289.283	-61.097
-201.891	-31.724	-512.803	-80.579	-111.891	-24.034	-284.203	-61.046
-199.891	-31.350	-507.723	-79.629	-109.891	-24.019	-279.123	-61.008
-197.891	-30.991	-502.643	-78.717	-107.891	-24.009	-274.043	-60.983
-195.891	-30.644	-497.563	-77.836	-105.891	-24.003	-268.963	-60.968
-193.891	-30.307	-492.483	-76.980	-103.891	-24.000	-263.883	-60.960
-191.891	-29.982	-487.403	-76.154	229.085	-24.000	581.876	-60.960

TABLE III.- Continued

(b) Upper block

x_l, in.	z_l, in.	x_l, cm	z_l, cm	x_l, in.	z_l, in.	x_l, cm	z_l, cm
-432.625	-4.375	-1098.868	-11.113	-247.625	-31.900	-628.968	-81.026
-334.375	-39.240	-849.313	-99.670	-180.625	-10.130	-458.788	-25.730
-331.625	-40.206	-842.328	-102.123	-173.625	-7.856	-441.008	-19.954
-327.625	-41.530	-832.168	-105.486	-171.625	-7.206	-435.928	-18.303
-323.625	-42.504	-822.007	-107.960	-169.625	-6.556	-430.848	-16.652
-319.625	-43.100	-811.848	-109.474	-167.625	-5.906	-425.768	-15.001
-315.625	-43.398	-801.688	-110.231	-165.625	-5.257	-420.688	-13.353
-311.625	-43.546	-791.528	-110.607	-163.625	-4.608	-415.608	-11.704
-307.625	-43.614	-781.368	-110.780	-161.625	-3.961	-410.528	-10.061
-303.625	-43.622	-771.208	-110.800	-159.625	-3.315	-405.448	-8.420
-299.625	-43.568	-761.048	-110.663	-157.625	-2.670	-400.368	-6.782
-295.625	-43.432	-750.888	-110.317	-155.625	-2.026	-395.288	-5.146
-291.625	-43.178	-740.728	-109.672	-153.625	-1.384	-390.208	-3.515
-289.625	-42.980	-735.648	-109.169	-151.625	-.745	-385.128	-1.892
-287.625	-42.743	-730.568	-108.567	-149.625	-.109	-380.048	-.277
-285.625	-42.466	-725.488	-107.864	-147.625	.522	-374.968	1.326
-283.625	-42.149	-720.408	-107.058	-145.625	1.148	-369.888	2.916
-281.625	-41.794	-715.328	-106.157	-143.625	1.766	-364.808	4.486
-279.625	-41.400	-710.248	-105.156	-141.625	2.377	-359.728	6.038
-277.625	-40.966	-705.168	-104.054	-139.625	2.978	-354.648	7.564
-275.625	-40.492	-700.088	-102.850	-137.625	3.568	-349.568	9.063
-273.625	-39.979	-695.008	-101.547	-135.625	4.147	-344.488	10.533
-271.625	-39.428	-689.928	-100.147	-133.625	4.714	-339.408	11.974
-269.625	-38.848	-684.848	-98.674	-131.625	5.272	-334.328	13.391
-267.625	-38.251	-679.768	-97.158	-129.625	5.818	-329.248	14.778
-265.625	-37.642	-674.688	-95.611	-127.625	6.352	-324.168	16.134
-263.625	-37.024	-669.608	-94.041	-125.625	6.875	-319.088	17.463
-261.625	-36.398	-664.528	-92.451	-123.625	7.388	-314.008	18.766
-259.625	-35.766	-659.448	-90.846	-121.625	7.889	-308.928	20.038
-257.625	-35.129	-654.368	-89.228	-119.625	8.380	-303.848	21.285
-255.625	-34.488	-649.288	-87.600	-117.625	8.859	-298.768	22.502
-253.625	-33.844	-644.208	-85.964	-115.625	9.328	-293.688	23.693
-251.625	-33.198	-639.128	-84.323	-113.625	9.786	-288.608	24.856
-249.625	-32.550	-634.048	-82.677	-111.625	10.234	-283.528	25.994
-249.125,	-32.387	-632.778	-82.263	-109.625	10.672	-278.448	27.107

TABLE III.- Concluded

(b) Concluded

x_l, in.	z_l, in.	x_l, cm	z_l, cm	x_l, in.	z_l, in.	x_l, cm	z_l, cm
-107.625	11.100	-273.368	28.194	-31.625	21.553	-80.328	54.745
-105.625	11.517	-268.288	29.253	-29.625	21.707	-75.248	55.136
-103.625	11.925	-263.208	30.290	-27.625	21.855	-70.168	55.512
-101.625	12.322	-258.128	31.298	-25.625	21.998	-65.088	55.875
-99.625	12.710	-253.048	32.283	-23.625	22.135	-60.008	56.223
-97.625	13.088	-247.968	33.244	-21.625	22.267	-54.928	56.558
-95.625	13.456	-242.888	34.178	-19.625	22.394	-49.848	56.881
-93.625	13.816	-237.808	35.093	-17.625	22.516	-44.768	57.191
-91.625	14.168	-232.728	35.987	-15.625	22.632	-39.688	57.485
-89.625	14.512	-227.648	36.860	-13.625	22.744	-34.608	57.770
-87.625	14.848	-222.568	37.714	-11.625	22.851	-29.528	58.042
-85.625	15.175	-217.488	38.545	-9.625	22.953	-24.448	58.301
-83.625	15.496	-212.408	39.360	-7.625	23.049	-19.368	58.544
-81.625	15.811	-207.328	40.160	-5.625	23.141	-14.288	58.778
-79.625	16.119	-202.248	40.942	-3.625	23.227	-9.208	58.997
-77.625	16.421	-197.168	41.709	-1.625	23.310	-4.128	59.207
-75.625	16.714	-192.088	42.454	.375	23.388	.953	59.406
-73.625	17.001	-187.008	43.183	2.375	23.461	6.033	59.591
-71.625	17.280	-181.928	43.891	4.375	23.530	11.113	59.766
-69.625	17.553	-176.848	44.585	6.375	23.594	16.193	59.929
-67.625	17.819	-171.768	45.260	8.375	23.653	21.273	60.079
-65.625	18.078	-166.688	45.918	10.375	23.707	26.353	60.216
-63.625	18.331	-161.608	46.561	12.375	23.756	31.433	60.340
-61.625	18.577	-156.528	47.186	14.375	23.800	36.513	60.452
-59.625	18.817	-151.448	47.795	16.375	23.841	41.593	60.556
-57.625	19.051	-146.368	48.390	18.375	23.878	46.673	60.650
-55.625	19.278	-141.288	48.966	20.375	23.909	51.753	60.729
-53.625	19.500	-136.208	49.530	22.375	23.936	56.833	60.797
-51.625	19.716	-131.128	50.079	24.375	23.958	61.913	60.853
-49.625	19.926	-126.048	50.612	26.375	23.975	66.993	60.897
-47.625	20.130	-120.968	51.130	28.375	23.987	72.073	60.927
-45.625	20.328	-115.888	51.633	30.375	23.996	77.153	60.950
-43.625	20.520	-110.808	52.121	32.375	23.998	82.233	60.955
-41.625	20.706	-105.728	52.593	34.375	23.999	87.313	60.957
-39.625	20.887	-100.648	53.053	35.375	24.000	89.853	60.960
-37.625	21.061	-95.568	53.495	73.375	24.000	186.373	60.960
-35.625	21.230	-90.488	53.924	98.656	28.000	250.586	71.120
-33.625	21.394	-85.408	54.341	185.375	28.000	470.853	71.120

TABLE IV.- CONTOURED-NOZZLE WALL COORDINATES FOR TEST SECTION 2

(a) Lower block

x_2,in.	z_2,in.	x_2,cm	z_2,cm	x_2,in.	z_2,in.	x_2,cm	z_2,cm
-541.545	-102.000	-1375.524	-259.080	-434.004	-25.298	-1102.370	-64.257
-502.489	-44.914	-1276.322	-114.082	-428.775	-24.971	-1089.089	-63.426
-501.545	-43.645	-1273.924	-110.858	-423.547	-24.710	-1075.809	-62.763
-499.545	-41.531	-1268.844	-105.489	-418.319	-24.505	-1062.530	-62.243
-497.545	-39.931	-1263.764	-101.425	-413.091	-24.353	-1049.251	-61.857
-495.545	-38.613	-1258.684	-98.077	-407.862	-24.245	-1035.969	-61.582
-493.545	-37.505	-1253.604	-95.263	-402.634	-24.178	-1022.690	-61.412
-491.545	-36.560	-1248.524	-92.862	-397.406	-24.151	-1009.411	-61.344
-489.545	-35.744	-1243.444	-90.790	-392.177	-24.150	-996.130	-61.341
-487.545	-35.034	-1238.364	-88.986	-386.949	-24.162	-982.850	-61.371
-485.545	-34.408	-1233.284	-87.396	-381.721	-24.178	-969.571	-61.412
-483.545	-33.854	-1228.204	-85.989	-376.493	-24.194	-956.292	-61.453
-481.545	-33.357	-1223.124	-84.727	-371.264	-24.211	-943.011	-61.496
-479.545	-32.901	-1218.044	-83.569	-366.036	-24.229	-929.731	-61.542
-477.265	-32.409	-1212.253	-82.319	-360.808	-24.248	-916.452	-61.590
-460.145	-28.849	-1168.768	-73.276	-355.580	-24.268	-903.173	-61.641
-454.917	-27.814	-1155.489	-70.648	-324.210	-24.391	-823.493	-61.953
-449.688	-26.951	-1142.208	-68.456	-308.525	-24.459	-783.654	-62.126
-444.460	-26.260	-1128.928	-66.700	95.980	-26.251	243.789	-66.678
-439.232	-25.721	-1115.649	-65.331				

TABLE IV.- Concluded

(b) Upper block

x_2,in.	z_2,in.	x_2,cm	z_2,cm	x_2,in.	z_2,in.	x_2,cm	z_2,cm
-550.125	3.000	-1397.318	7.620	-404.614	-14.531	-1027.720	-36.909
-502.895	-28.109	-1277.353	-71.397	-399.386	-13.407	-1014.440	-34.054
-502.125	-28.587	-1275.398	-72.611	-394.157	-12.283	-1001.159	-31.199
-500.125	-29.587	-1270.318	-75.151	-388.929	-11.158	-987.880	-28.341
-498.125	-30.299	-1265.238	-76.959	-383.701	-10.033	-974.601	-25.484
-496.125	-30.799	-1260.158	-78.229	-378.473	-8.908	-961.321	-22.626
-494.125	-31.129	-1255.078	-79.068	-373.244	-7.782	-948.040	-19.766
-492.125	-31.325	-1249.998	-79.566	-368.016	-6.655	-934.761	-16.904
-490.125	-31.409	-1244.918	-79.779	-362.788	-5.530	-921.482	-14.046
-489.413	-31.417	-1243.109	-79.799	-357.560	-4.420	-908.202	-11.227
-488.125	-31.395	-1239.838	-79.743	-326.190	1.583	-828.523	4.021
-486.125	-31.298	-1234.758	-79.497	-294.820	6.596	-748.843	16.754
-484.125	-31.124	-1229.678	-79.055	-279.136	8.816	-709.005	22.393
-482.125	-30.880	-1224.598	-78.435	-247.766	12.567	-629.326	31.920
-480.125	-30.578	-1219.518	-77.668	-232.081	14.213	-589.486	36.101
-478.125	-30.230	-1214.438	-76.784	-200.711	17.166	-509.806	43.602
-476.125	-29.843	-1209.358	-75.801	-169.342	19.654	-430.129	49.921
-473.865	-29.377	-1203.617	-74.618	-137.972	21.615	-350.449	54.902
-462.125	-26.862	-1173.798	-68.229	-122.287	22.394	-310.609	56.881
-456.897	-25.742	-1160.518	-65.385	-90.918	23.694	-230.932	60.183
-451.668	-24.623	-1147.237	-62.542	-75.233	24.225	-191.092	61.532
-446.440	-23.503	-1133.958	-59.698	-43.863	25.063	-111.412	63.660
-441.212	-22.383	-1120.678	-56.853	-12.494	25.624	-31.735	65.085
-435.984	-21.262	-1107.399	-54.005	18.876	25.901	47.945	65.789
-430.755	-20.142	-1094.118	-51.161	34.561	25.962	87.785	65.943
-425.527	-19.020	-1080.839	-48.311	50.246	26.015	127.625	66.078
-420.299	-17.899	-1067.559	-45.463	83.250	26.121	211.455	66.347
-415.071	-16.777	-1054.280	-42.614	185.250	28.000	470.535	71.120
-409.842	-15.654	-1040.999	-39.761				

TABLE V.- VARIATION OF MACH NUMBER WITH

POSITION OF LOWER NOZZLE BLOCK

(a) Test section 1

Mach number	Block position
1.469	230
1.50	253
1.55	292
1.60	333
1.65	372
1.70	414
1.75	456
1.769	472
1.80	498
1.85	539
1.90	580
1.95	620
2.00	660
2.05	698
2.10	735
2.15	771
2.160	777
2.20	806
2.25	840
2.30	872
2.35	903
2.354	907
2.40	933
2.45	962
2.50	990
2.540	1011
2.55	1016
2.60	1041
2.65	1064
2.70	1087
2.75	1108
2.80	1128
2.85	1148
2.869	1155

TABLE V.- Continued

(b) Test section 2

M	Block position for $R \times 10^{-6}$ per ft (per m) of -						
	0.5 (1.64)	1.0 (3.28)	2.0 (6.56)	3.0 (9.84)	4.0 (13.12)	5.0 (16.41)	6.0 (19.69)
2.25	12 349	12 272	12 172	12 130	12 113	12 082	12 063
2.30	12 845	12 765	12 658	12 629	12 609	12 580	12 561
2.35	13 324	13 241	13 146	13 110	13 089	13 060	13 040
2.40	13 785	13 700	13 607	13 574	13 550	13 523	13 503
2.45	14 228	14 141	14 050	14 020	13 994	13 968	13 947
2.50	14 654	14 564	14 476	14 448	14 421	14 396	14 374
2.55	15 062	14 971	14 885	14 859	14 831	14 807	14 784
2.60	15 451	15 360	15 277	15 253	15 223	15 200	15 177
2.65	15 817	15 729	15 648	15 624	15 596	15 574	15 552
2.70	16 168	16 082	16 002	15 978	15 952	15 931	15 910
2.75	16 503	16 419	16 341	16 317	16 293	16 273	16 253
2.80	16 823	16 741	16 665	16 640	16 618	16 599	16 580
2.85	17 129	17 049	16 975	16 949	16 929	16 911	16 892
2.90	17 420	17 347	17 270	17 244	17 225	17 208	17 190
2.95	17 697	17 622	17 551	17 525	17 508	17 491	17 475
3.00	17 955	17 880	17 813	17 787	17 772	17 756	17 741
3.05	18 201	18 125	18 058	18 031	18 017	18 000	17 987
3.10	18 435	18 358	18 292	18 264	18 251	18 233	18 221
3.15	18 658	18 580	18 514	18 486	18 473	18 455	18 445
3.20	18 871	18 791	18 726	18 698	18 685	18 666	18 657
3.25	19 073	18 995	18 932	18 903	18 890	18 870	18 861
3.30	19 266	19 190	19 129	19 102	19 089	19 069	19 059
3.35	19 449	19 375	19 318	19 291	19 279	19 259	19 248
3.40	19 623	19 551	19 497	19 471	19 459	19 440	19 427
3.45	19 789	19 718	19 668	19 642	19 630	19 612	19 598
3.50	19 947	19 877	19 830	19 805	19 793	19 775	19 760
3.55	20 096	20 029	19 984	19 960	19 948	19 931	19 914
3.60	20 238	20 173	20 129	20 107	20 095	20 078	20 061
3.65	20 373	20 310	20 266	20 245	20 233	20 217	20 201
3.70	20 502	20 441	20 397	20 376	20 364	20 349	20 334
3.75	20 624	20 565	20 521	20 501	20 489	20 474	20 460
3.80	20 740	20 683	20 639	20 620	20 607	20 593	20 581
3.85	20 851	20 795	20 751	20 734	20 720	20 707	20 695
3.90	20 956	20 902	20 858	20 841	20 828	20 815	20 804
3.95	21 055	21 003	20 960	20 944	20 930	20 918	20 908

TABLE V.- Concluded

(b) Concluded

M	Block position for $R \times 10^{-6}$ per ft (per m) of -						
	0.5 (1.64)	1.0 (3.28)	2.0 (6.56)	3.0 (9.84)	4.0 (13.12)	5.0 (16.41)	6.0 (19.69)
4.00	21 149	21 099	21 057	21 041	21 027	21 016	21 006
4.05	21 239	21 190	21 150	21 134	21 120	21 109	21 099
4.10	21 325	21 277	21 238	21 223	21 208	21 197	21 188
4.15	21 403	21 360	21 323	21 307	21 293	21 281	21 273
4.20	21 474	21 437	21 402	21 387	21 373	21 362	21 354
4.25	21 542	21 511	21 478	21 463	21 450	21 439	21 431
4.30	21 606	21 581	21 550	21 535	21 524	21 513	21 505
4.35	21 668	21 648	21 618	21 605	21 594	21 584	21 575
4.40	21 731	21 712	21 683	21 670	21 661	21 651	21 642
4.45	21 796	21 775	21 747	21 734	21 725	21 714	21 706
4.50	21 858	21 834	21 807	21 794	21 785	21 774	21 766
4.55	21 917	21 891	21 865	21 852	21 842	21 832	21 824
4.60	21 973	21 945	21 921	21 907	21 897	21 886	21 879

TABLE VI.- VARIATION OF SECOND-MINIMUM CONTRACTION RATIO

WITH NOZZLE BLOCK POSITION FOR TEST SECTION 2

Nozzle block position	Contraction ratio
12 600	1.186
14 350	1.214
16 500	1.248
17 100	1.255
17 650	1.261
18 100	1.292
18 600	1.306
18 950	1.311
19 300	1.321
19 700	1.325
20 050	1.332
20 400	1.339
20 500	1.346
20 750	1.423
20 950	1.431
21 370	1.439
21 700	1.449
21 950	1.582

L-72-607

Figure 1.- Photograph of the Langley Unitary Plan Wind Tunnel.

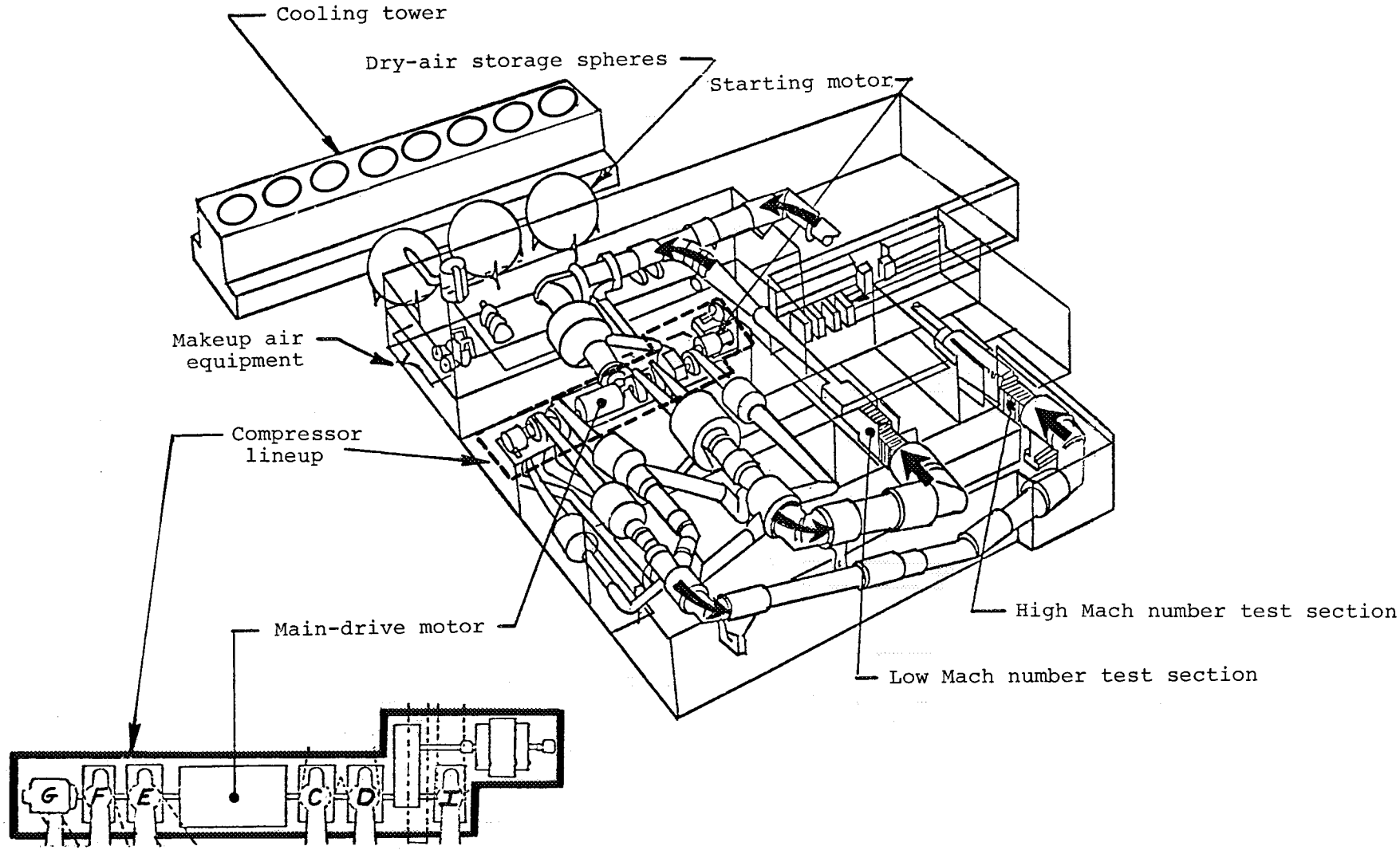

Figure 2.- Schematic drawing of the Langley Unitary Plan Wind Tunnel.

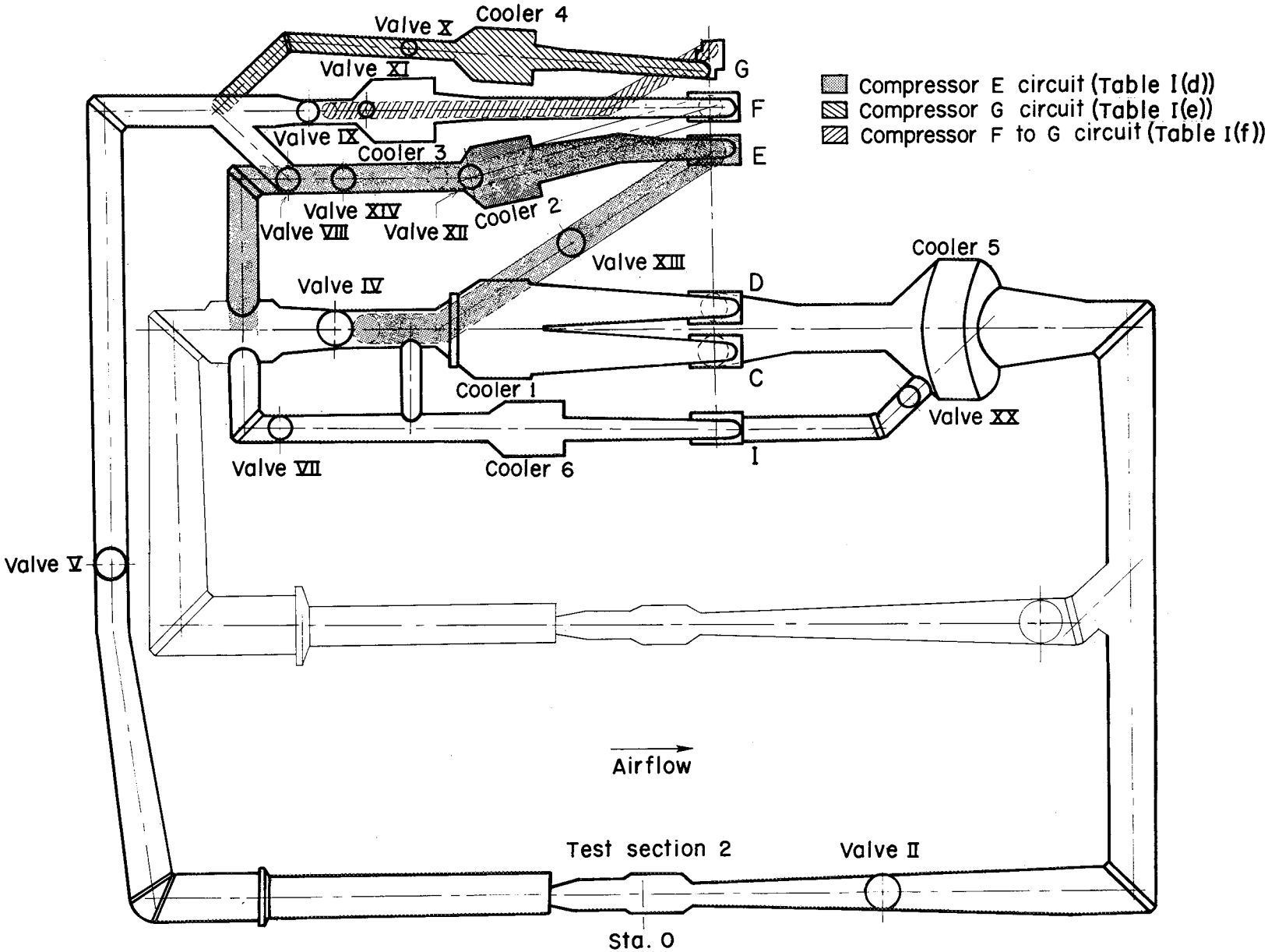

(a) High Mach number circuit. See table I(a).

Figure 3.- Arrangement of the Langley Unitary Plan Wind Tunnel.

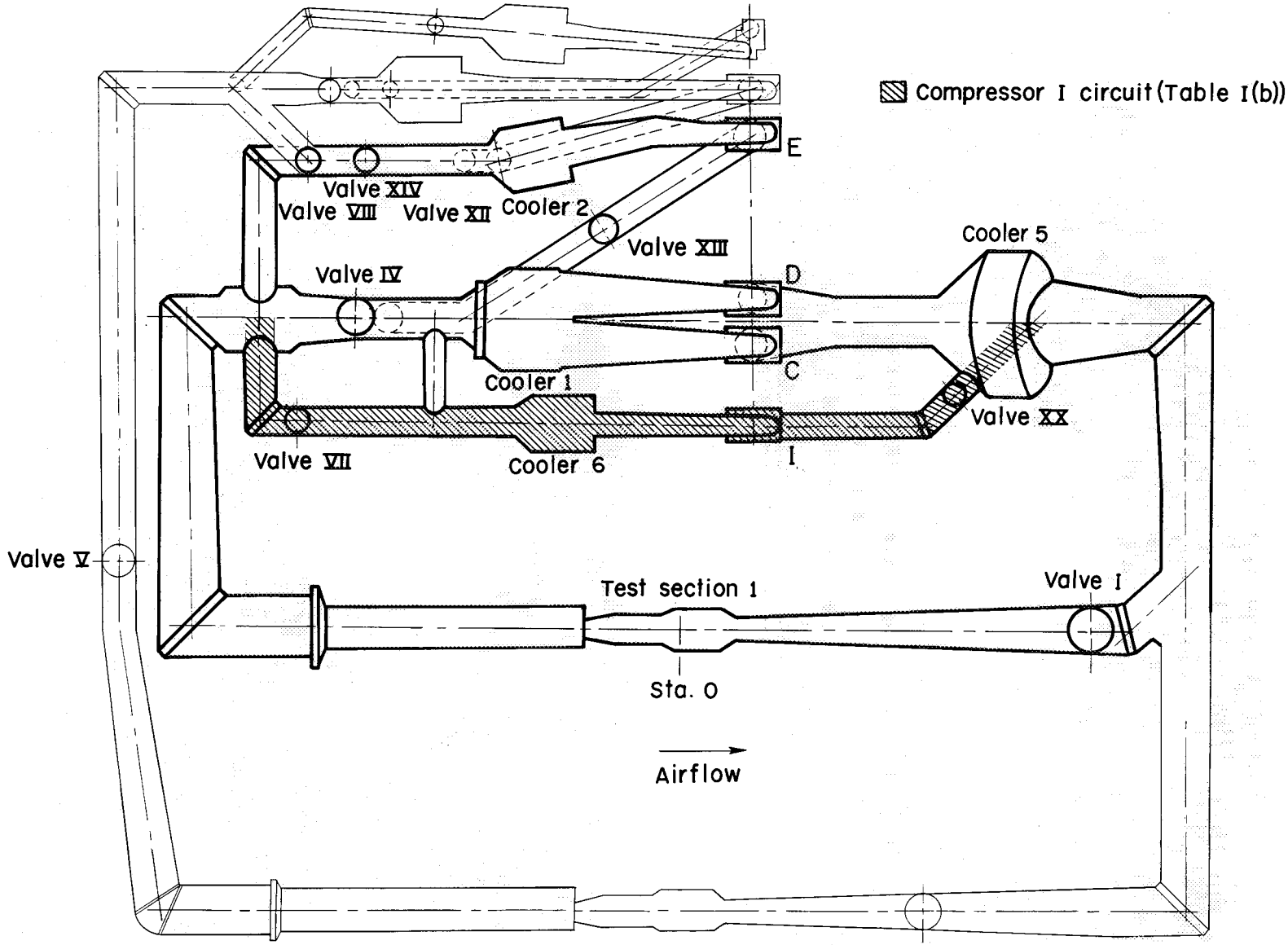

(b) Low Mach number circuit. See table II.

Figure 3.- Concluded.

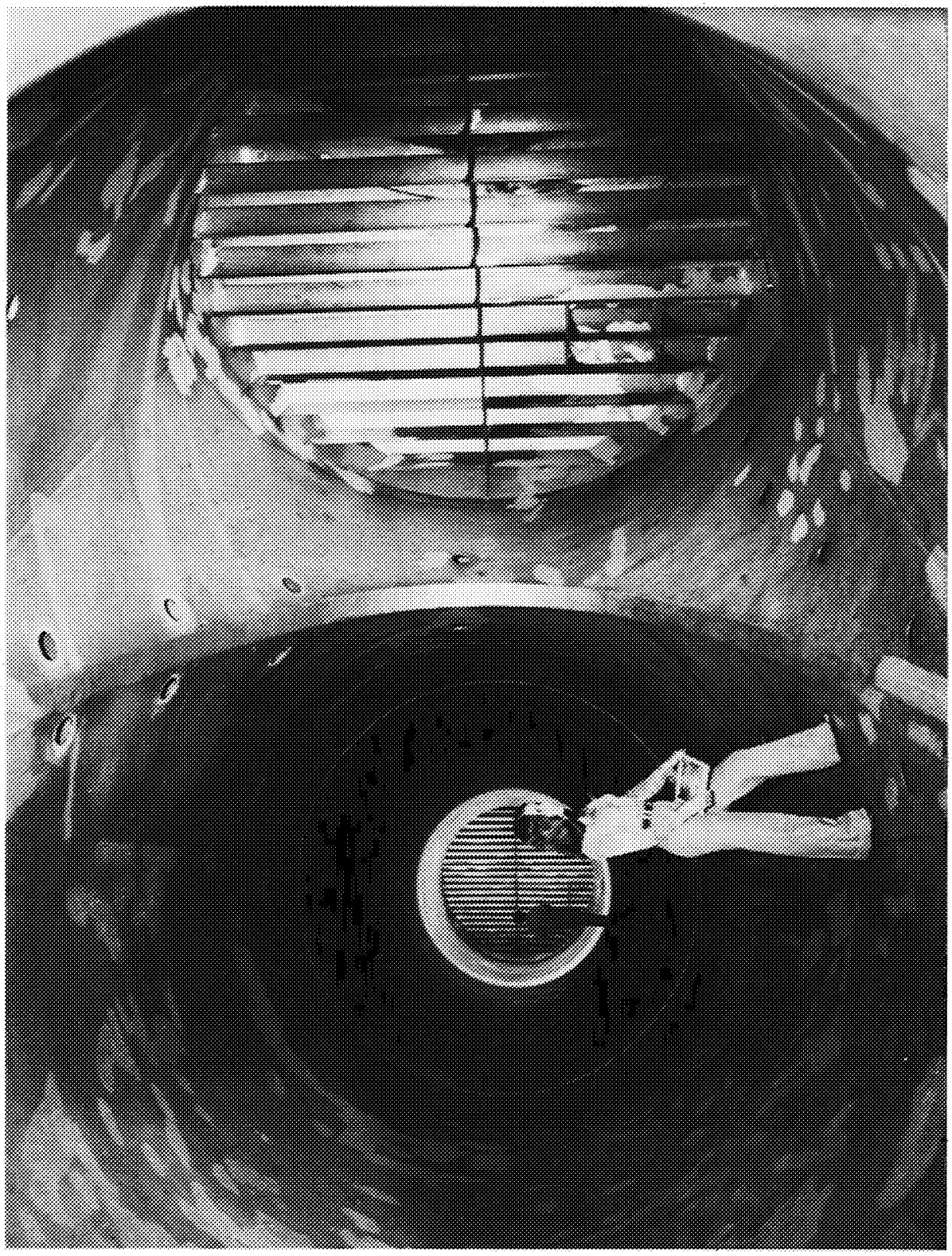

L-78-3565

Figure 4.- Photograph of tunnel duct juncture and turning vanes downstream of valve I.

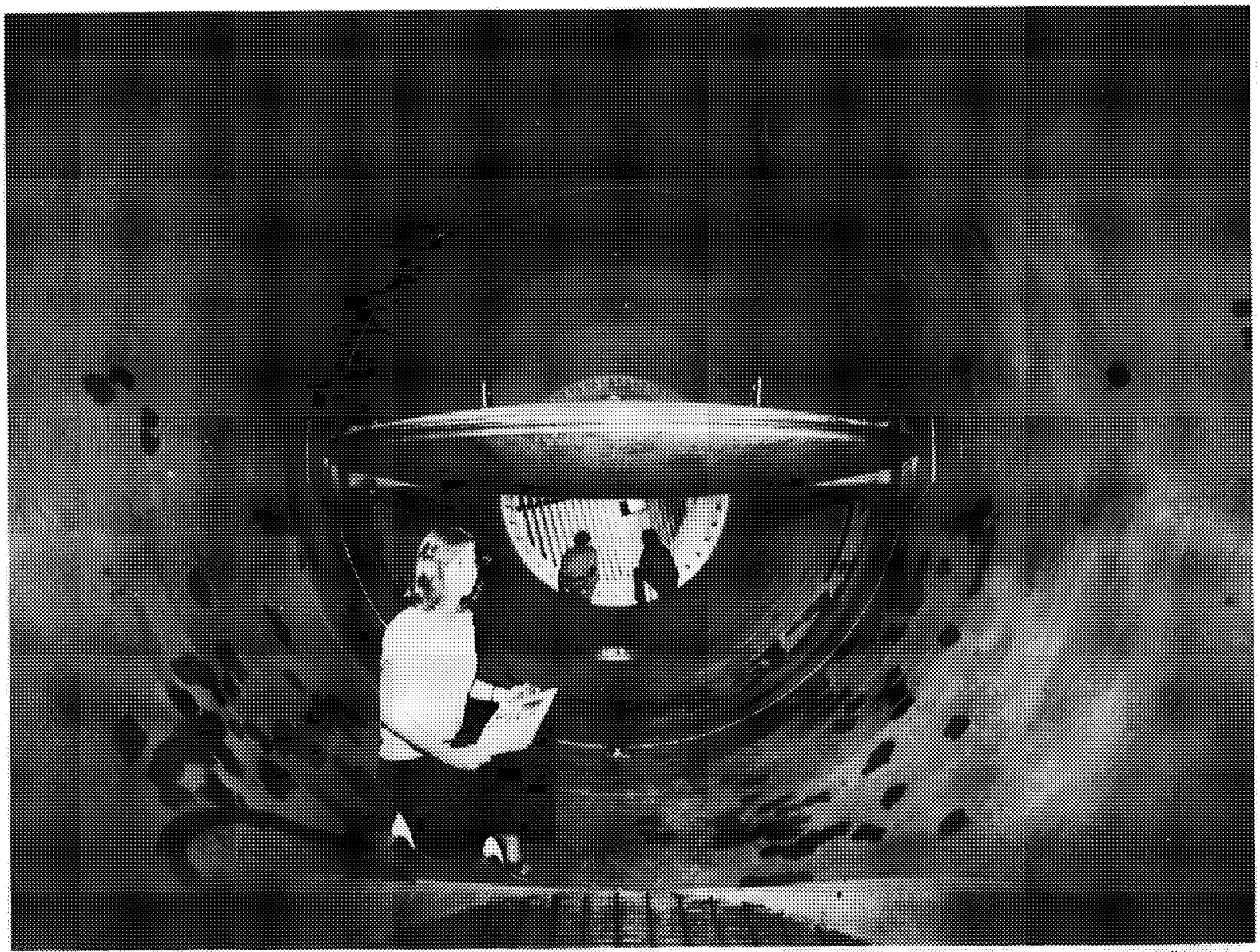

L-78-3564

Figure 5.- Photograph of typical configuration valve.

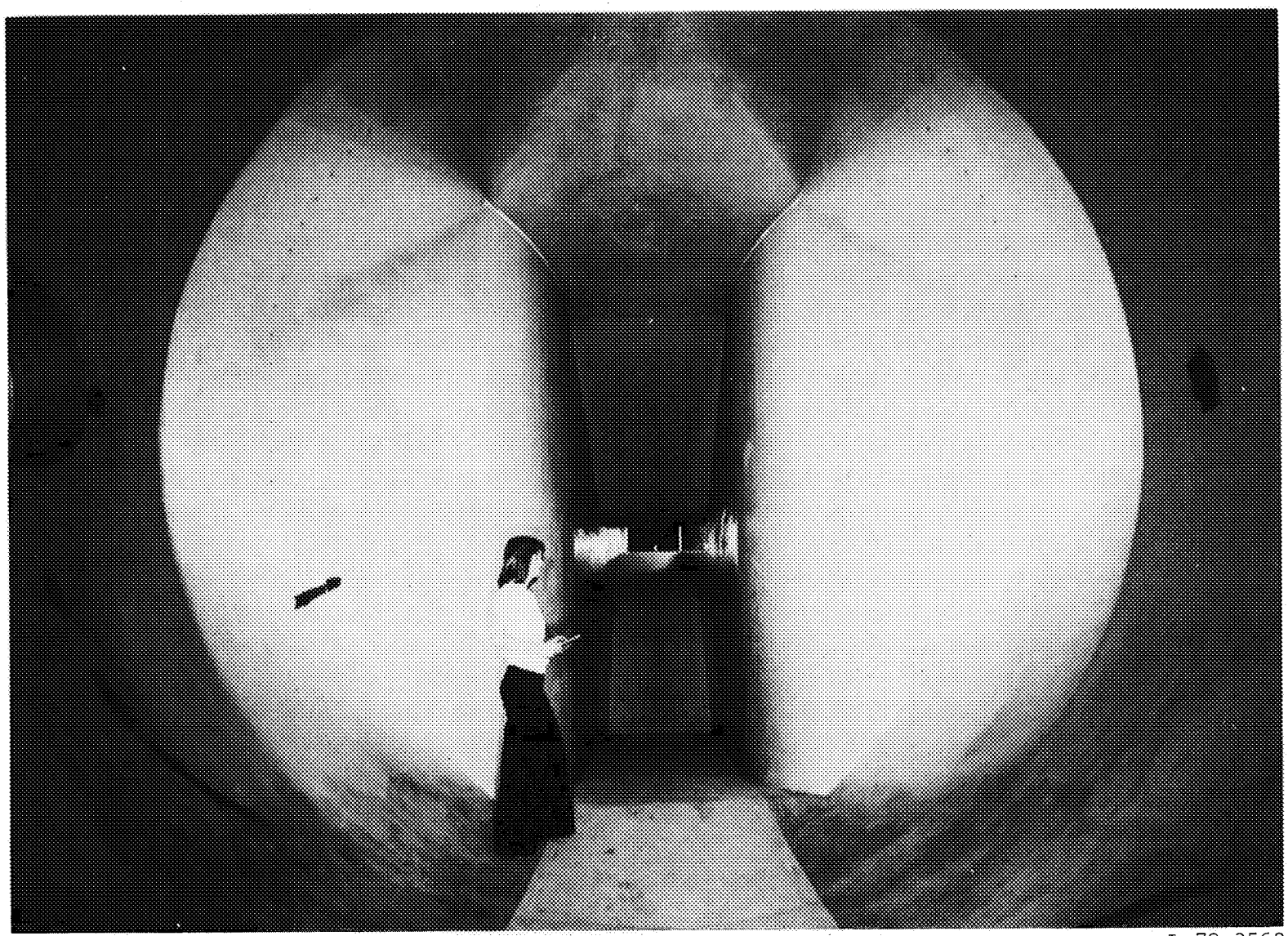

L-78-3562

Figure 6.- Photograph of settling chamber and transition to nozzle looking downstream in test section 1.

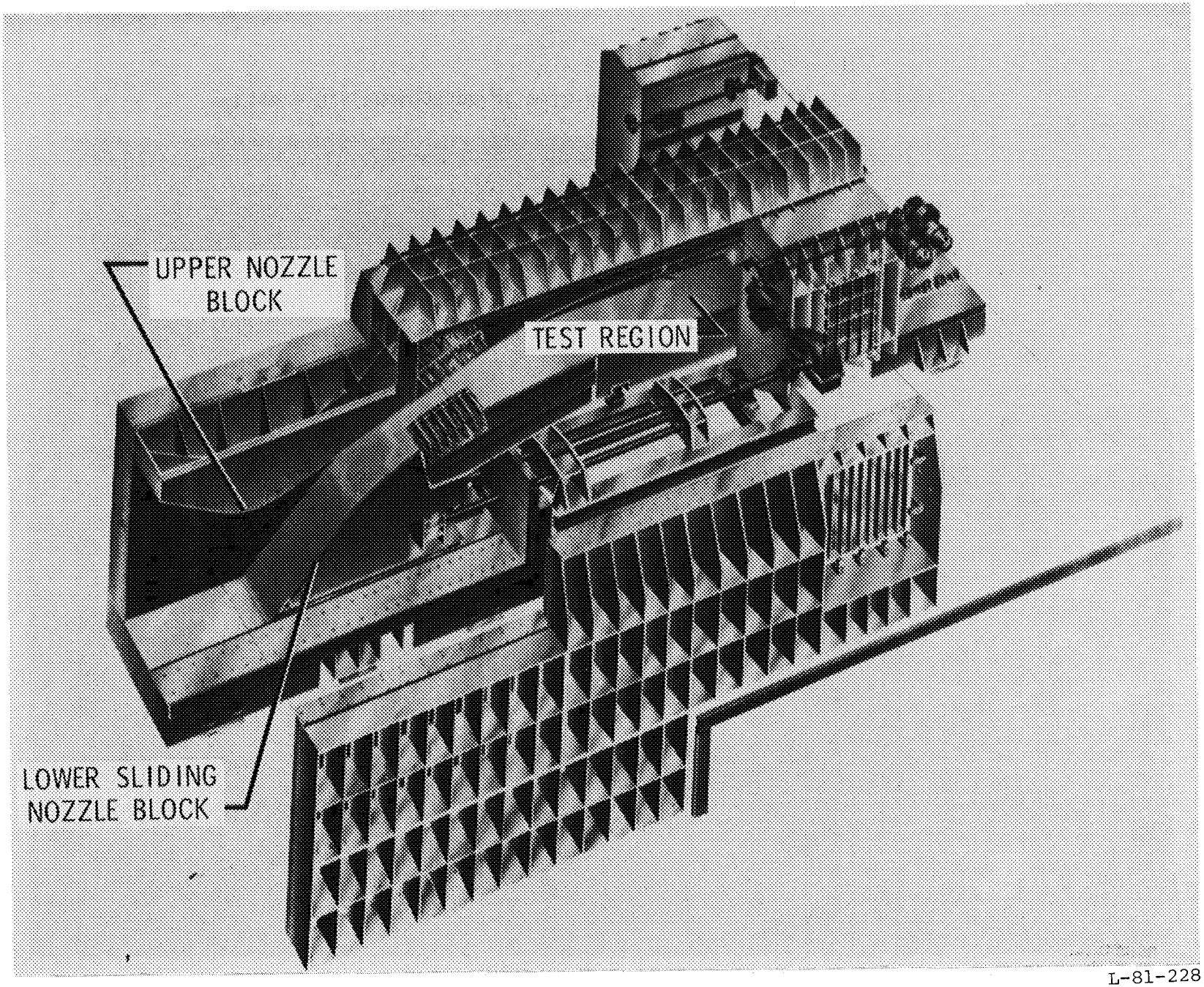

L-81-228

Figure 7.- Exploded view of test section 1, nozzle blocks, and superstructure.

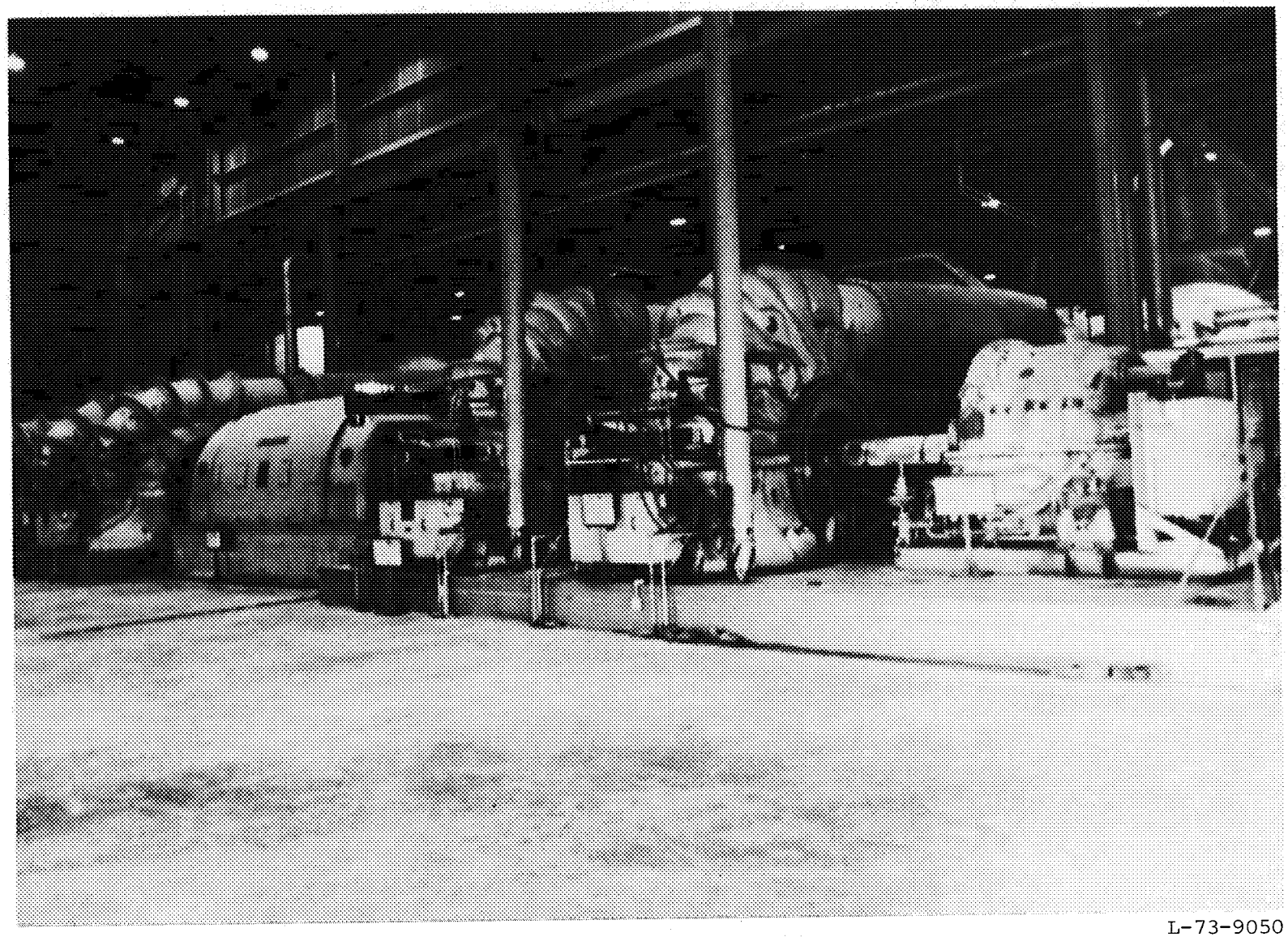

L-73-9050

Figure 8.- Photograph of main-drive motor and six compressors.

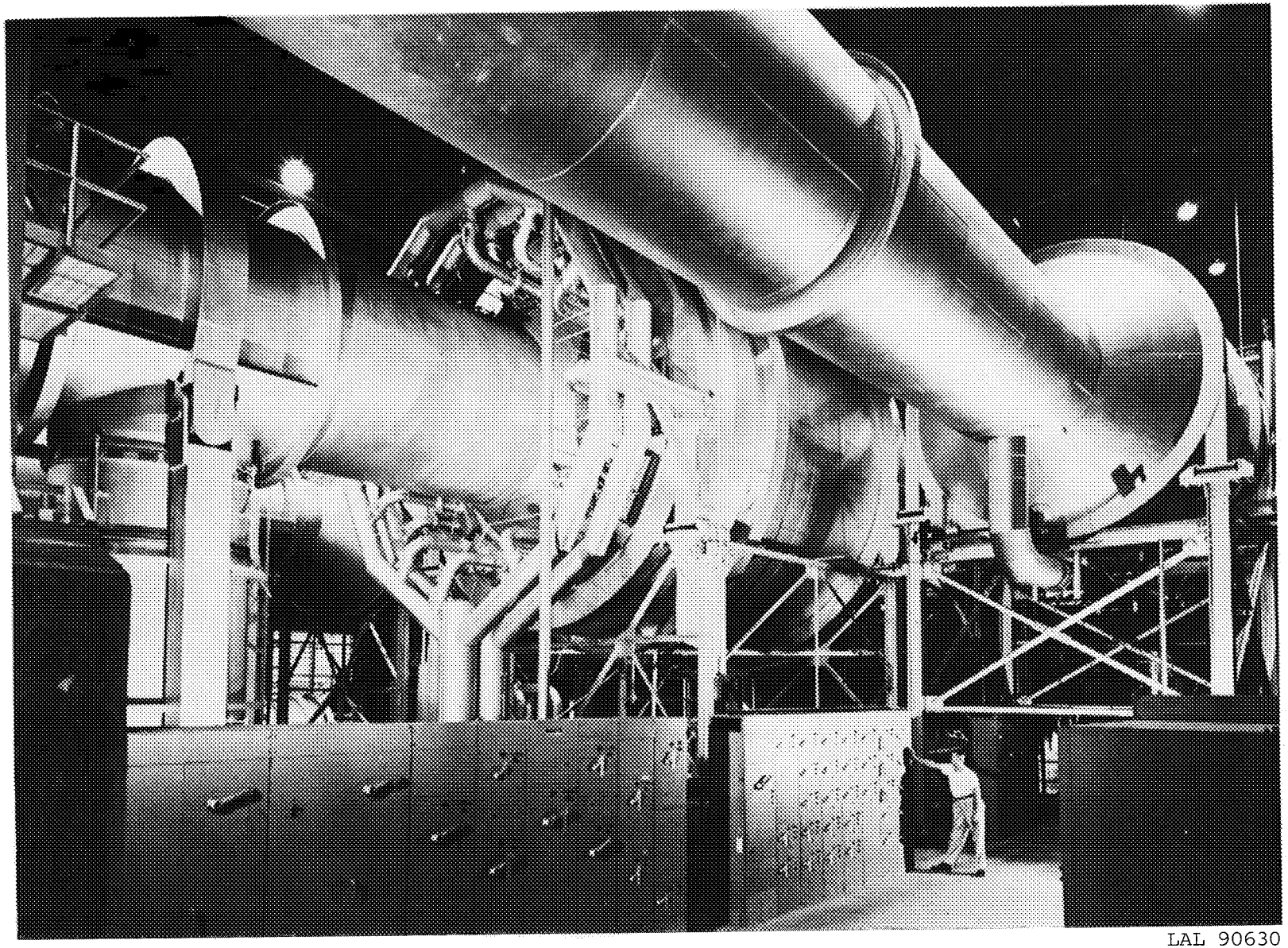

LAL 90630

Figure 9.- Photograph of heat exchangers and tunnel ducts downstream of compressors.

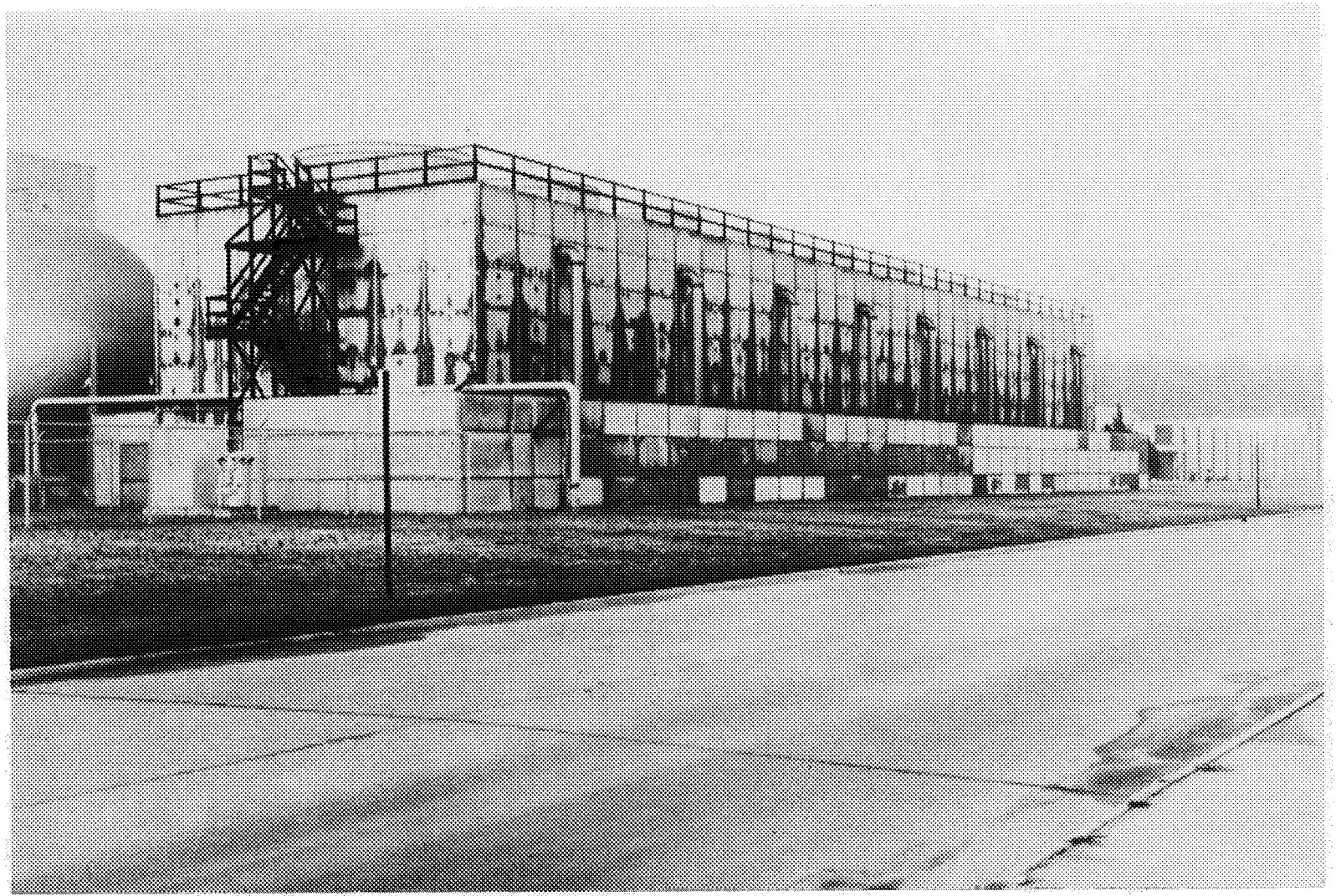

L-75-907

Figure 10.- Photograph of cooling tower.

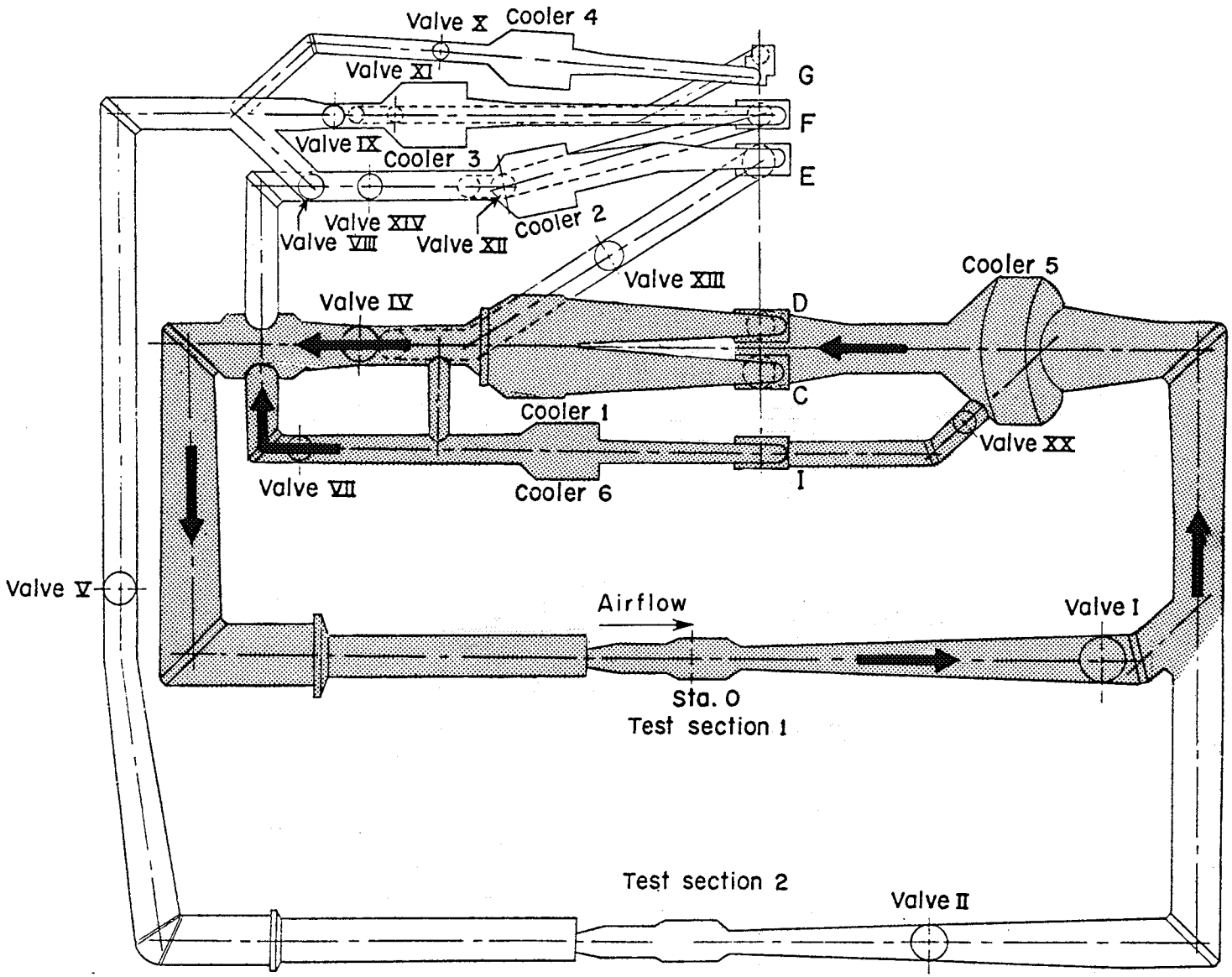

(a) Mode 1-IA. $1.46 < M < 2.16$.

Figure 11.- Tunnel-operating circuit configurations.

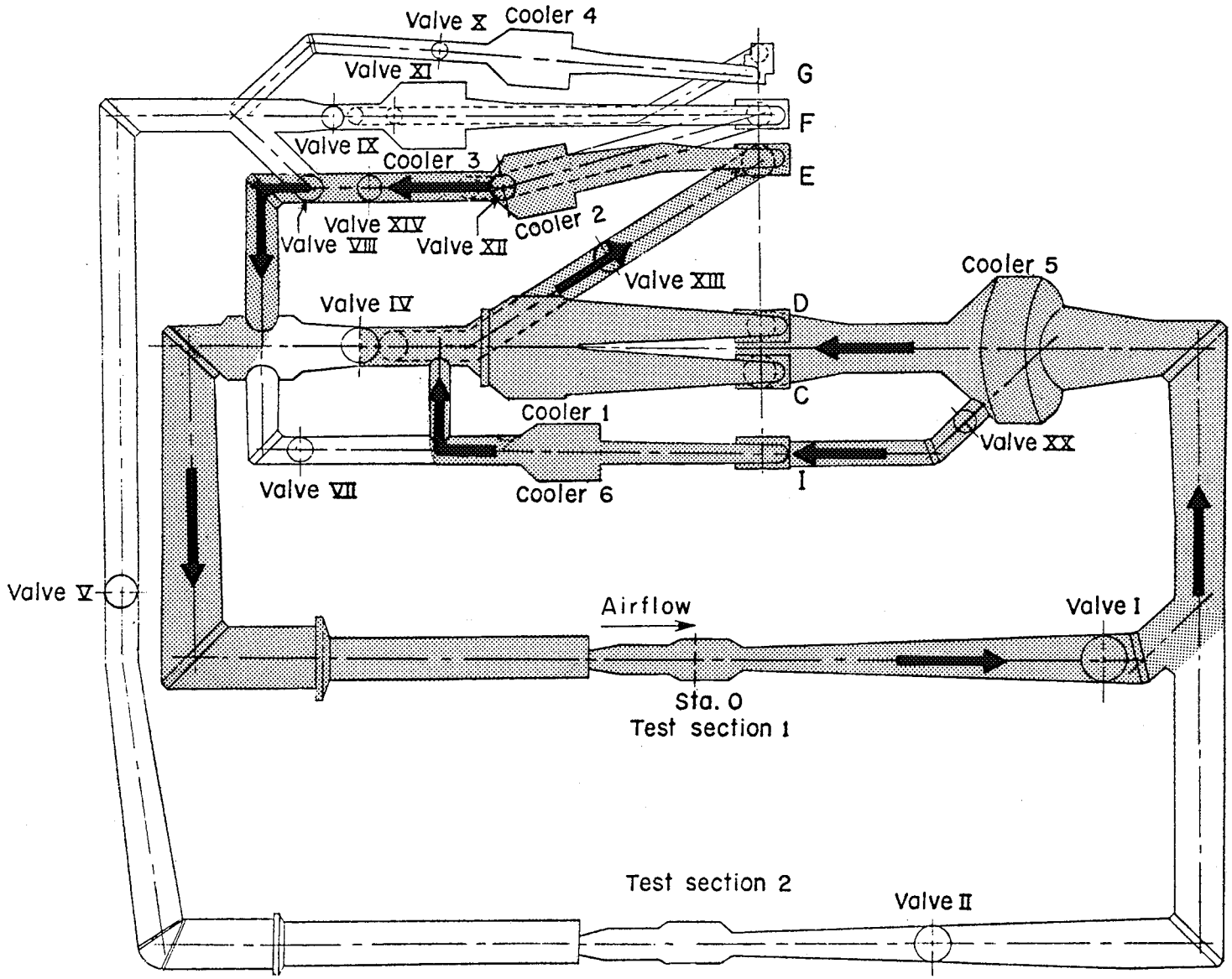

(b) Mode 1-II. $2.36 < M < 2.87$.

Figure 11.- Continued.

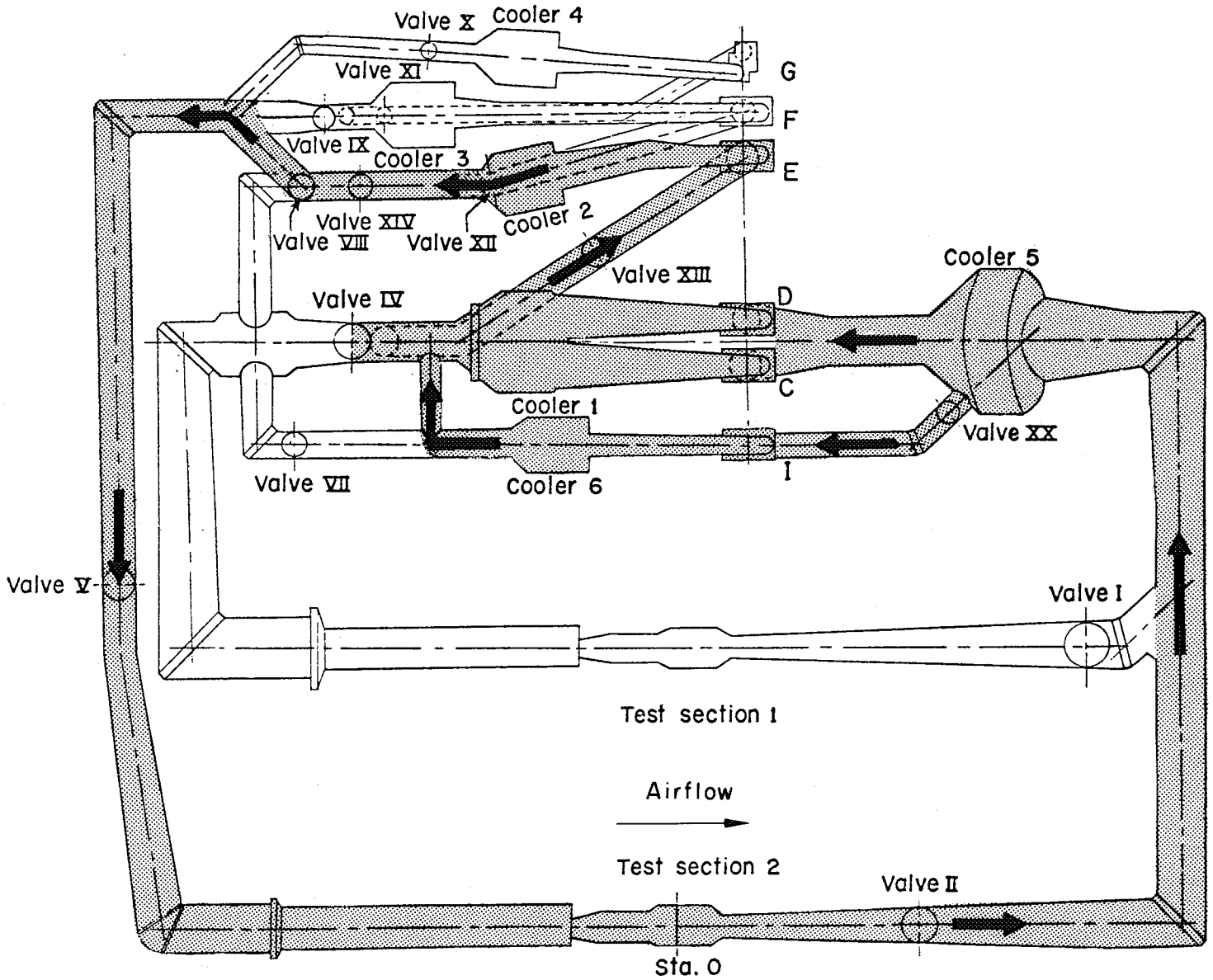

(c) Mode 2-II. $2.30 < M < 2.98$.

Figure 11.- Continued.

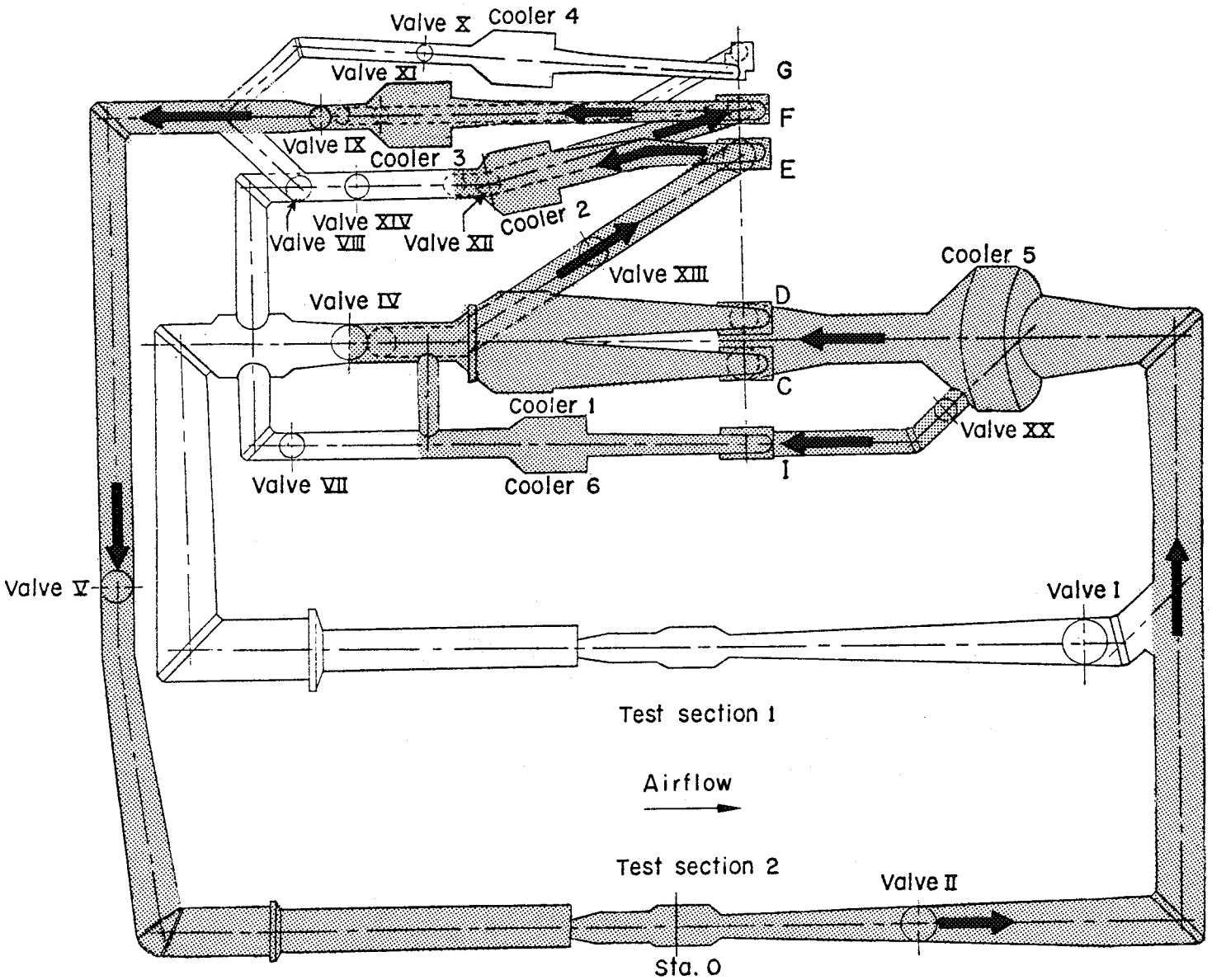

(d) Mode 2-III. $2.98 < M < 3.75$.

Figure 11.- Continued.

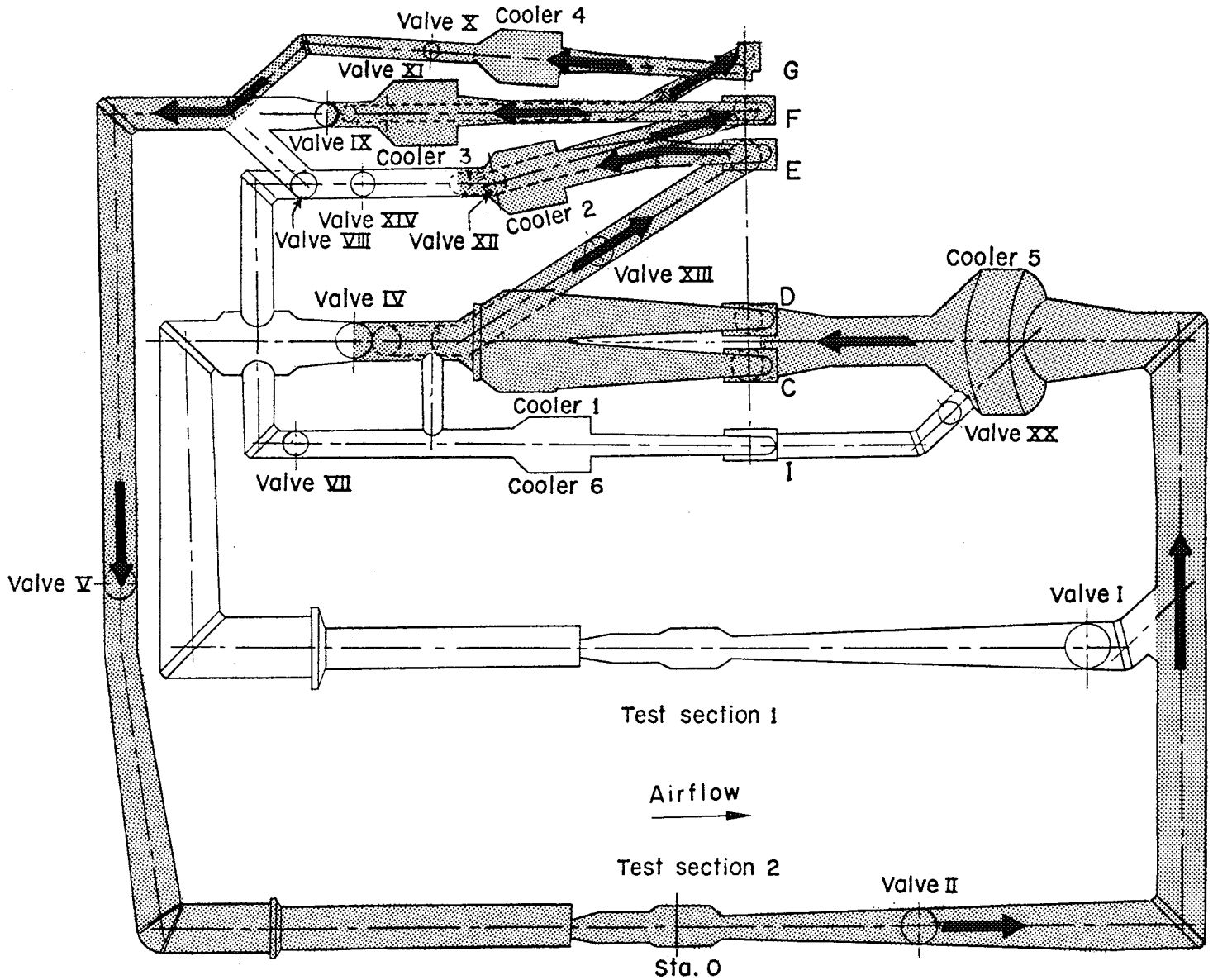

(e) Mode 2-IV. $3.84 < M < 4.63$.

Figure 11.- Concluded.

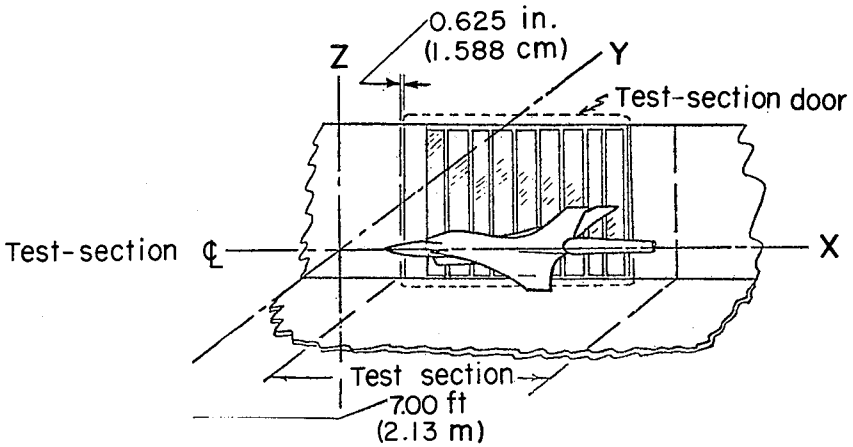

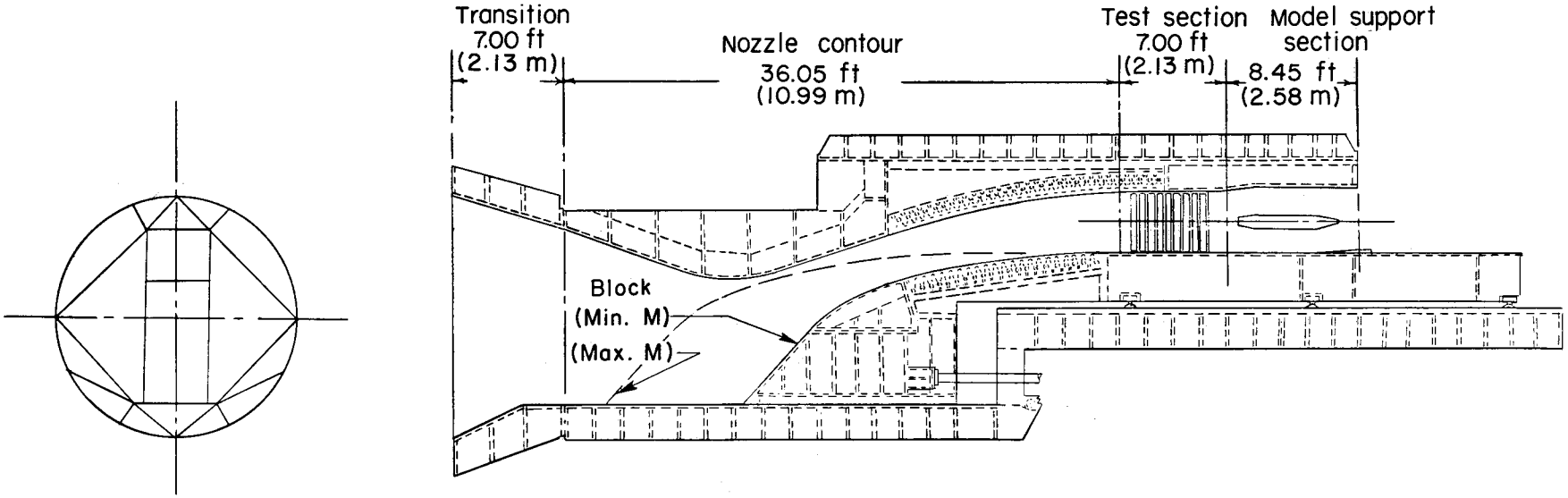

(a) Low Mach number circuit for test section 1.

Figure 12.- Test-section details and nozzle coordinate-system definition.

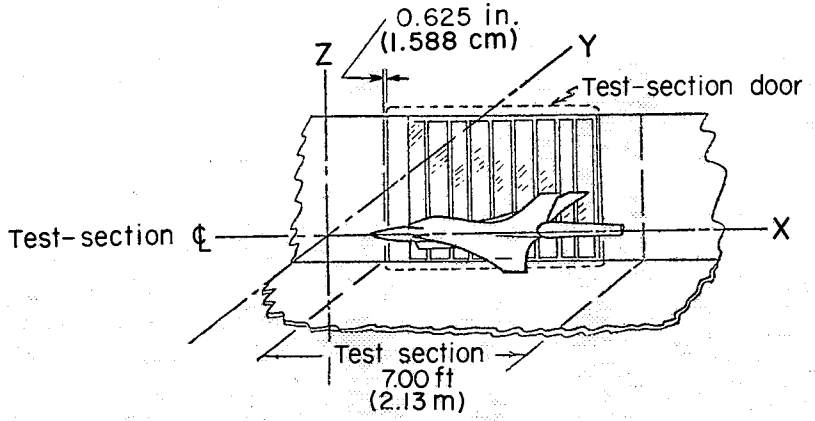

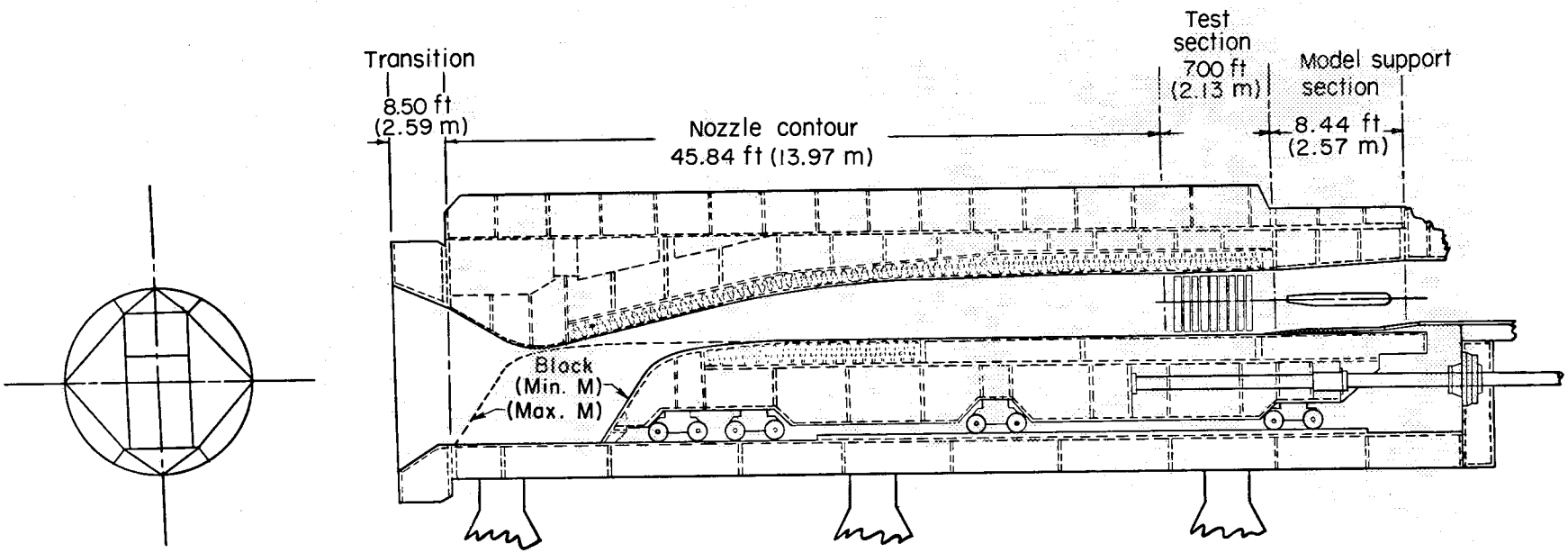

(b) High Mach number circuit for test section 2.

Figure 12.- Concluded.

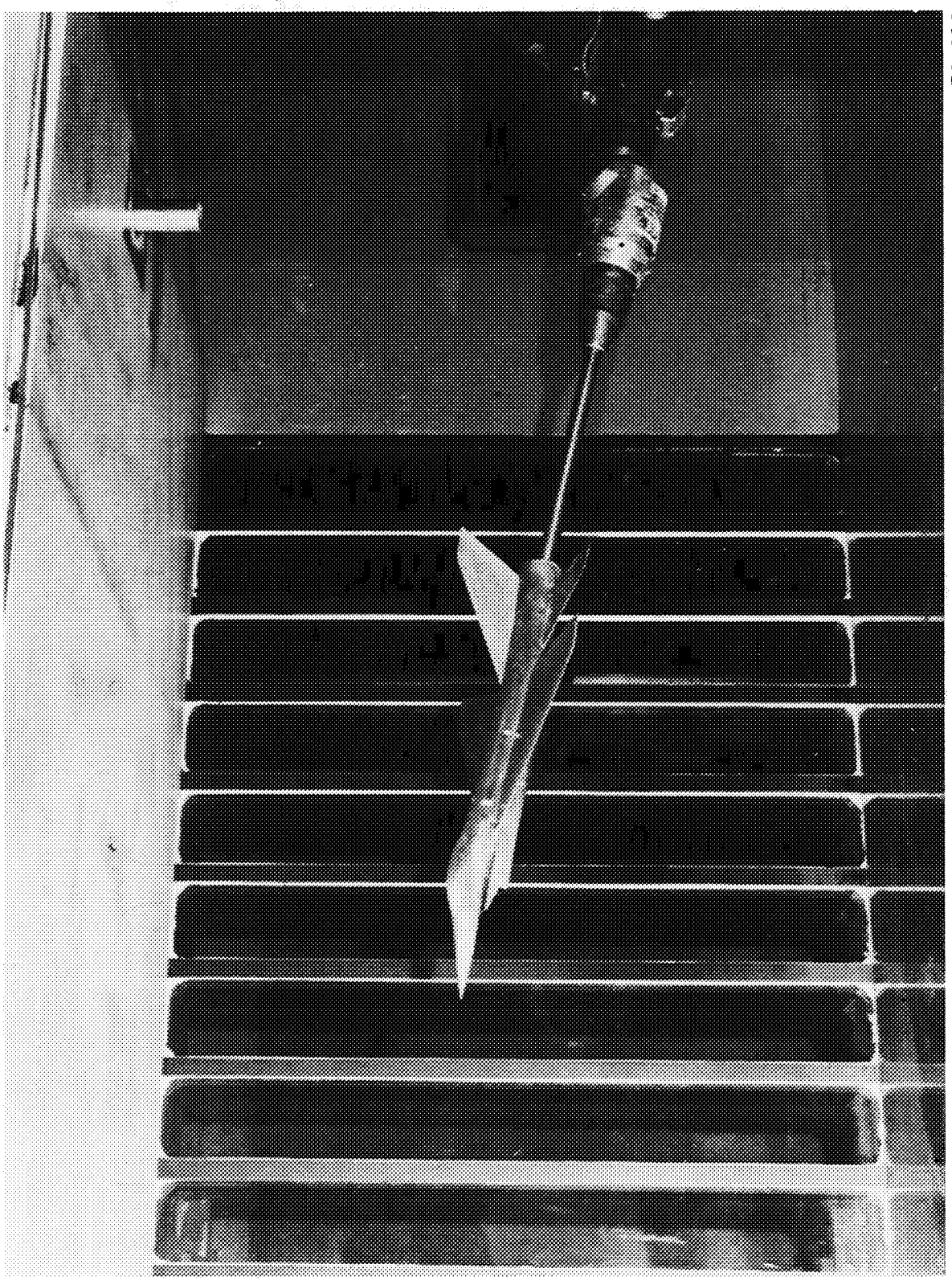

L-76-818

Figure 13.- Photograph of airplane model mounted in test section 1.

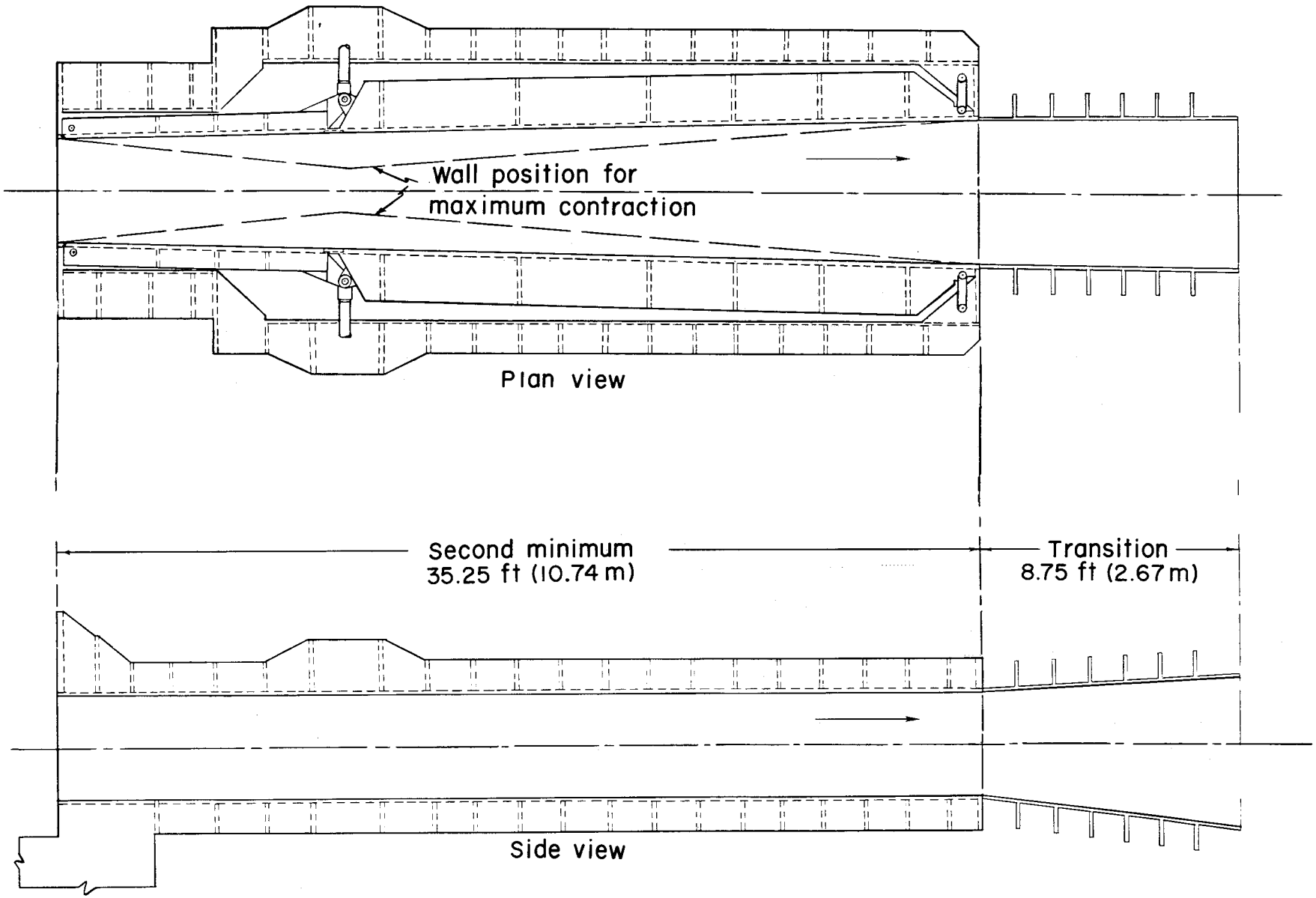

(a) Low Mach number circuit.

Figure 14.- Second-minimum details.

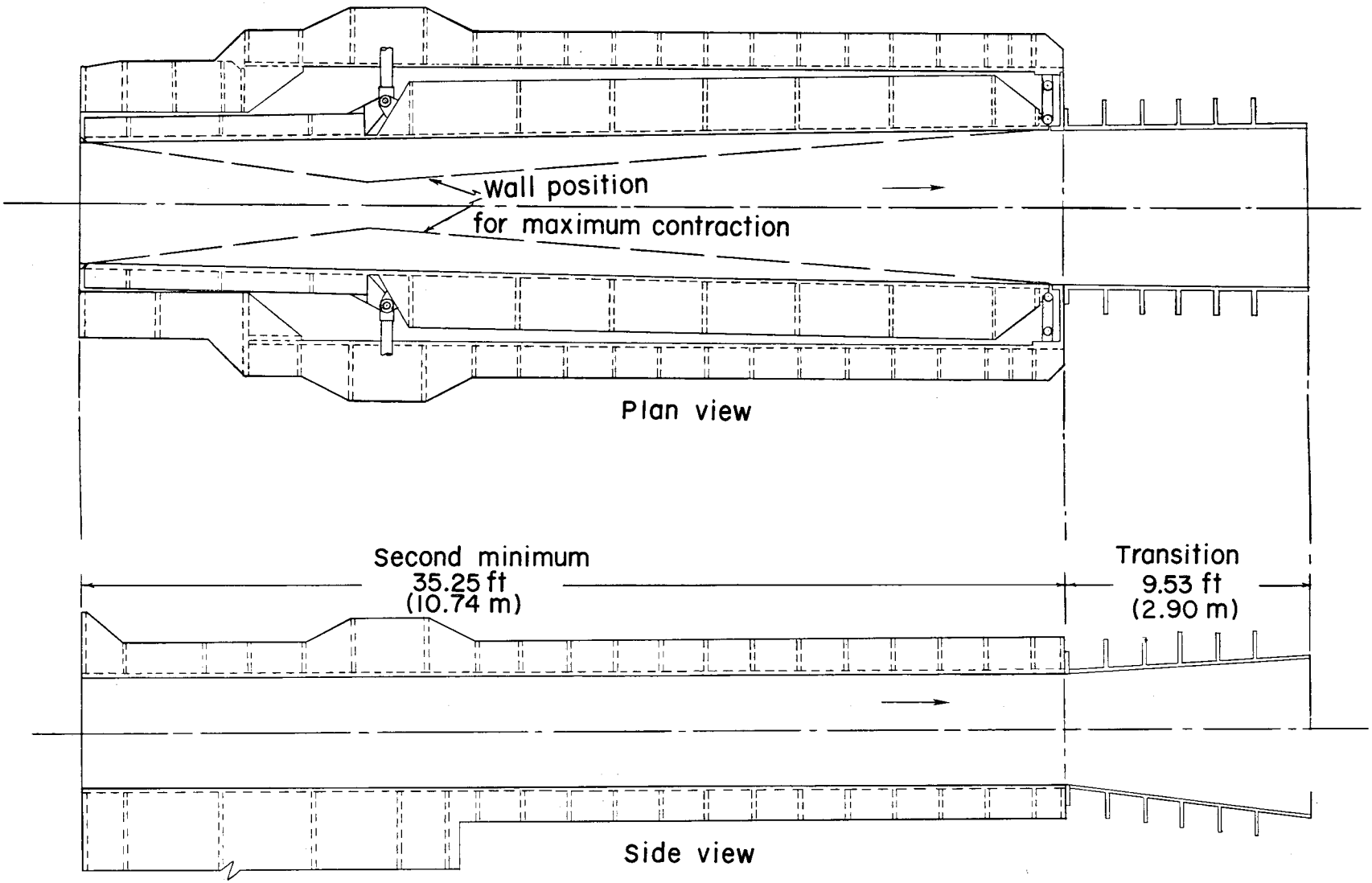

(b) High Mach number circuit.

Figure 14.- Concluded.

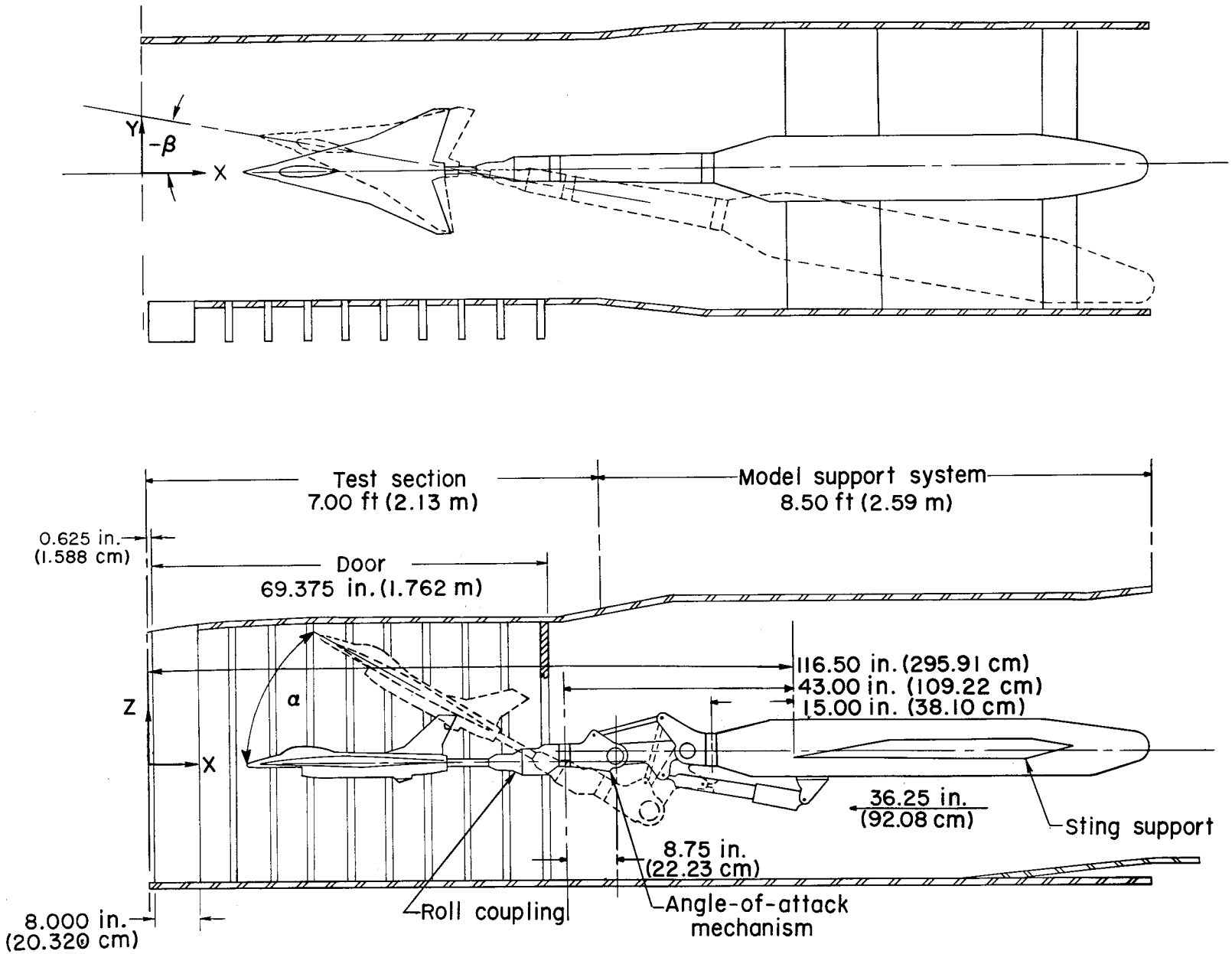

Figure 15.- Test section and model support system. Test sections 1 and 2 are similar.

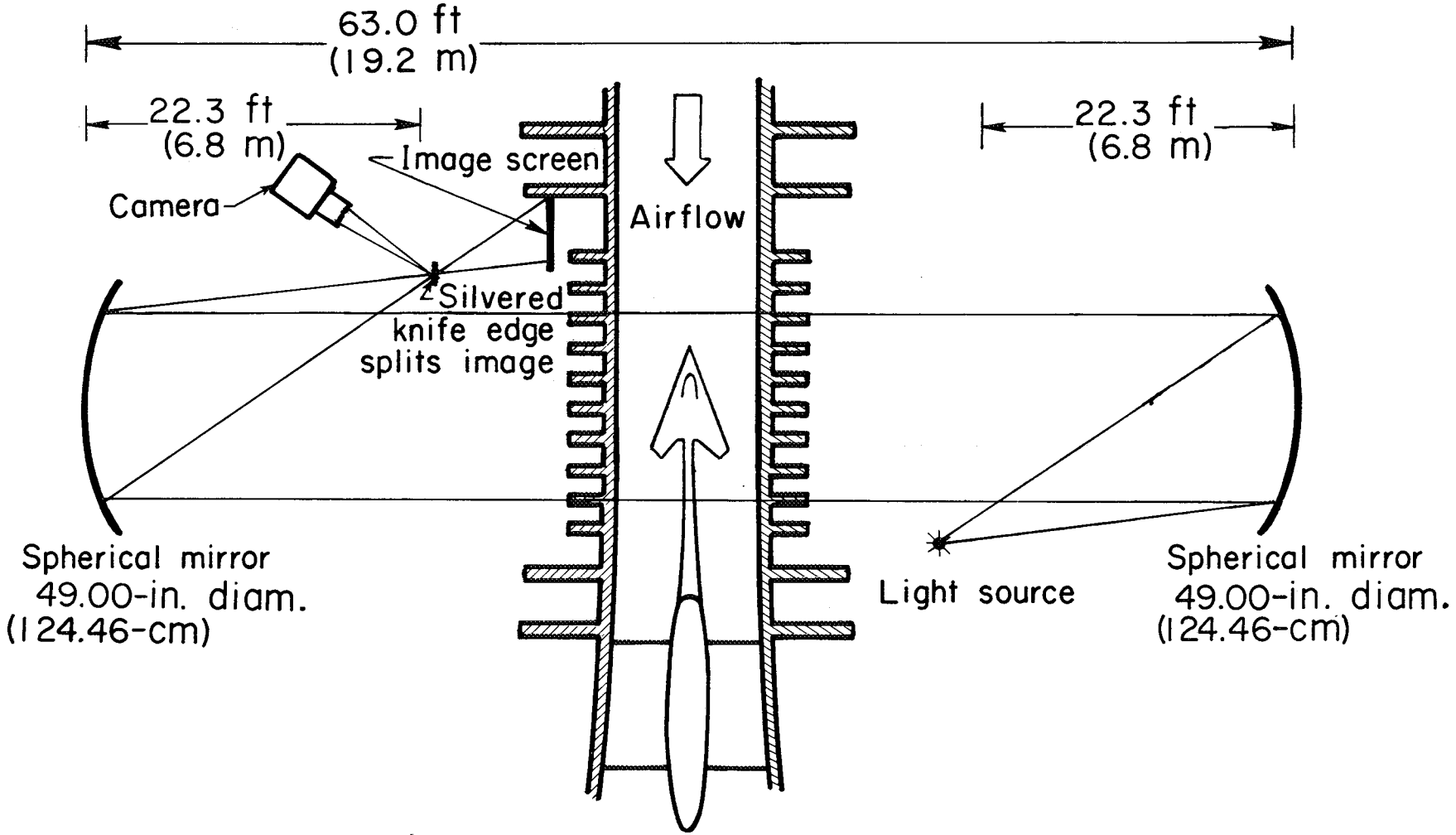

Figure 16.- Schematic drawing of schlieren system and test section.

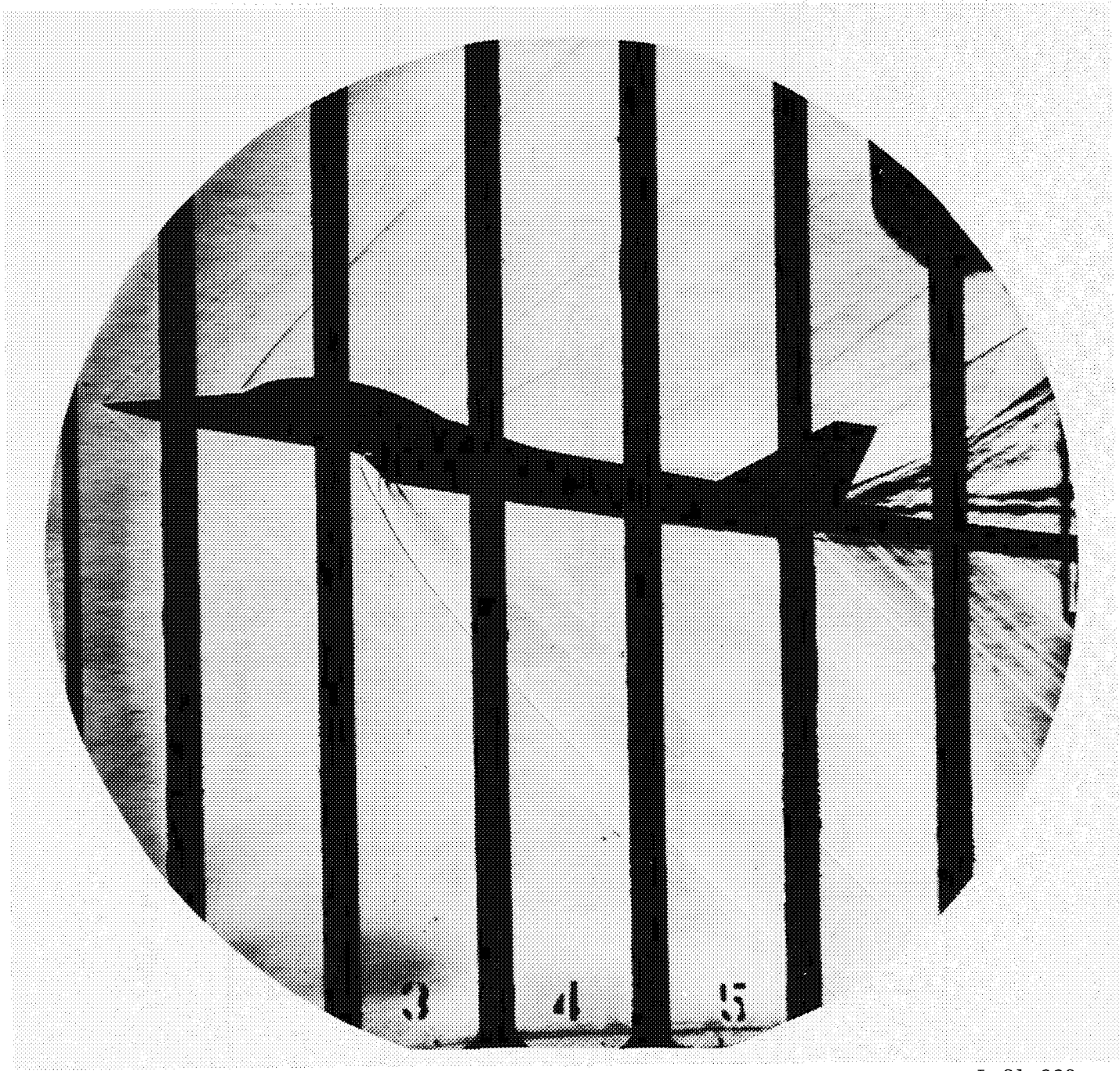

L-81-229

Figure 17.- Typical schlieren photograph of airplane model at M = 1.6.

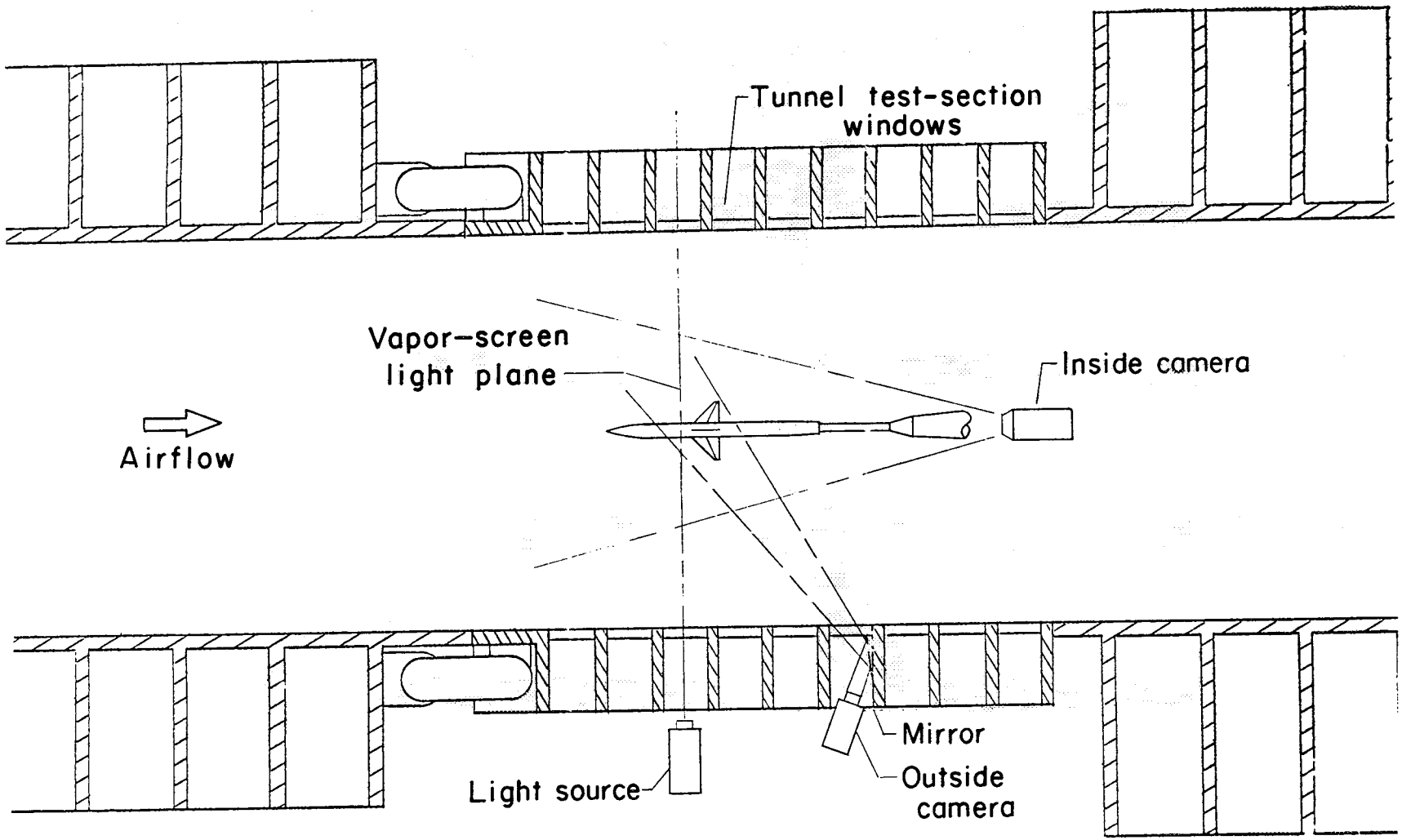

Figure 18.- Schematic drawing of vapor-screen light and camera setup.

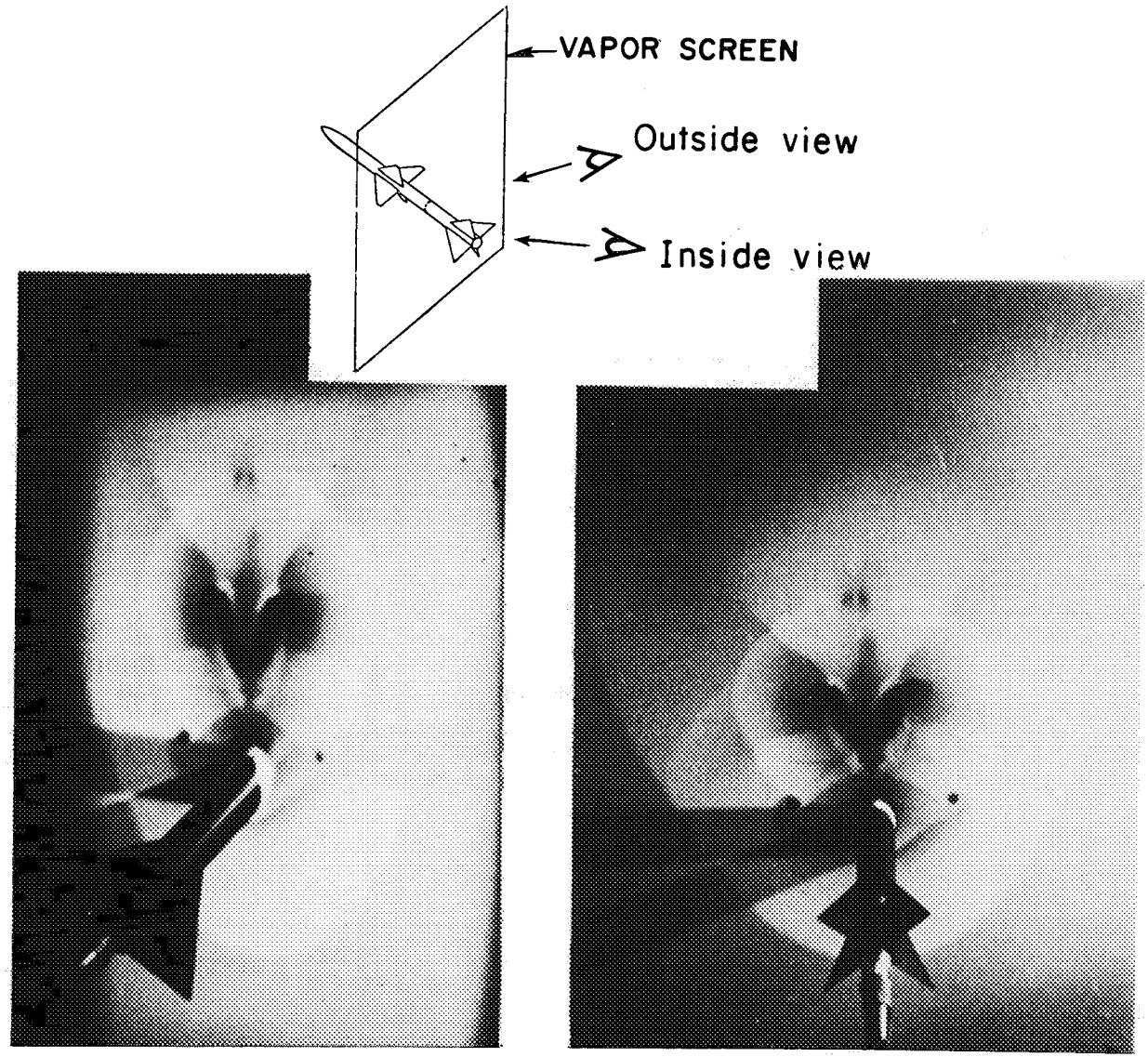

L-81-230

Figure 19.- Vapor-screen photographs of missile model in test section 2 at M = 2.36.

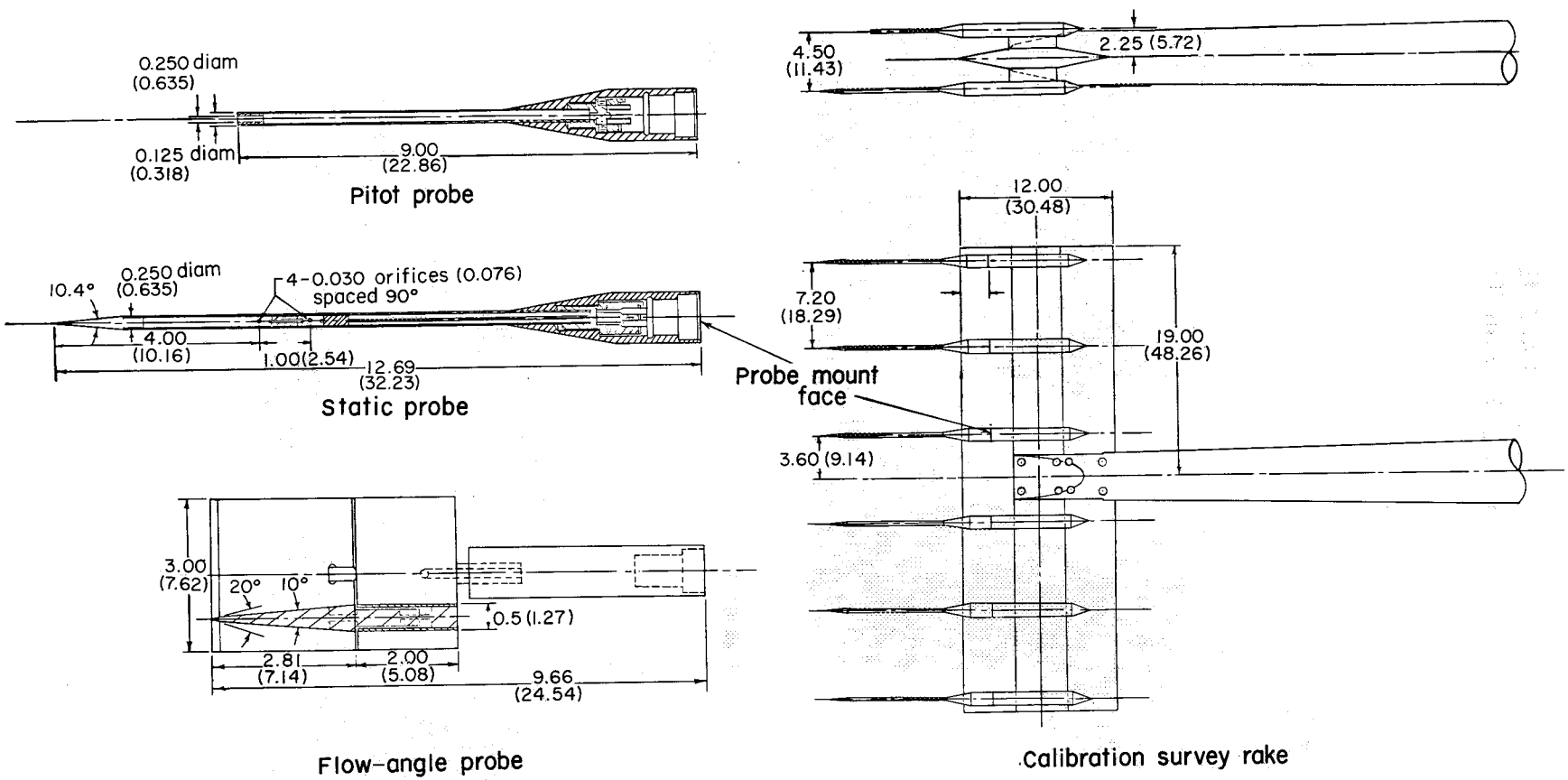

Figure 20.- Details of calibration survey rake and probes. All dimensions are in inches (centimeters) except as noted.

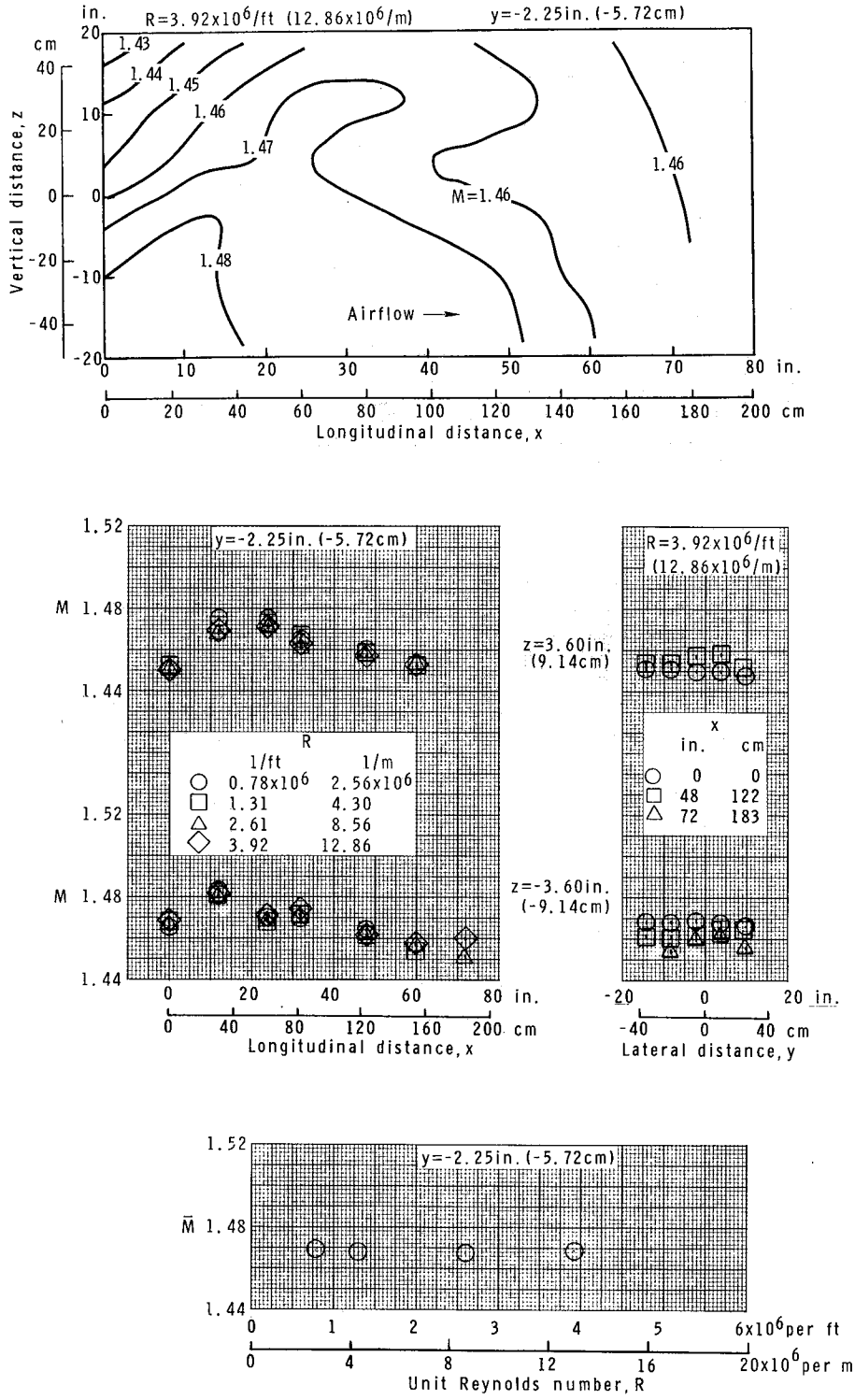

(a) M = 1.469.

Figure 21.- Mach number calibration for test section 1.

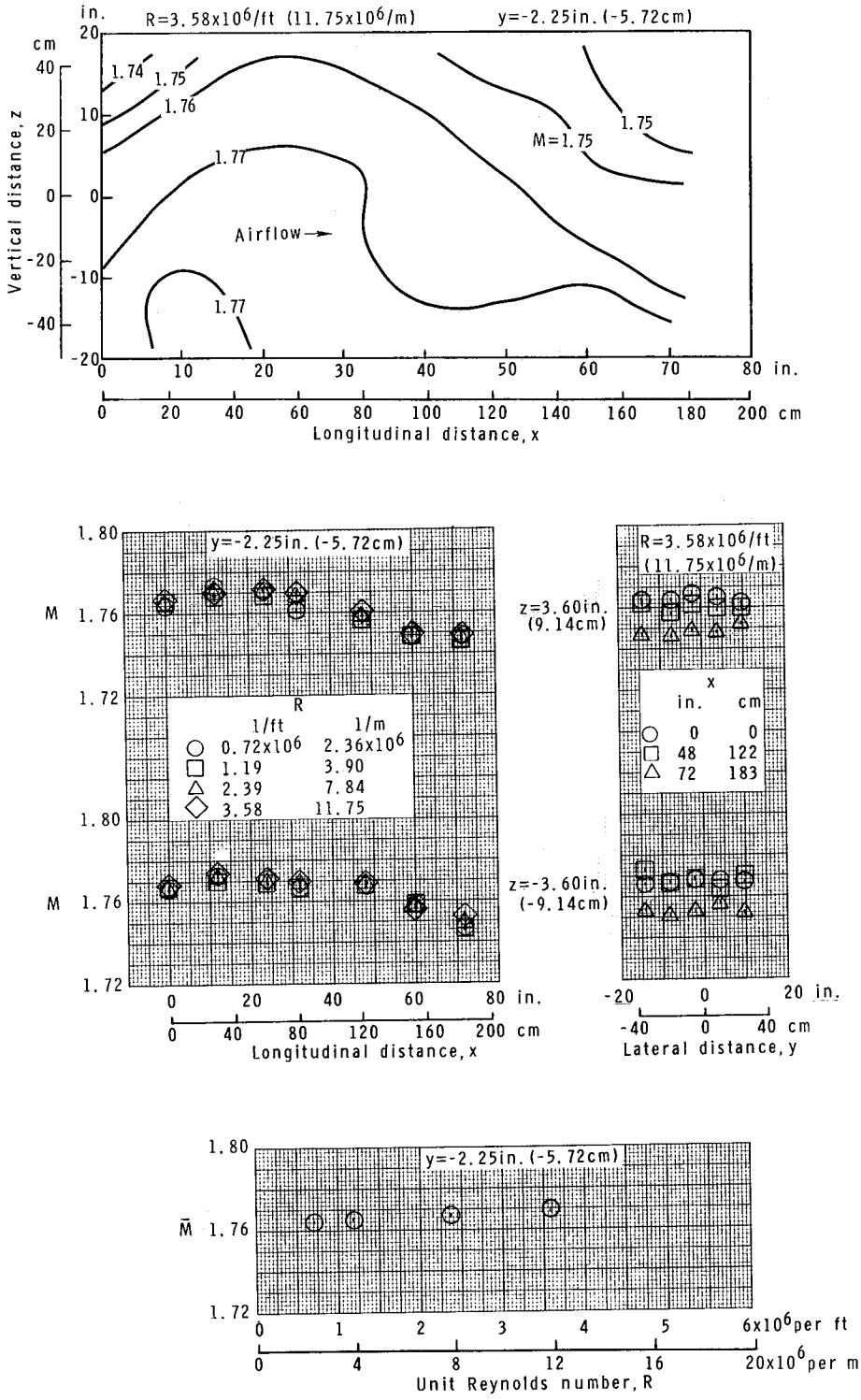

(b) M = 1.769.

Figure 21.- Continued.

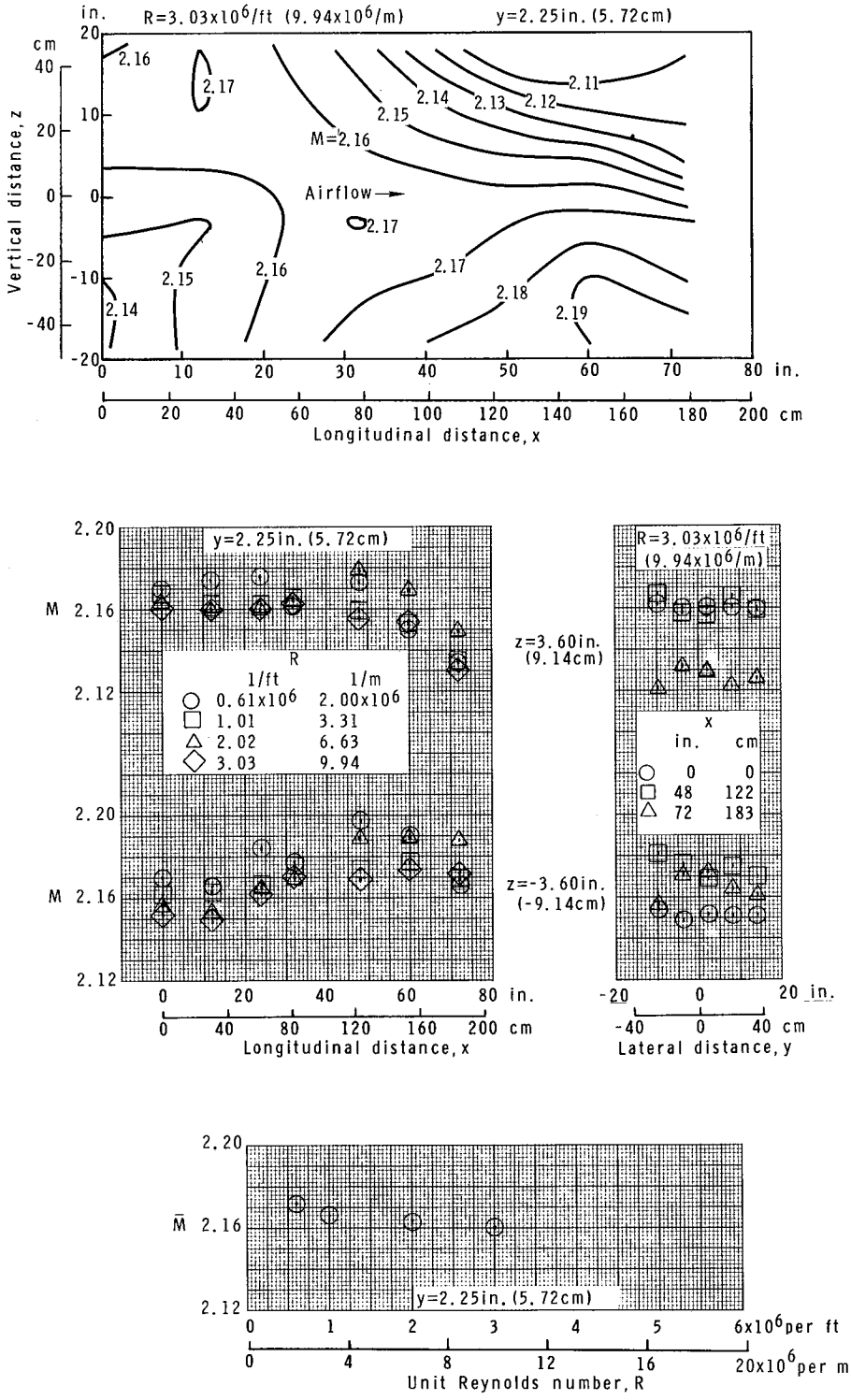

(c) M = 2.160.

Figure 21.- Continued.

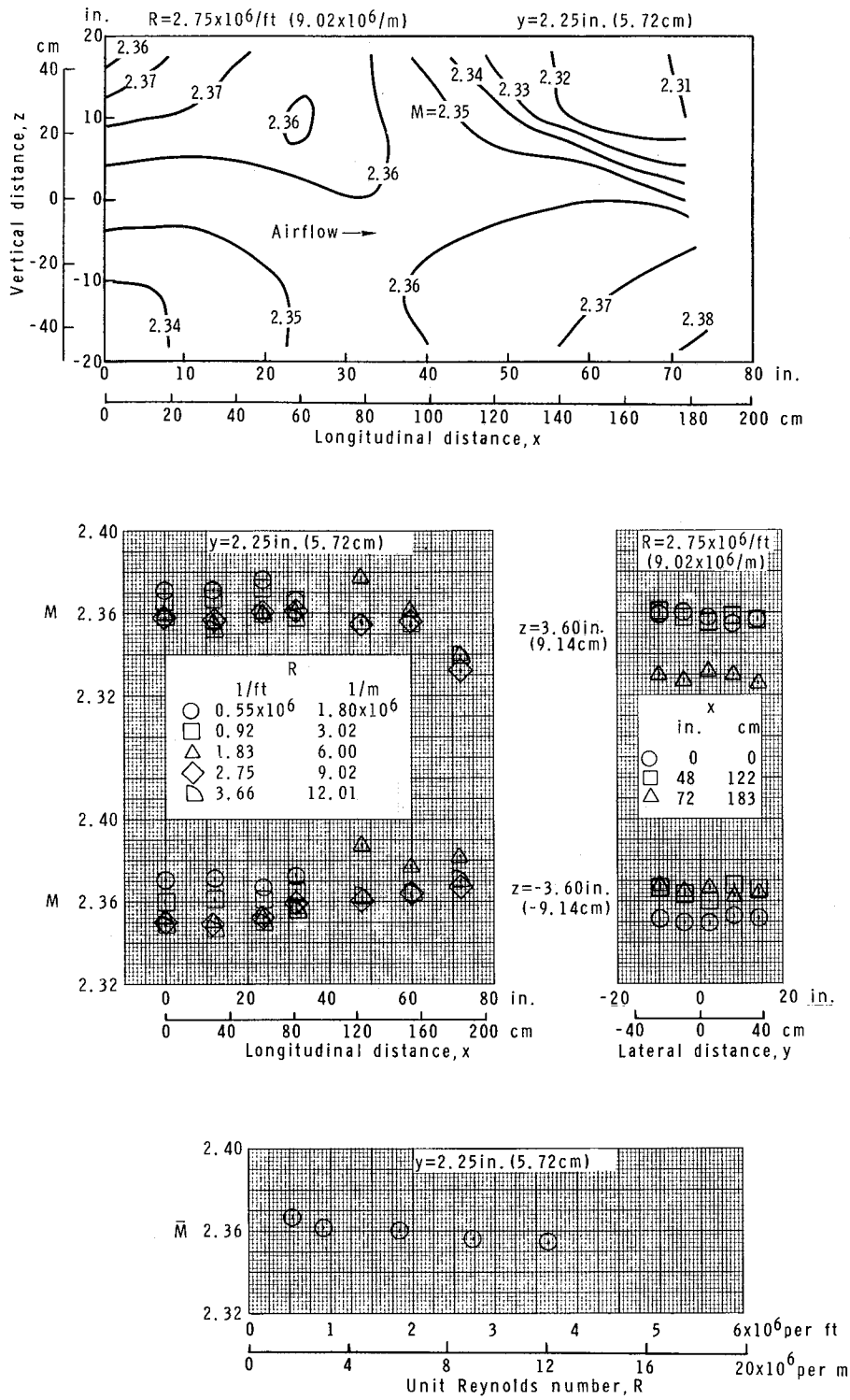

(d) M = 2.354.

Figure 21.- Continued.

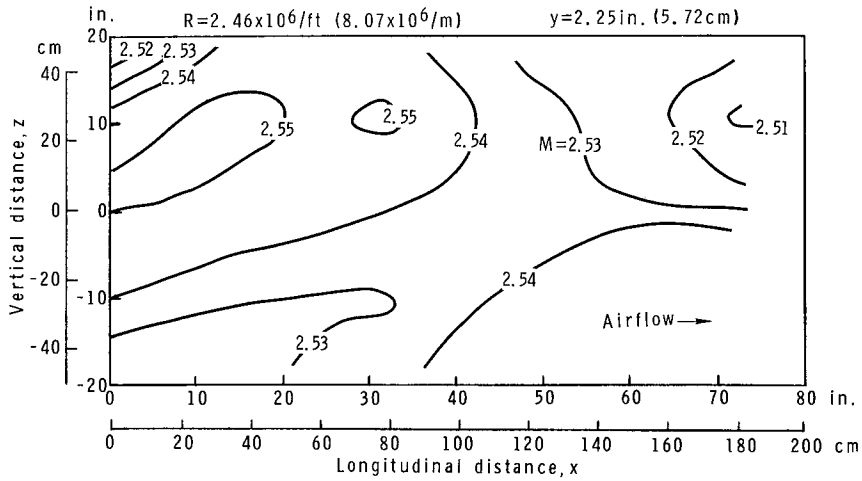

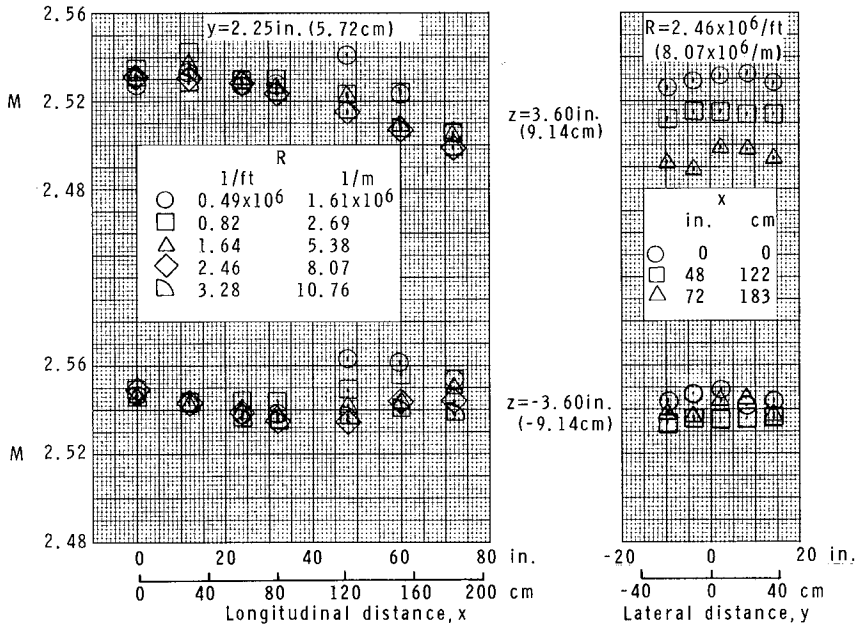

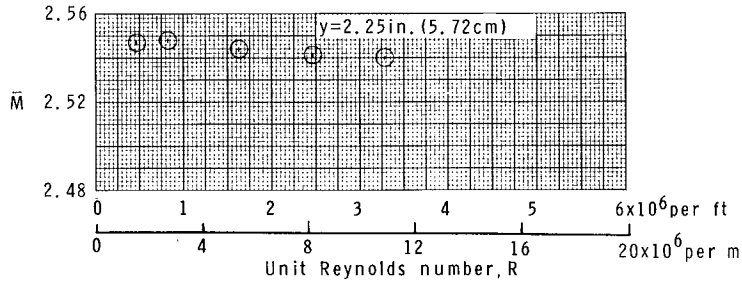

(e) M = 2.540.

Figure 21.- Continued.

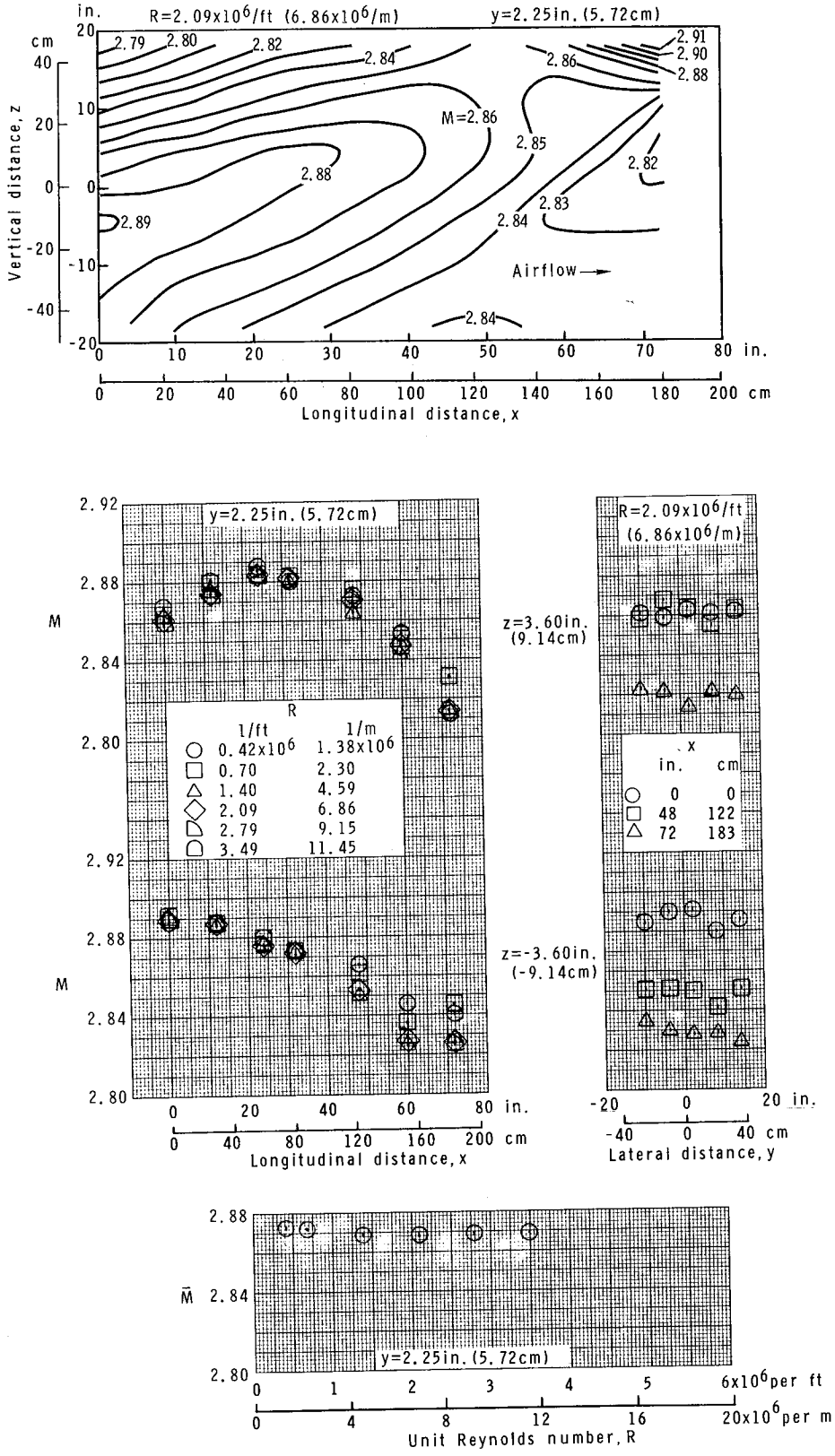

(f) M = 2.869.

Figure 21.- Concluded.

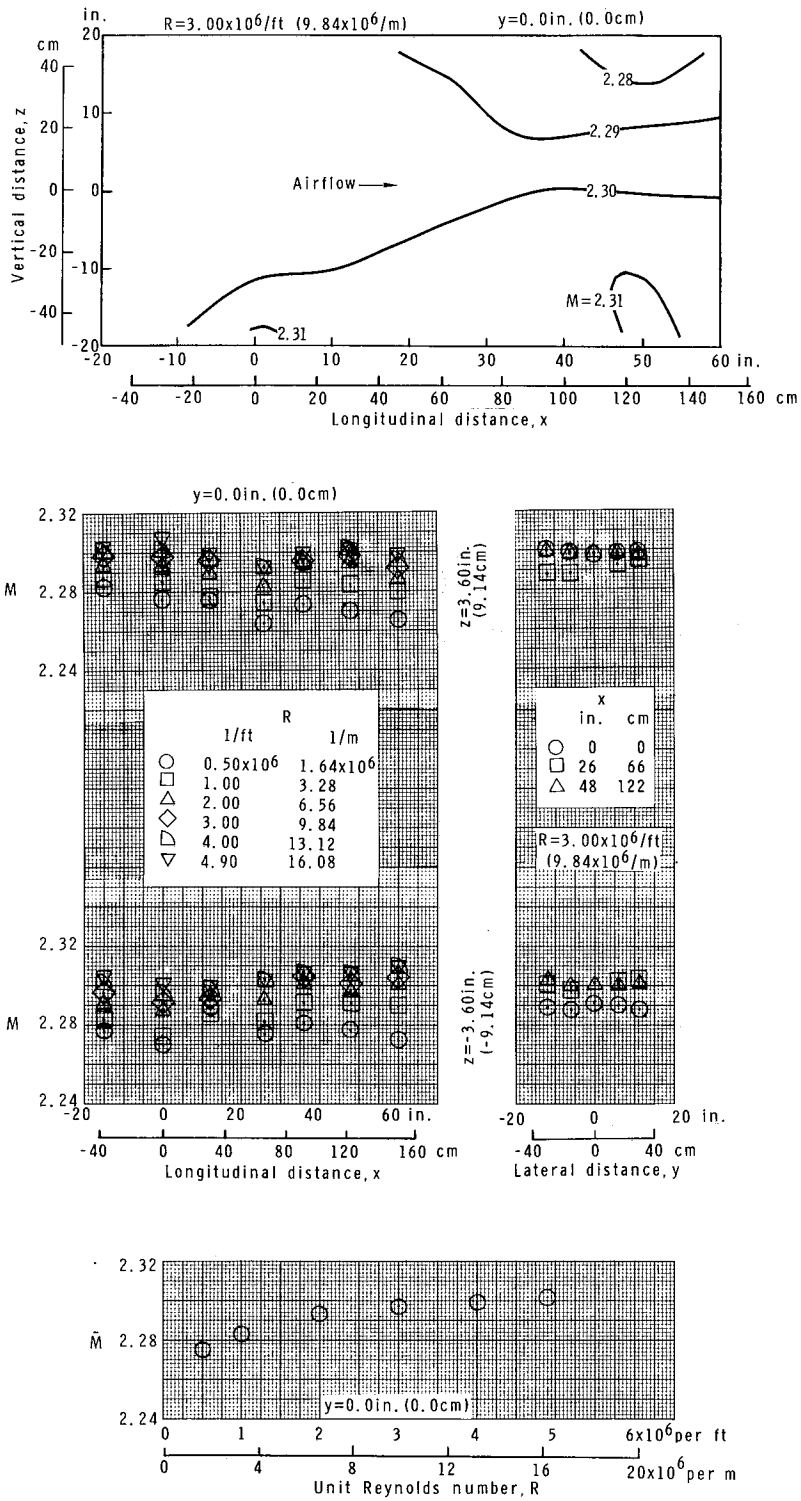

(a) M = 2.297.

Figure 22.- Mach number calibration for test section 2.

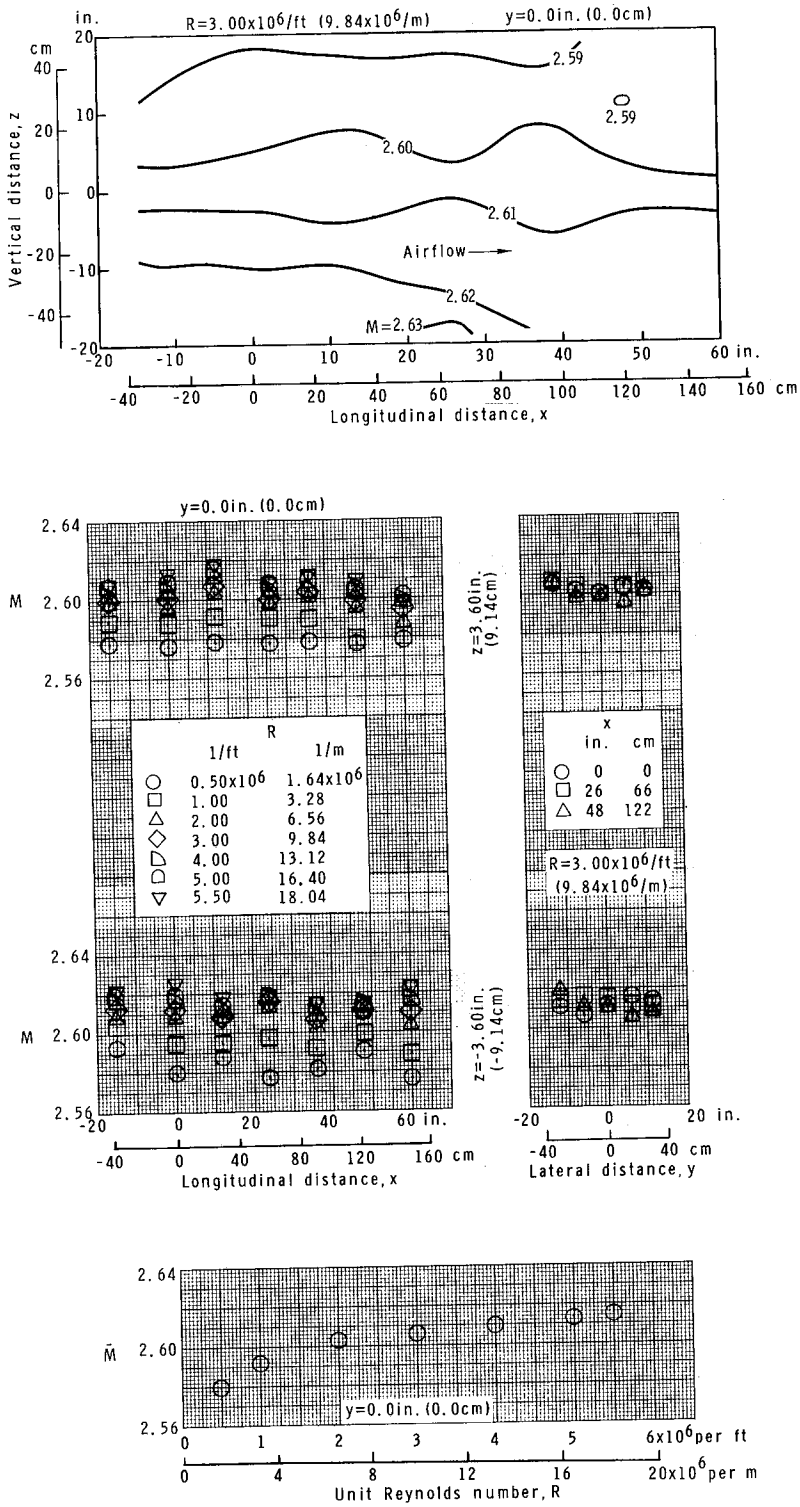

(b) M = 2.606.

Figure 22.- Continued.

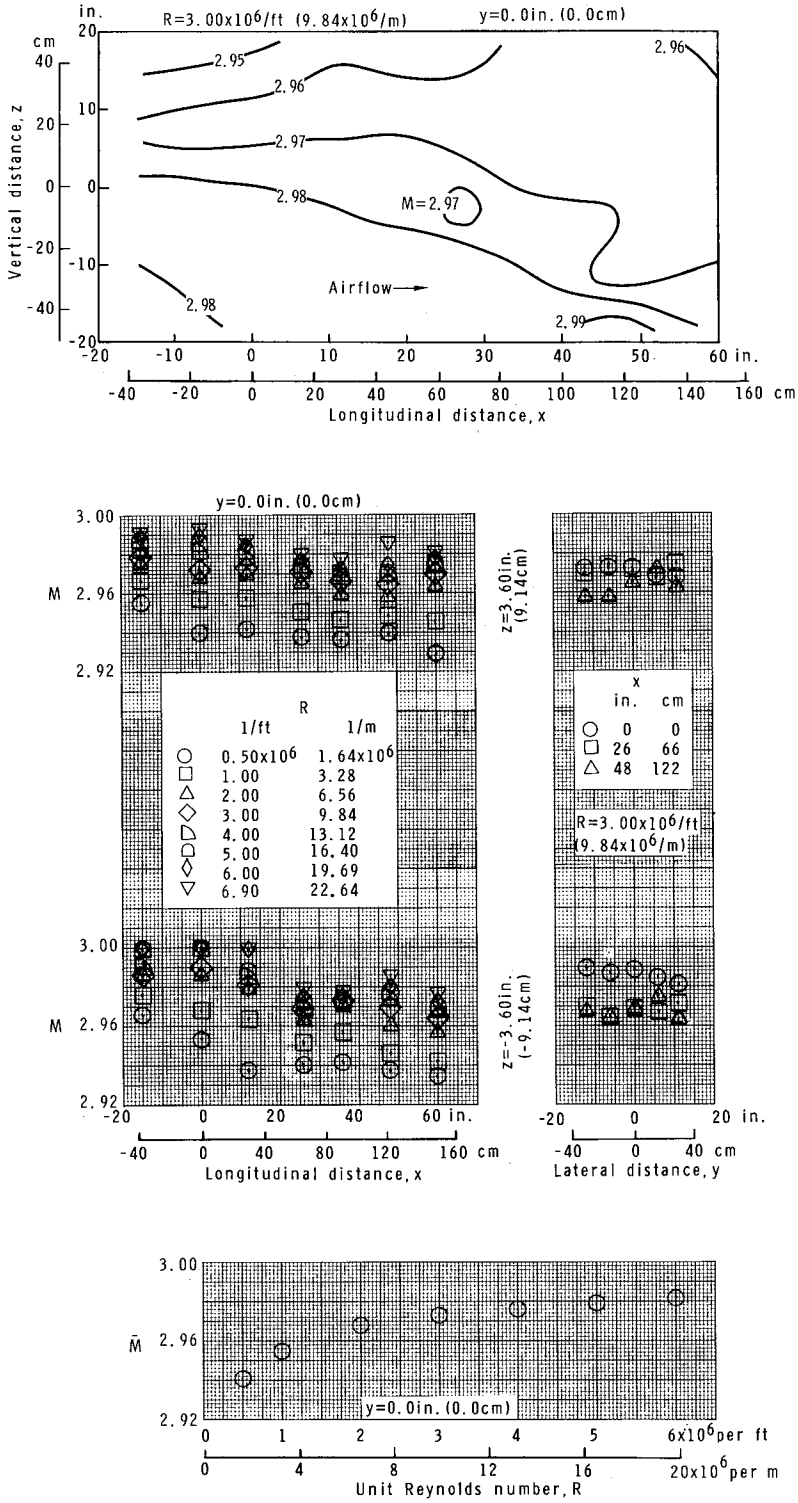

(c) M = 2.973.

Figure 22.- Continued.

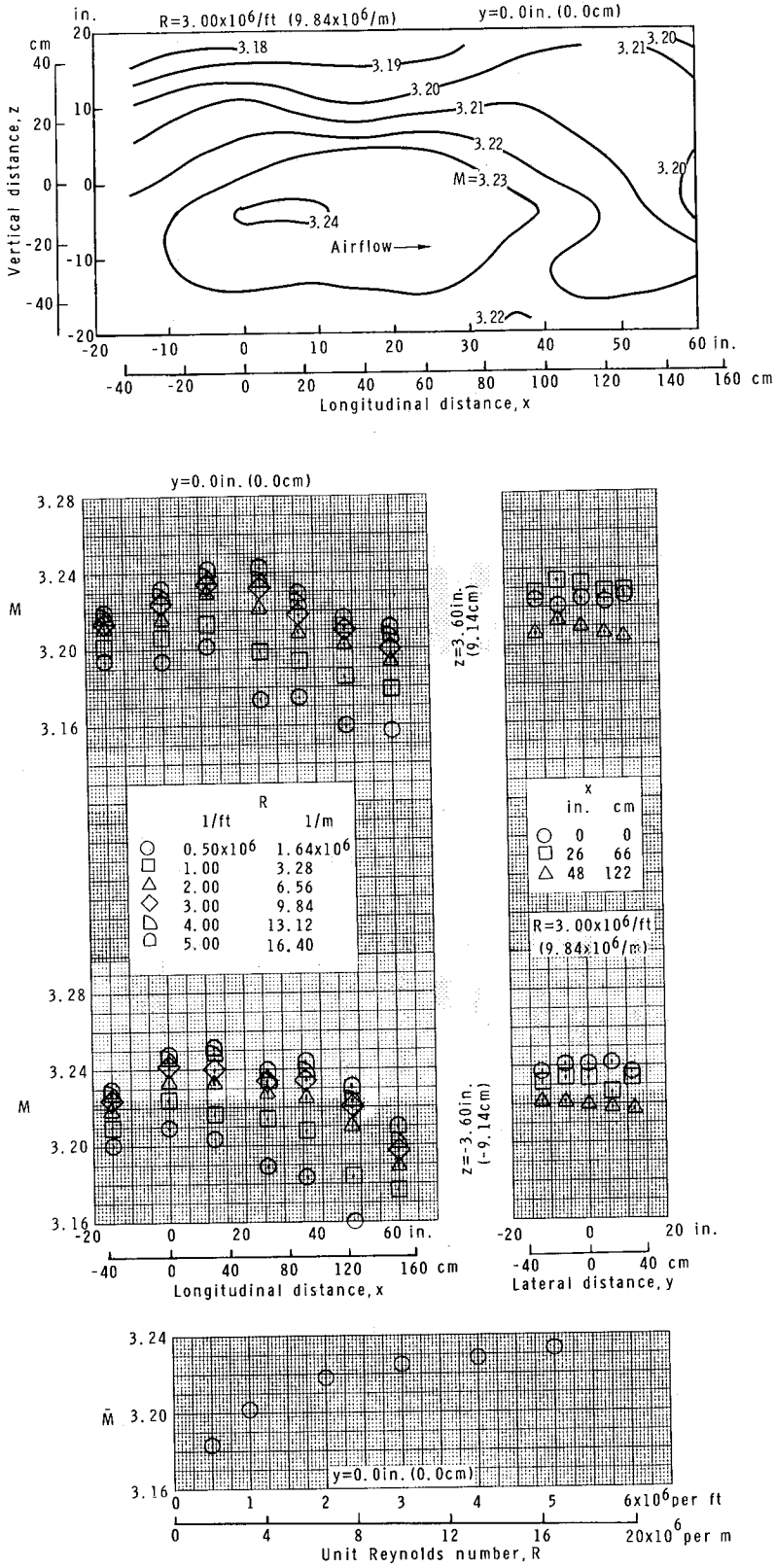

(d) M = 3.225.

Figure 22.- Continued.

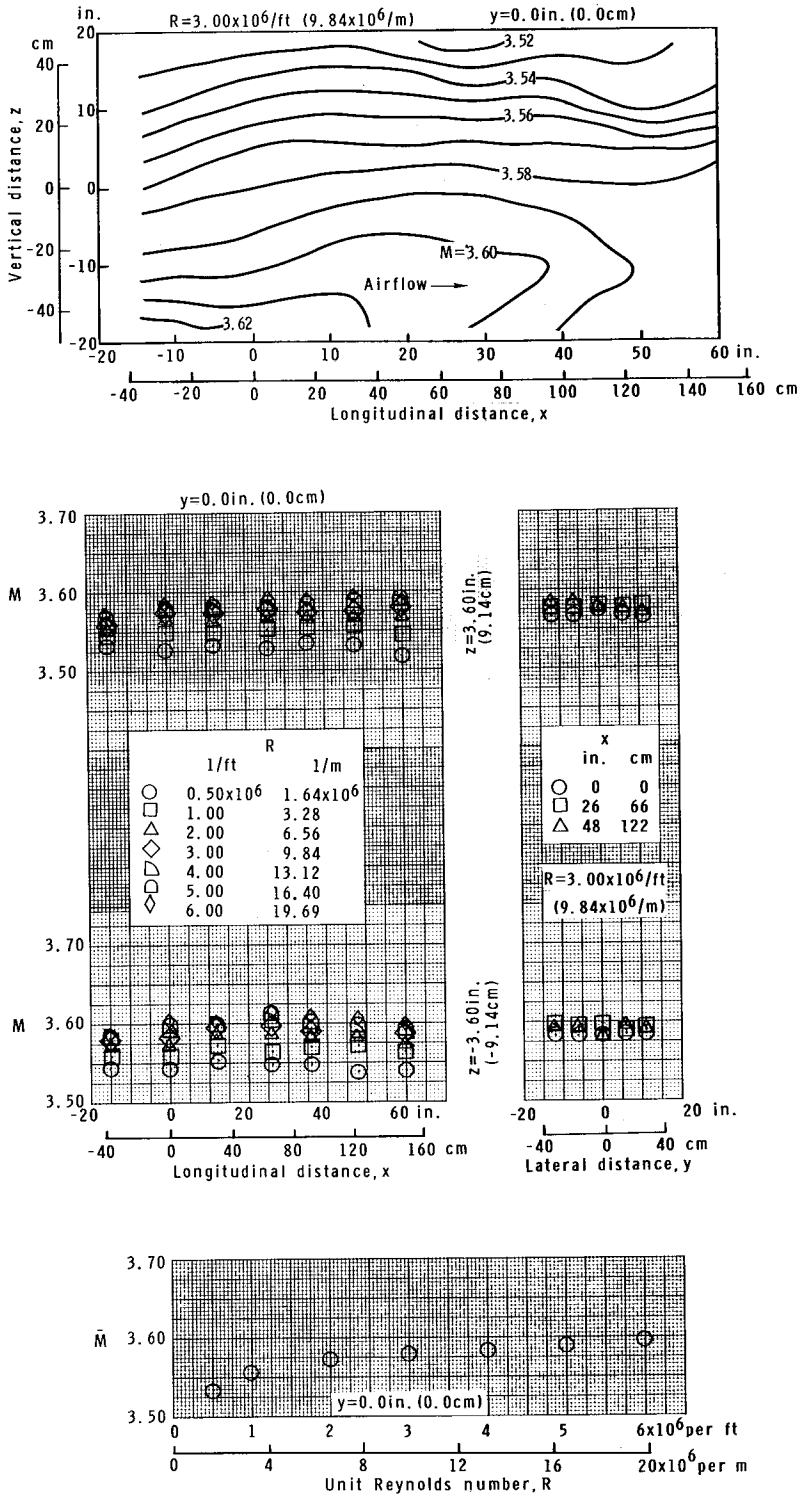

(e) M = 3.580.

Figure 22.- Continued.

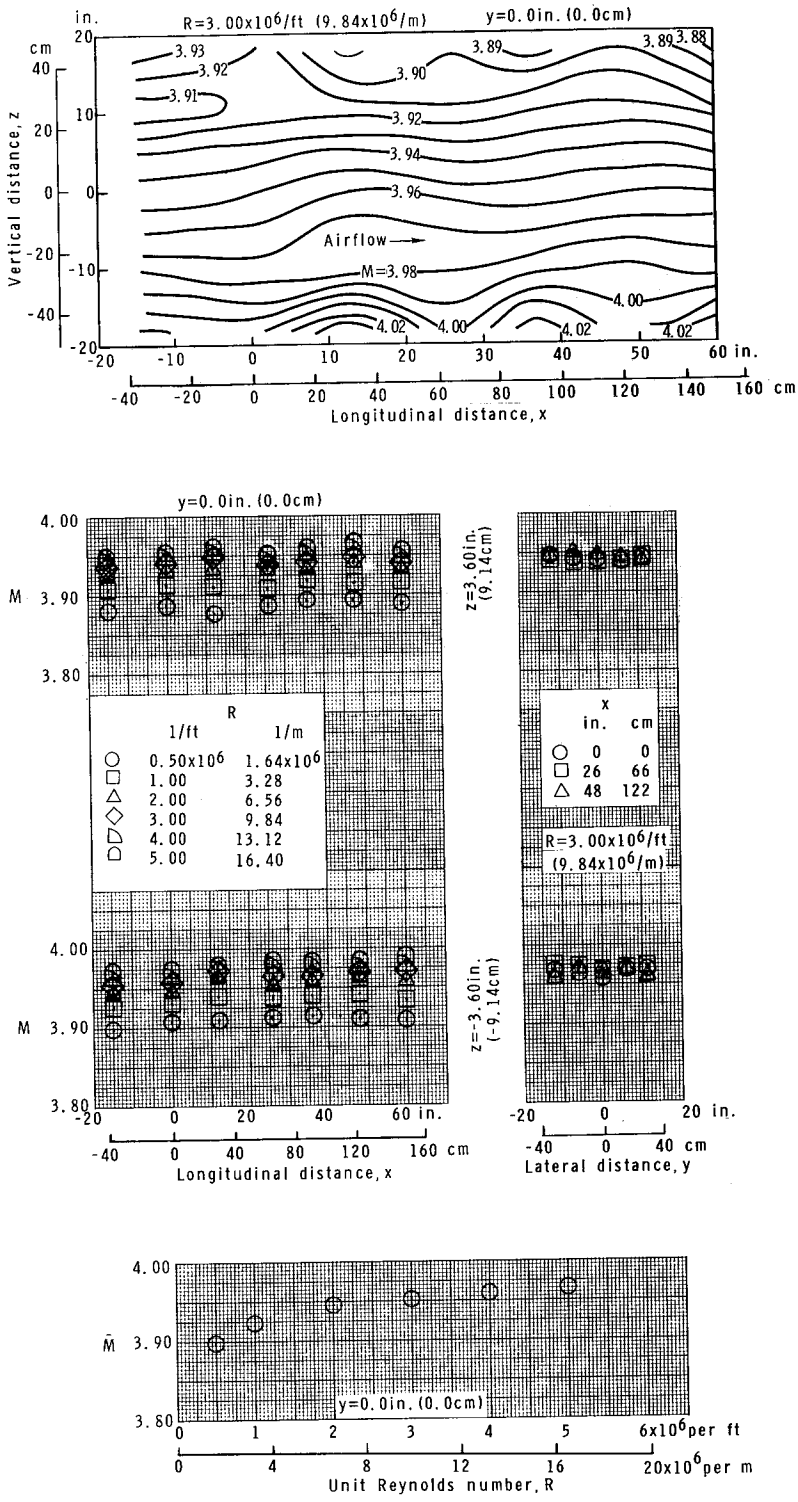

(f) M = 3.953.

Figure 22.- Continued.

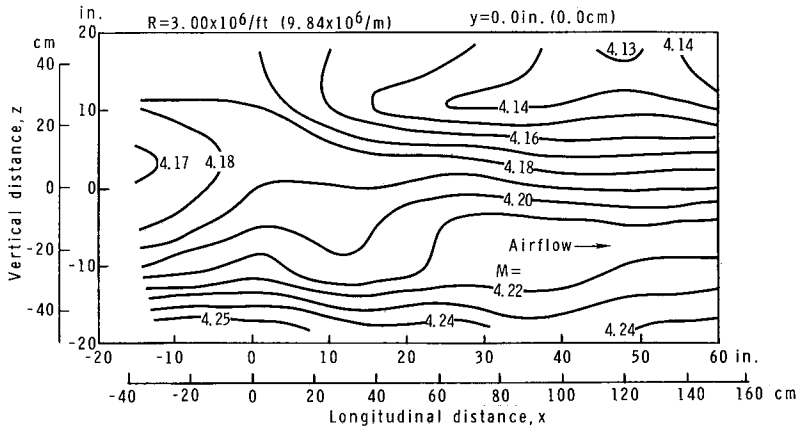

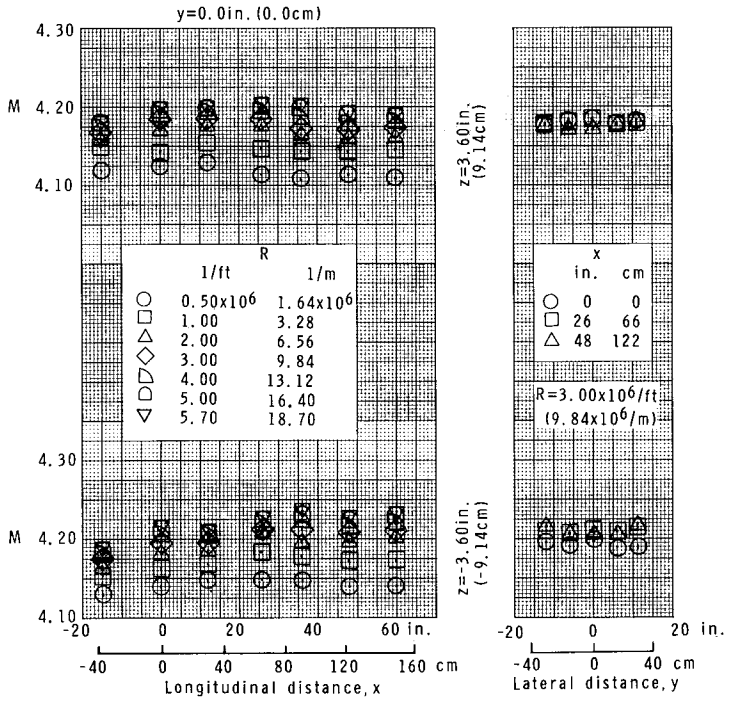

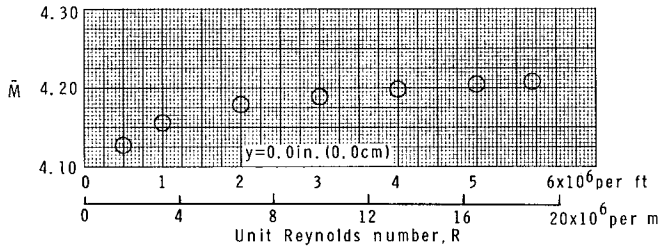

(g) M = 4.189.

Figure 22.- Continued.

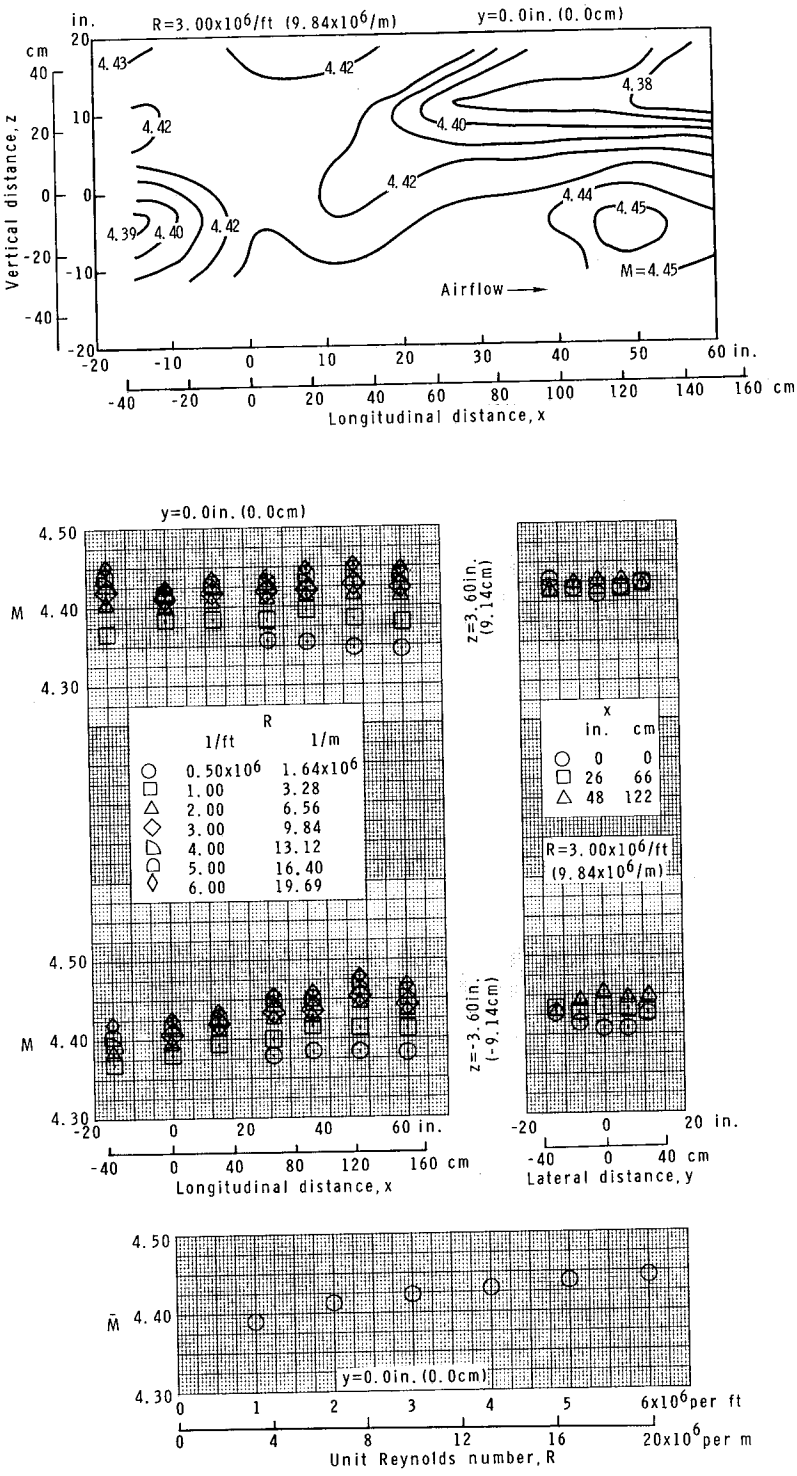

(h) M = 4.423.

Figure 22.- Continued.

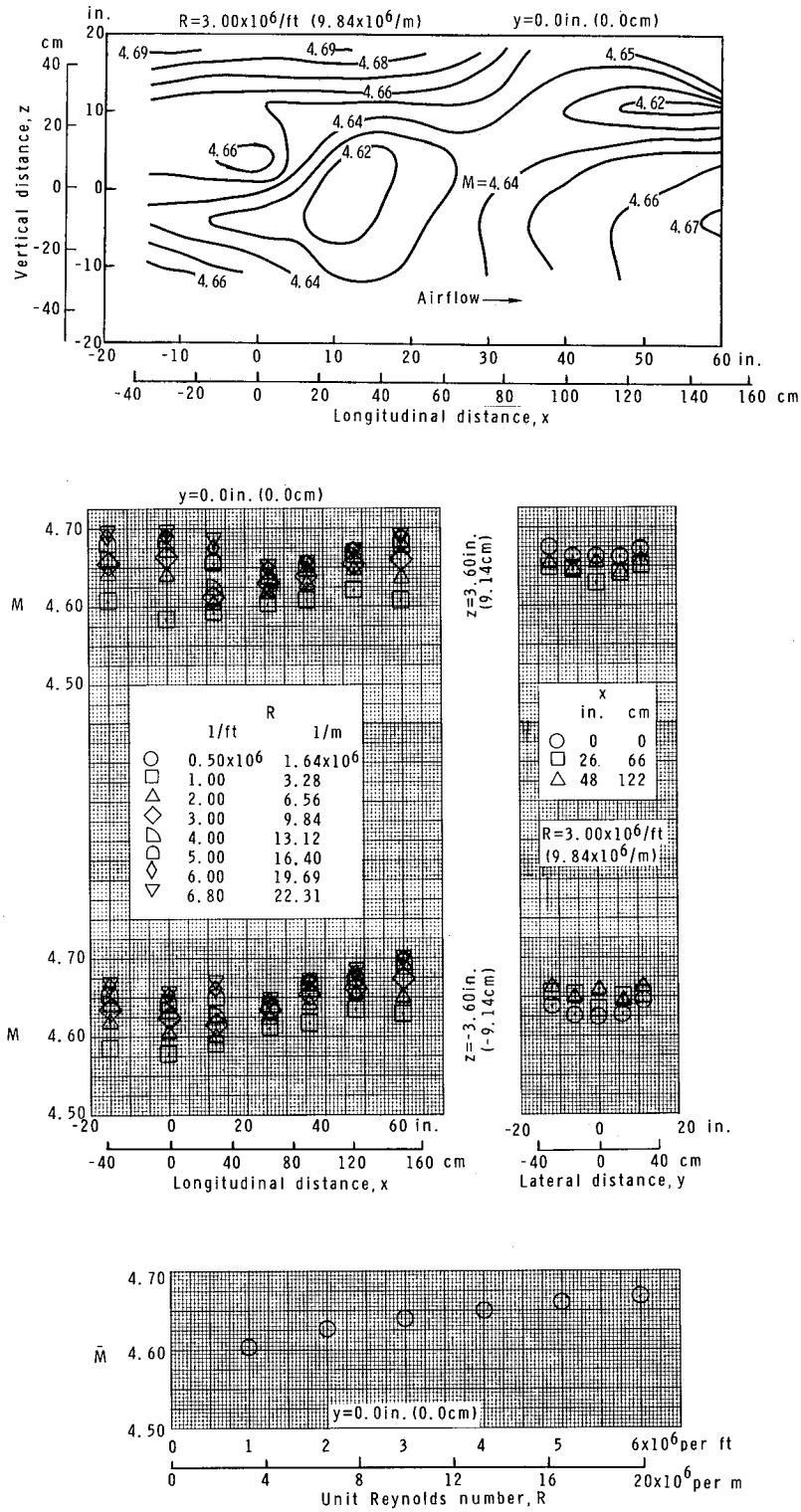

(i) M = 4.640.

Figure 22.- Concluded.

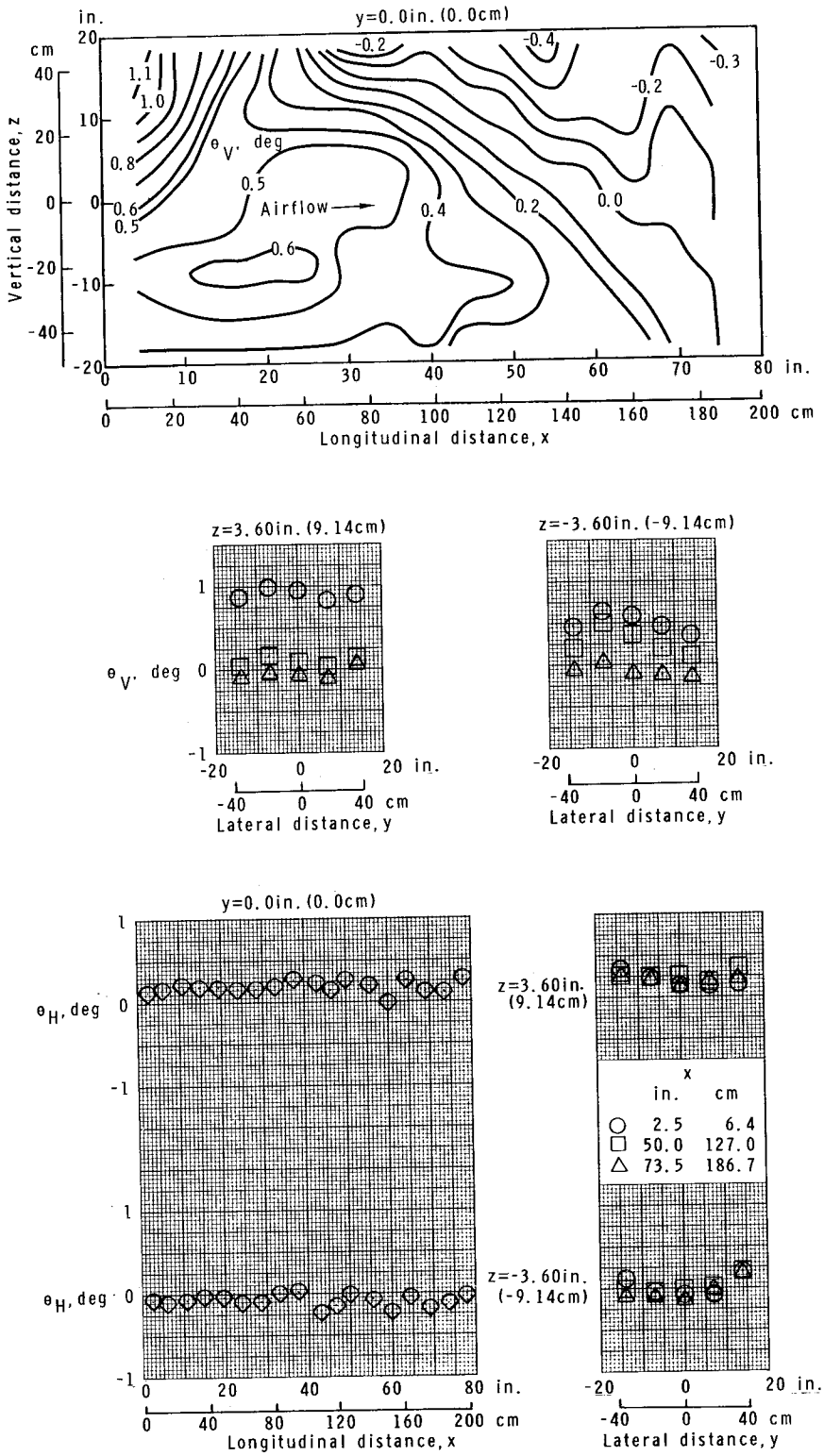

(a) M = 1.57; R = 1.62×10^6 per ft (5.31×10^6 per m).

Figure 23.- Flow-angle calibration for test section 1.

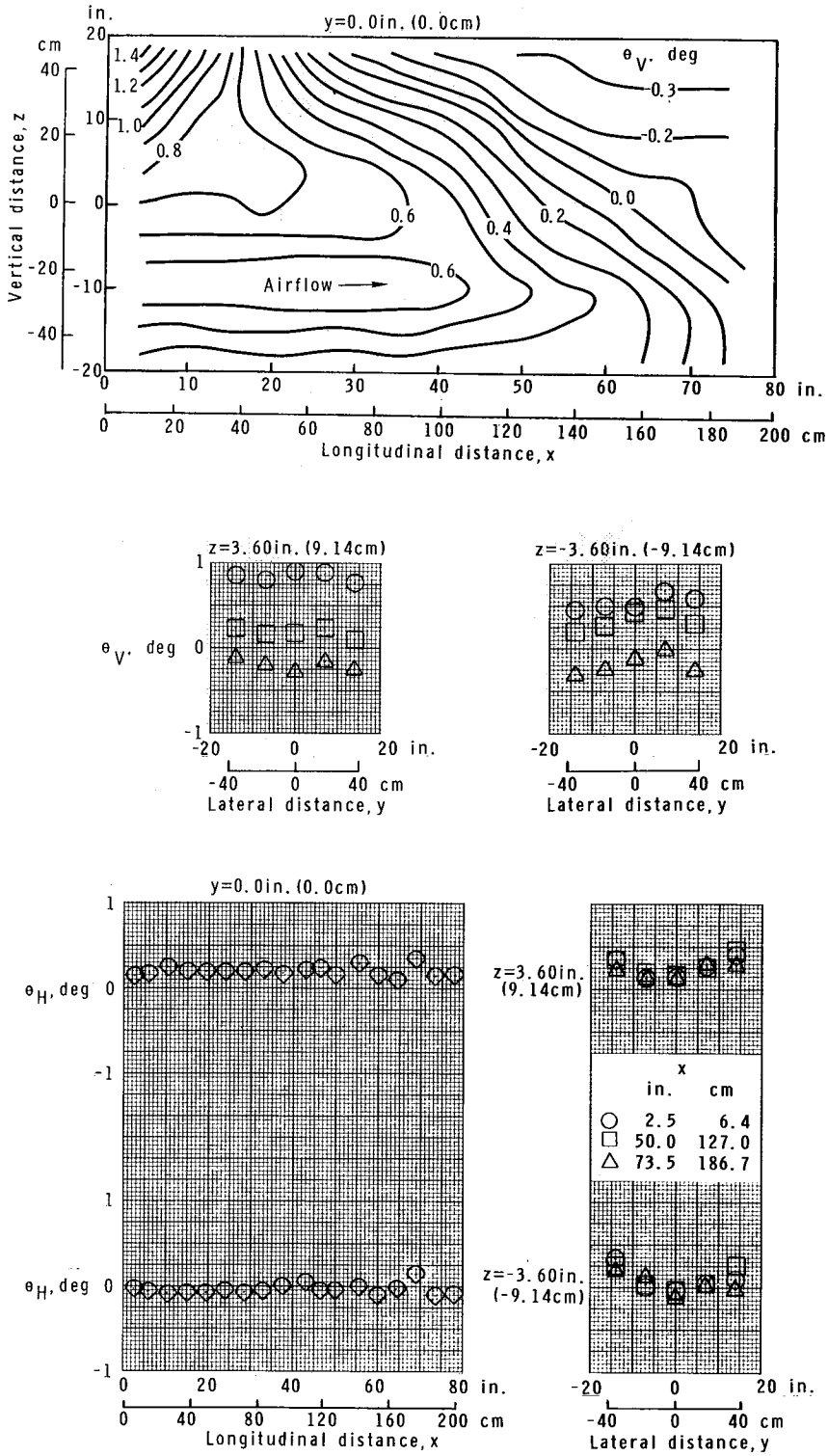

(b) M = 1.77; R = 1.51 × 10^6 per ft (4.95 × 10^6 per m).

Figure 23.- Continued.

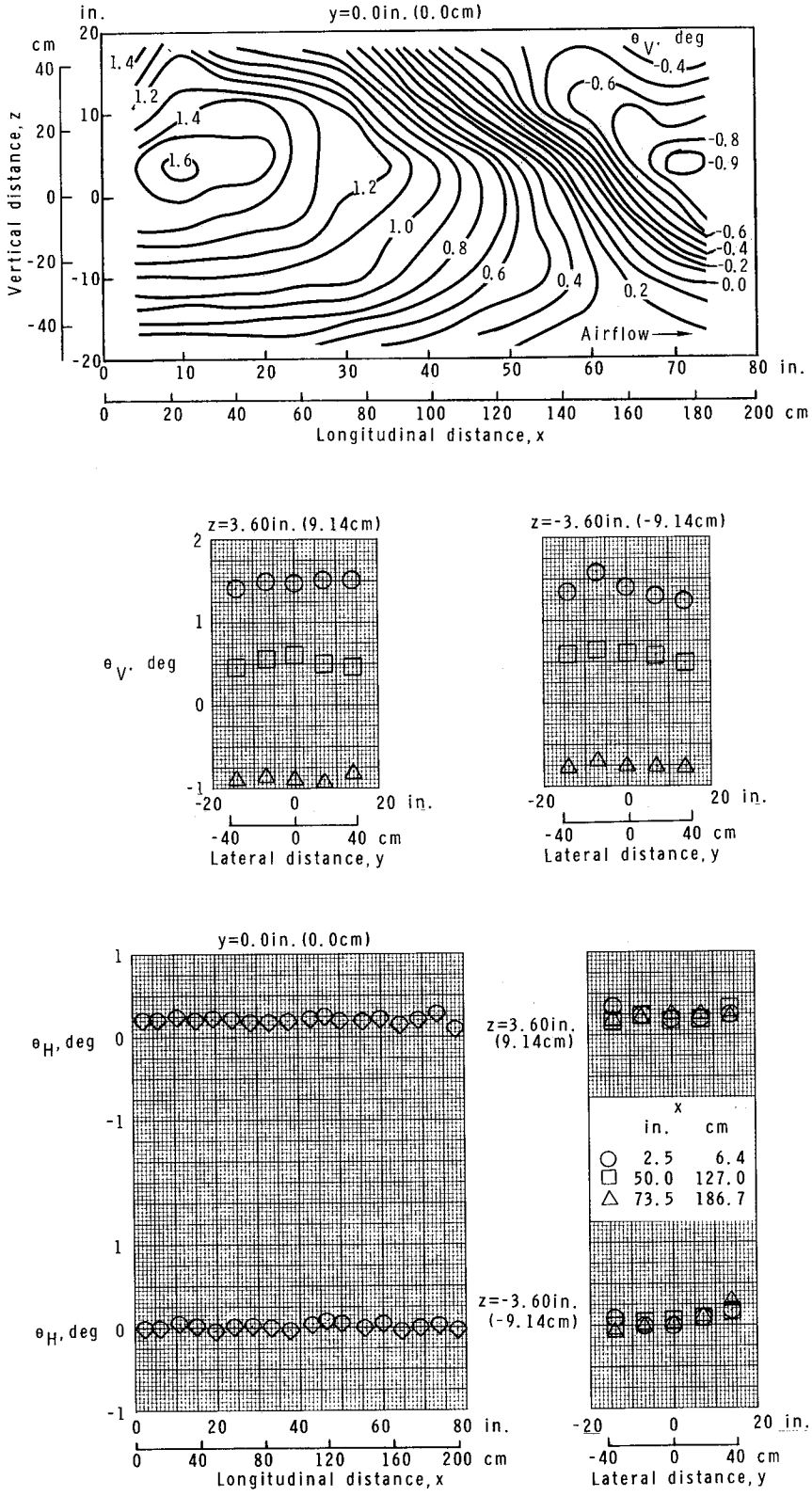

(c) M = 1.97; R = 1.63×10^6 per ft (5.35×10^6 per m).

Figure 23.- Continued.

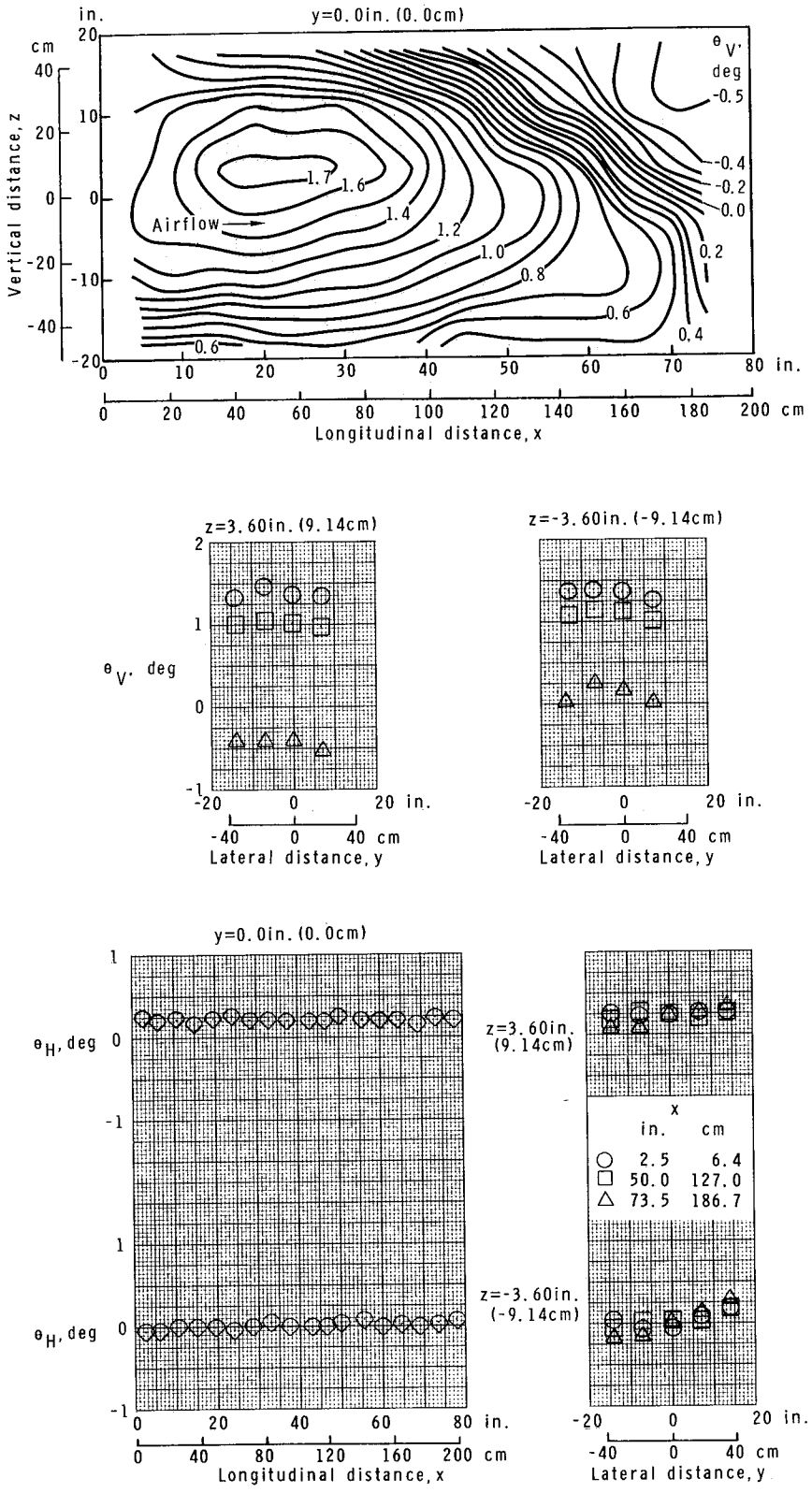

(d) M = 2.17; R = 1.49×10^6 per ft (4.89×10^6 per m).

Figure 23.- Continued.

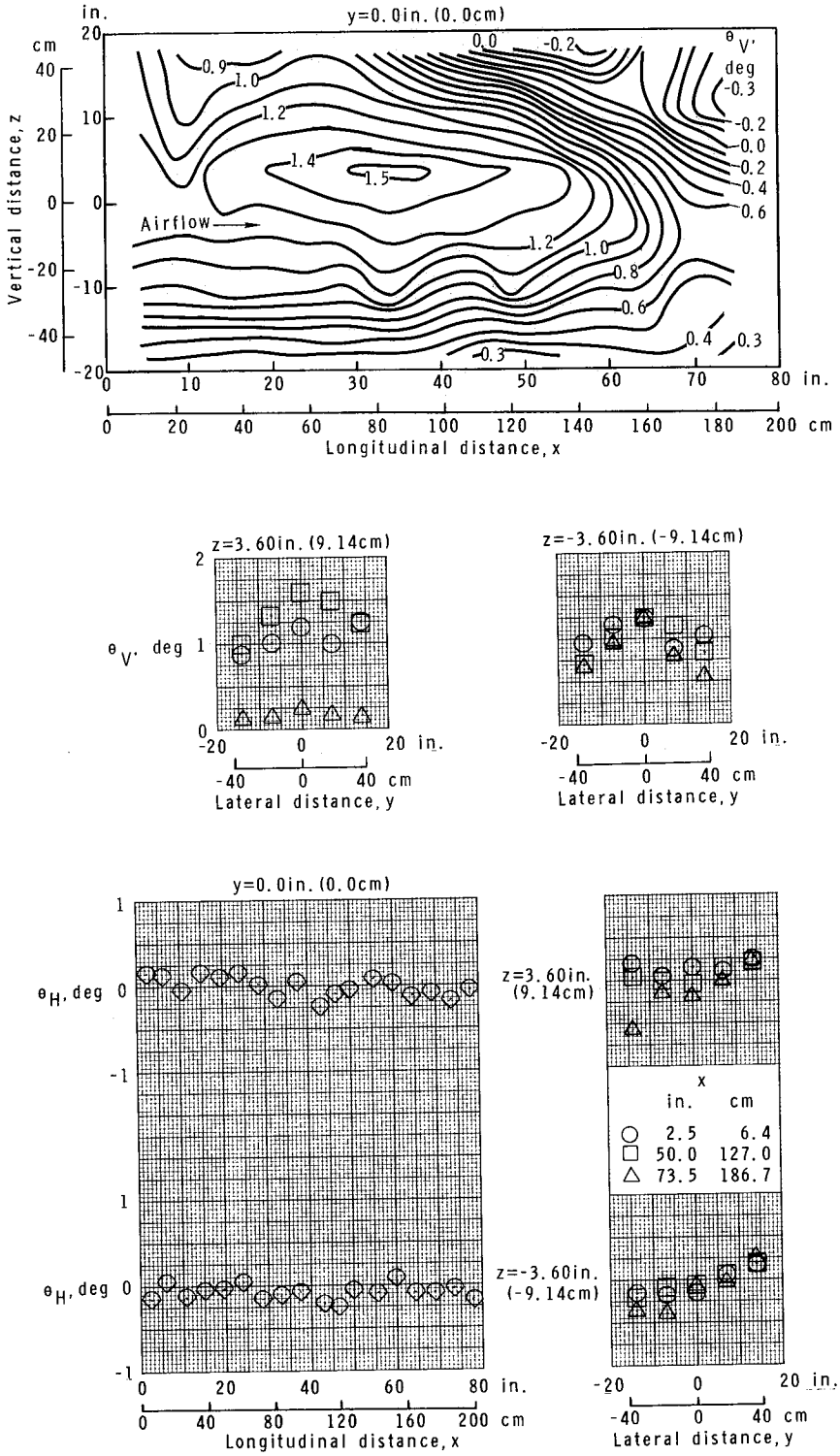

(e) M = 2.36; R = 1.46×10^6 per ft (4.79×10^6 per m).

Figure 23.- Continued.

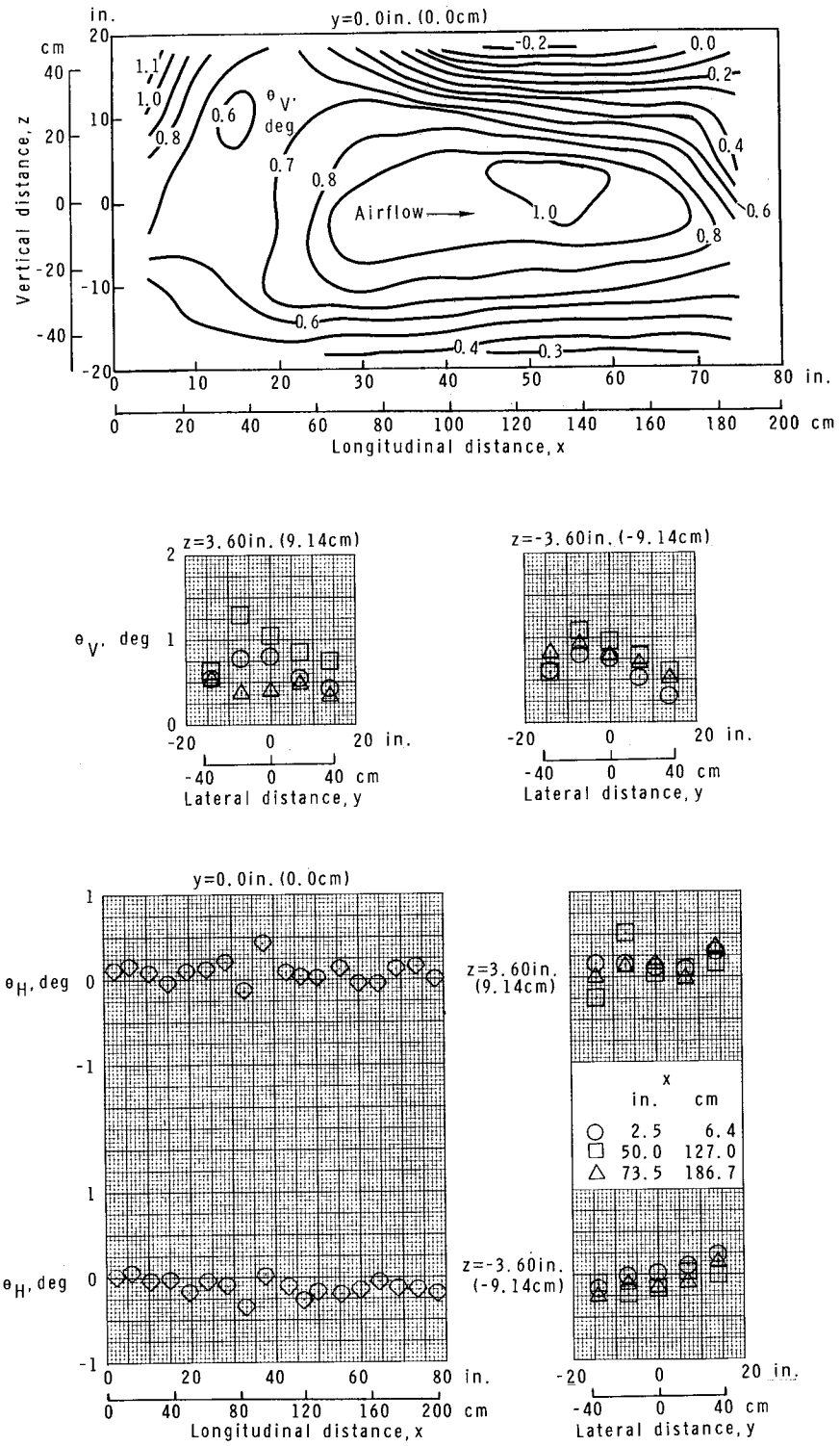

(f) M = 2.54; R = 1.66×10^6 per ft (5.45×10^6 per m).

Figure 23.- Continued.

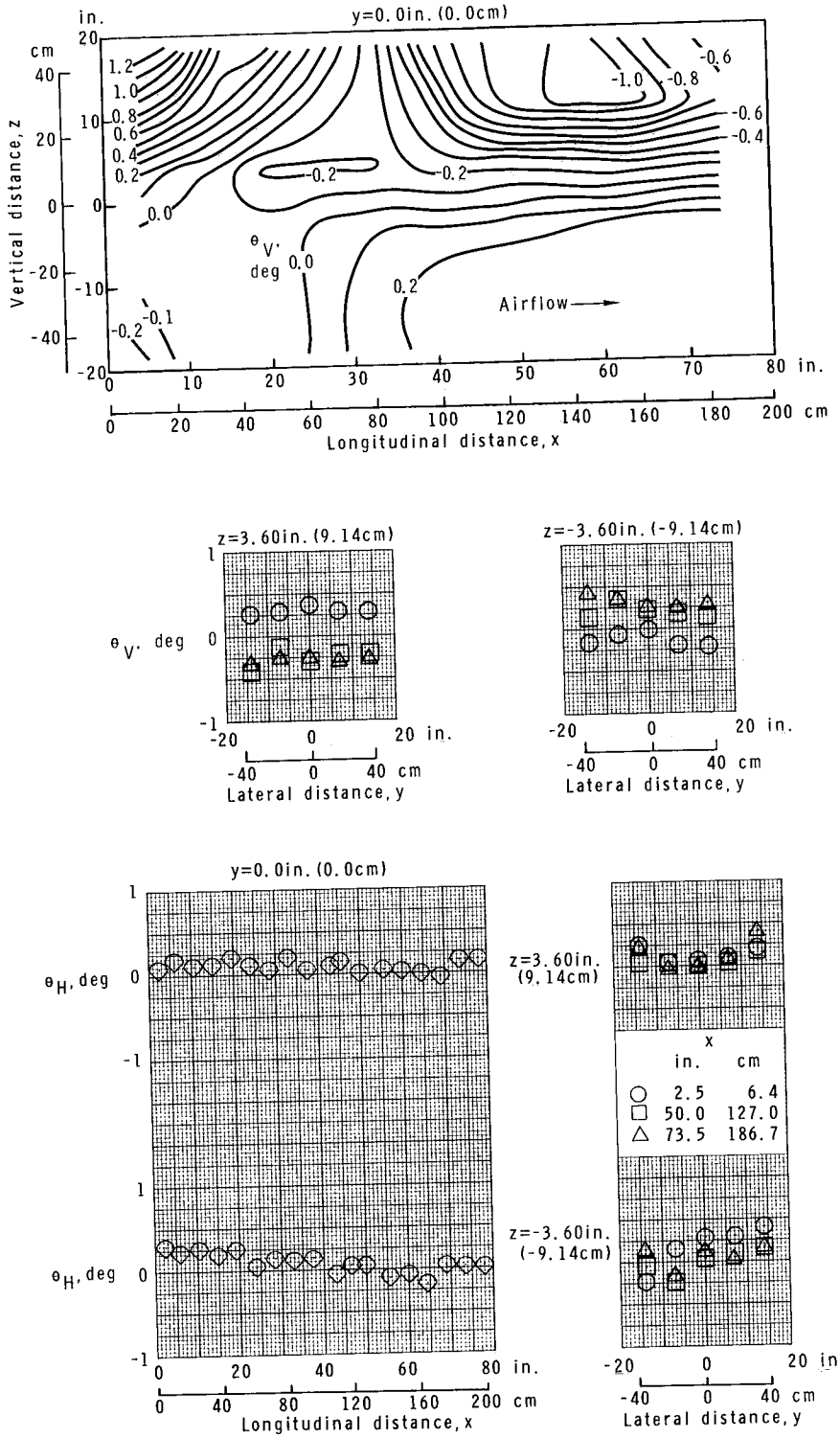

(g) M = 2.87; R = 1.82×10^6 per ft (5.97×10^6 per m).

Figure 23.- Concluded.

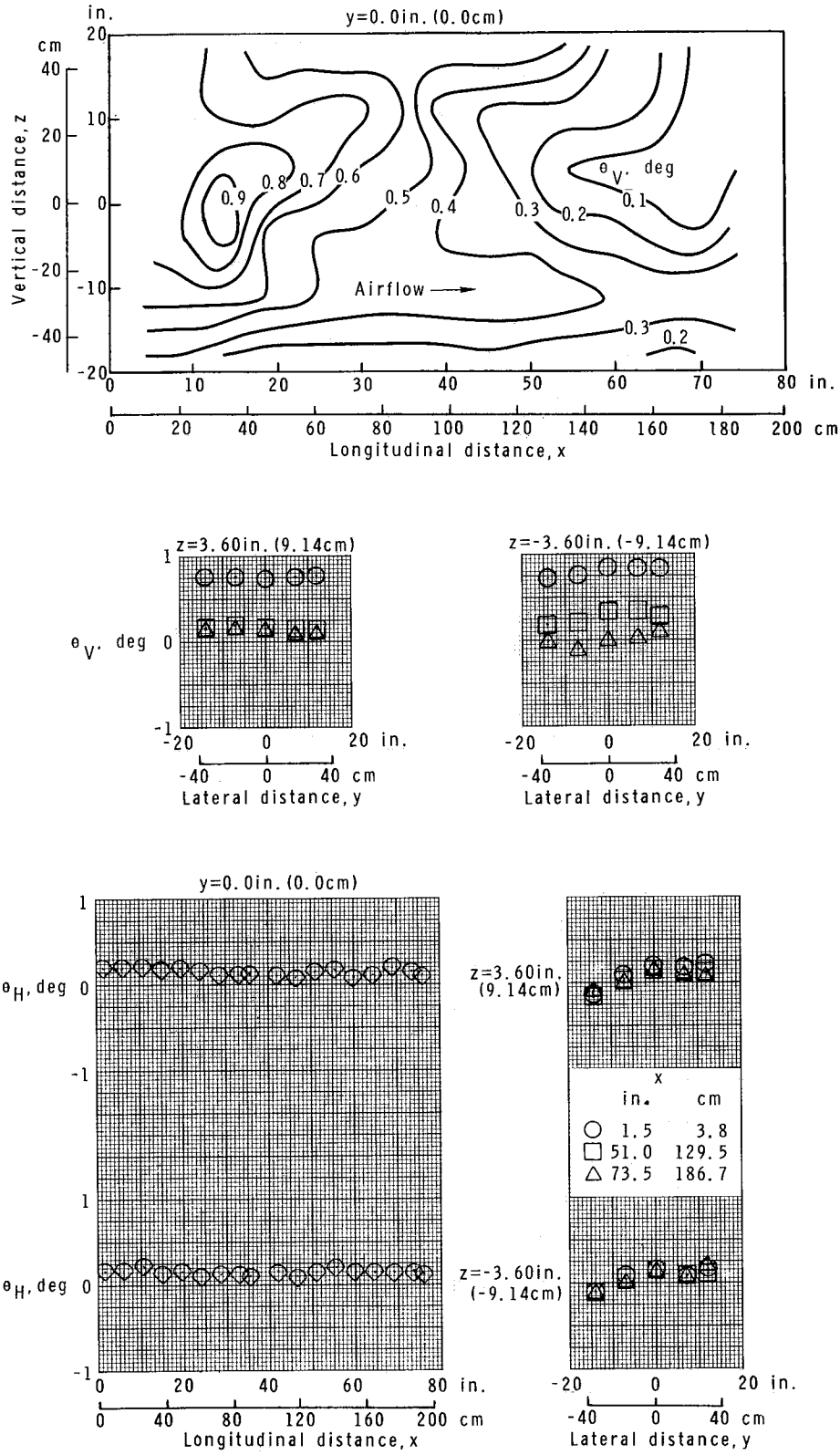

(a) M = 2.294; R = 1.51 × 10^6 per ft (4.95 × 10^6 per m).

Figure 24.- Flow-angle calibration for test section 2.

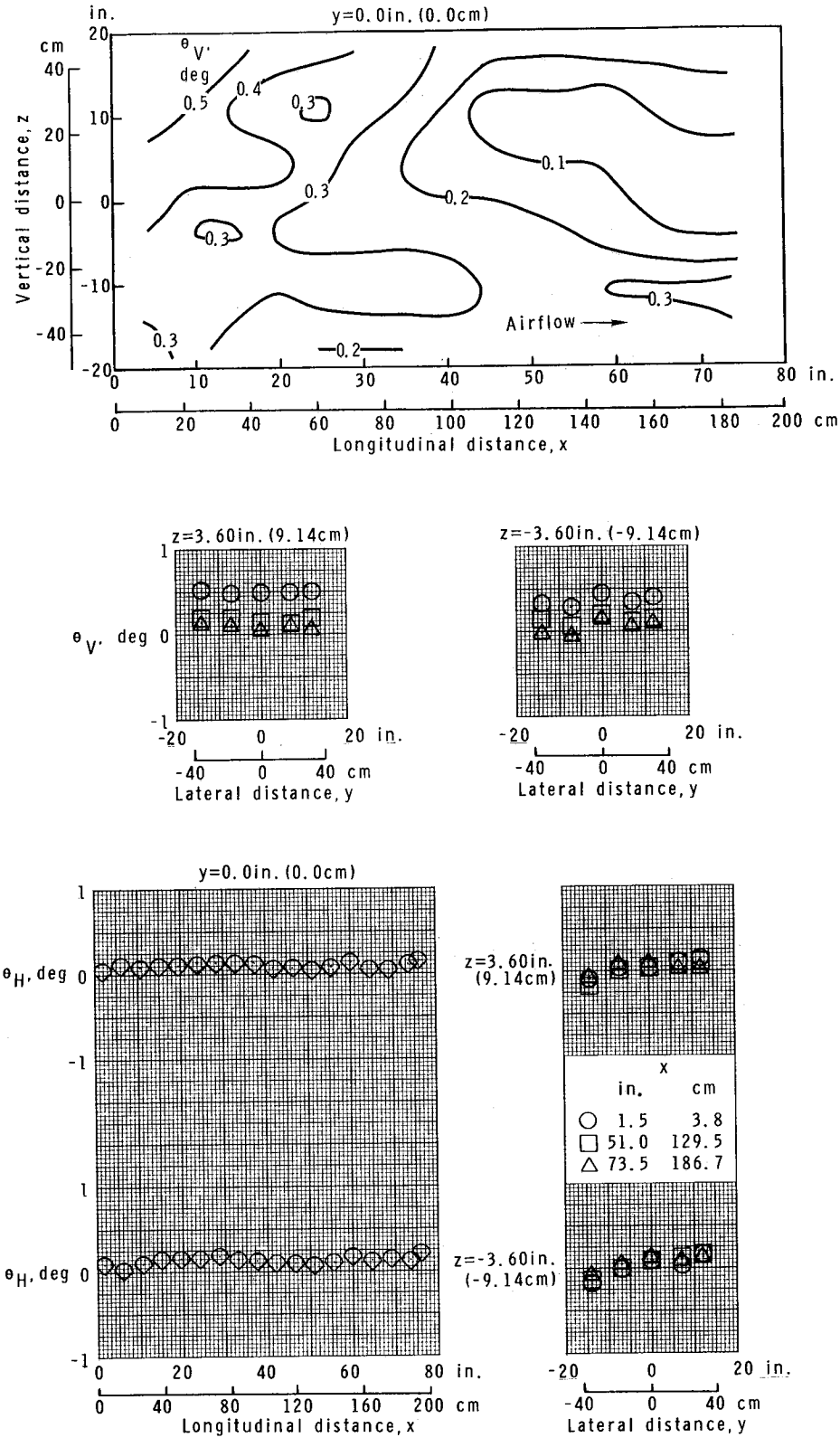

(b) M = 2.489; R = 1.54×10^6 per ft (5.05×10^6 per m).

Figure 24.- Continued.

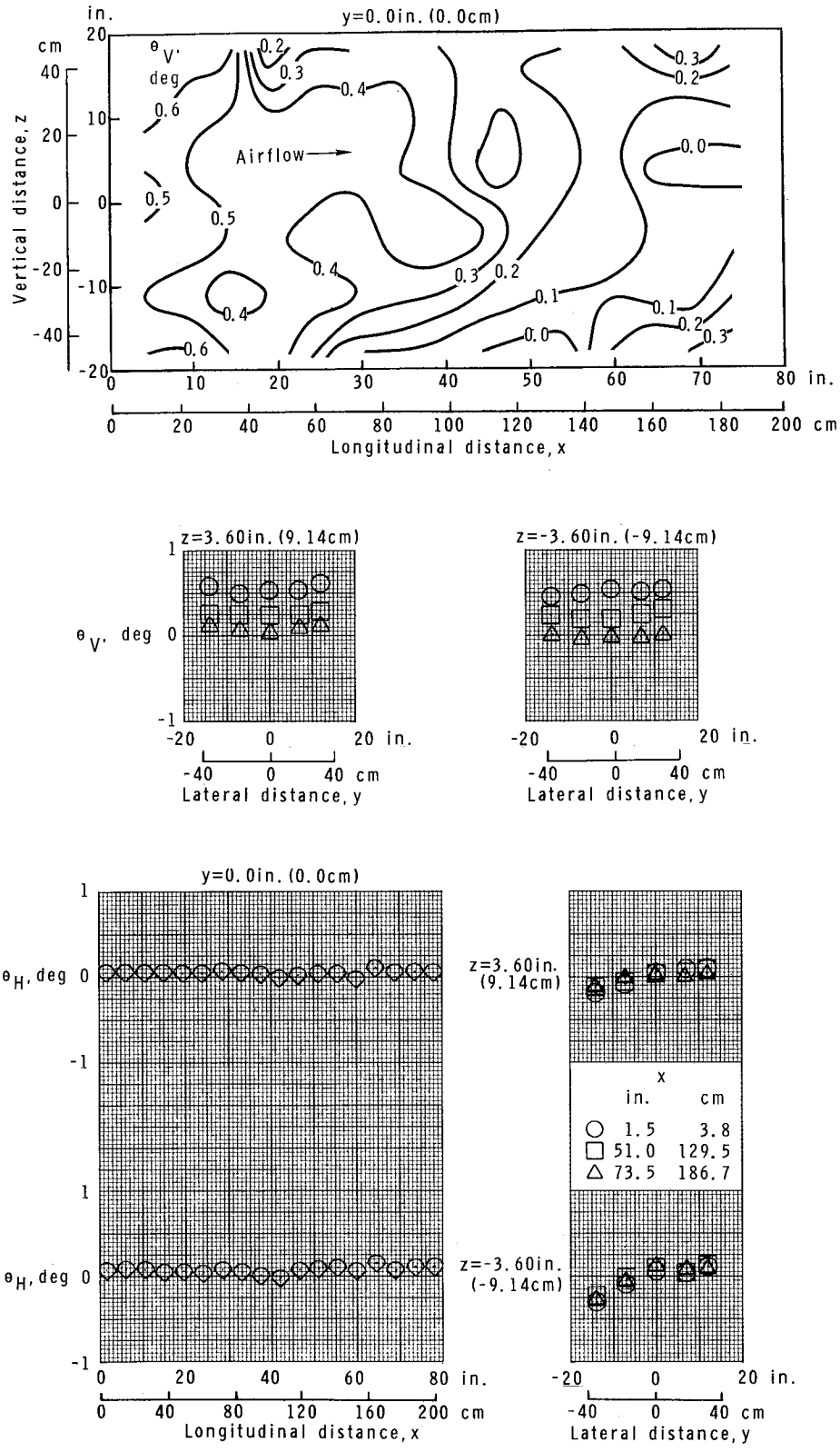

(c) M = 2.750; R = 1.64 × 10^6 per ft (5.38 × 10^6 per m).

Figure 24.- Continued.

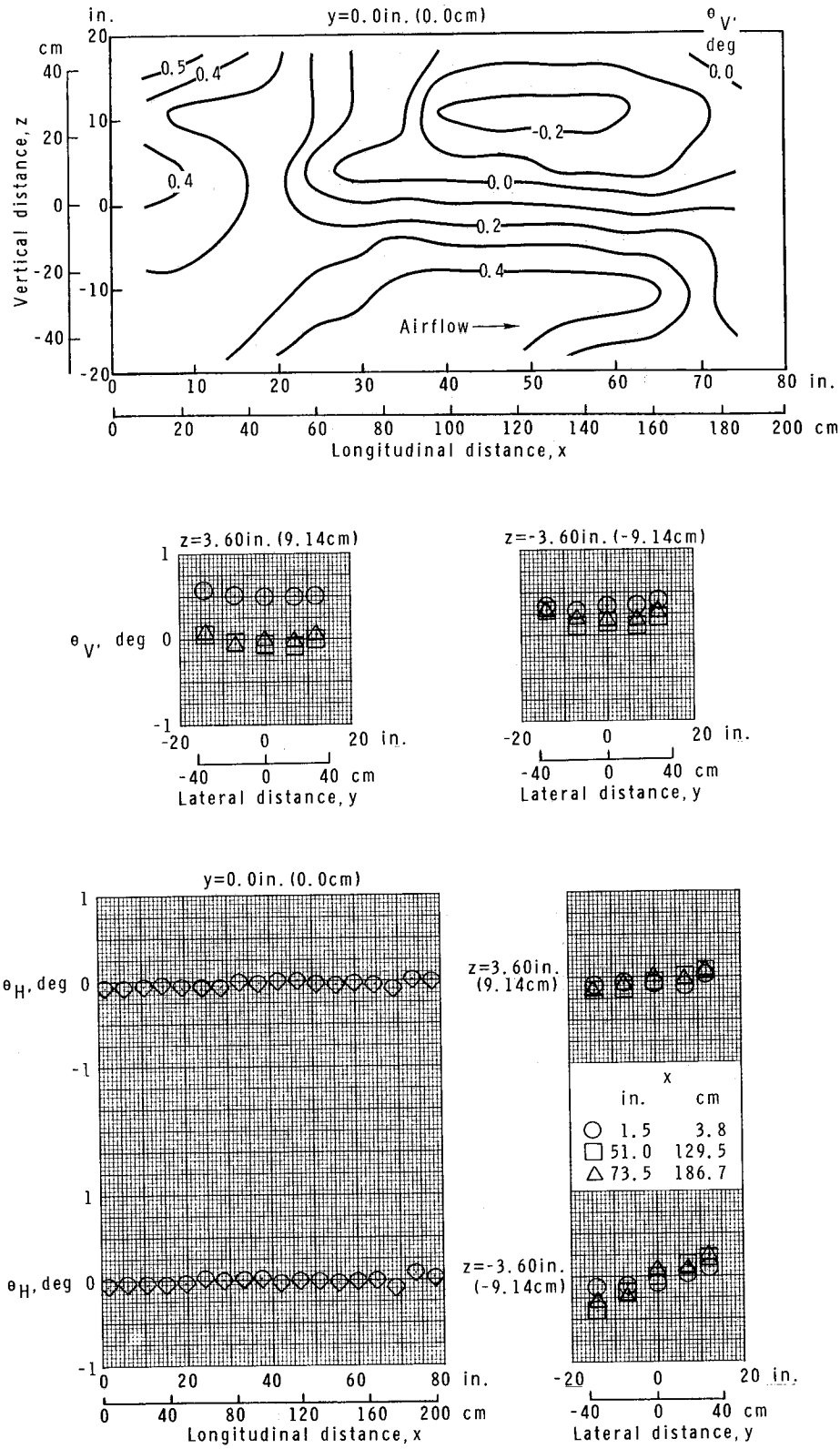

(d) M = 3.218; R = 1.96×10^6 per ft (6.43×10^6 per m).

Figure 24.- Continued.

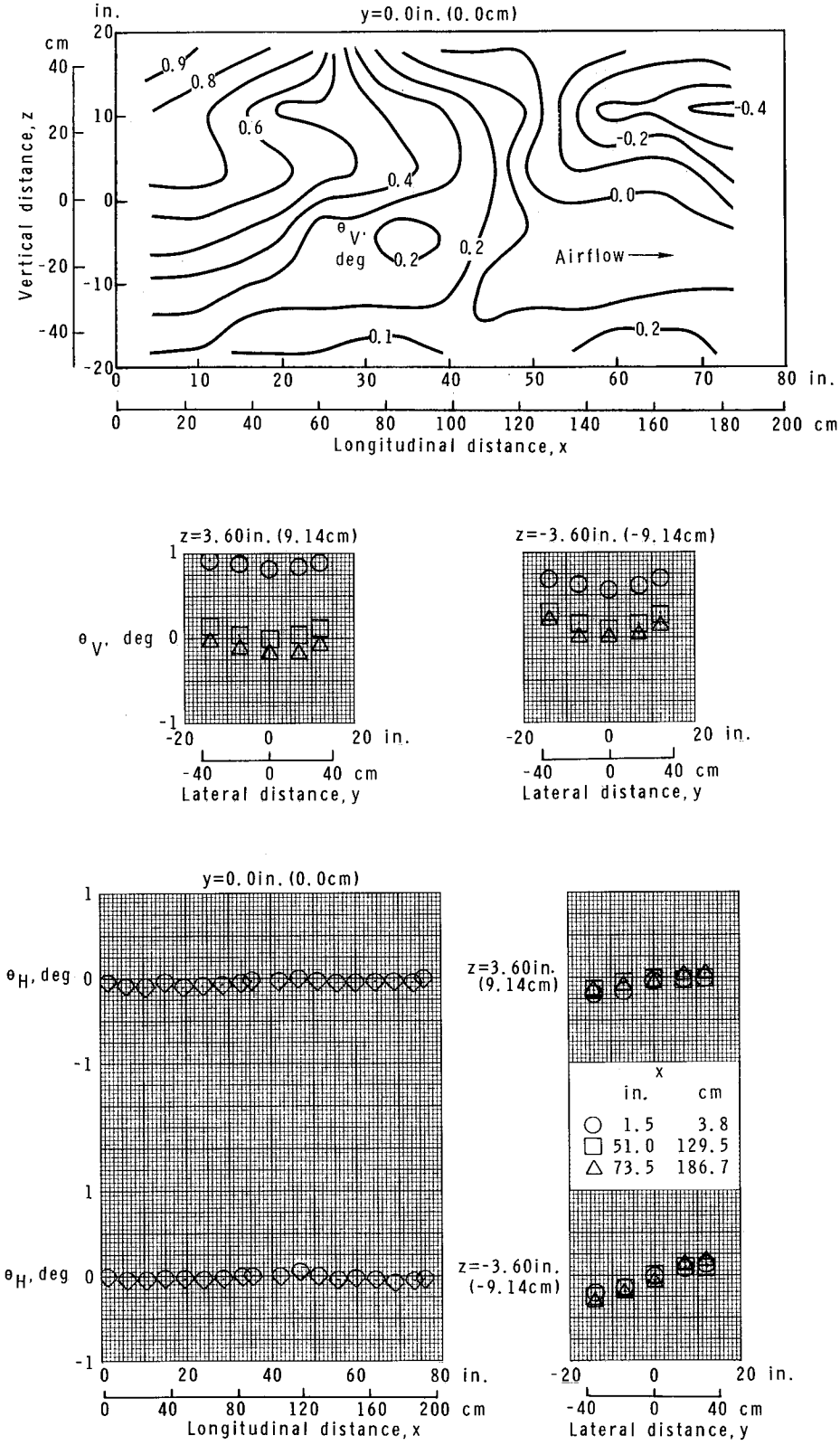

(e) M = 3.703; R = 2.25×10^6 per ft (7.38×10^6 per m).

Figure 24.- Continued.

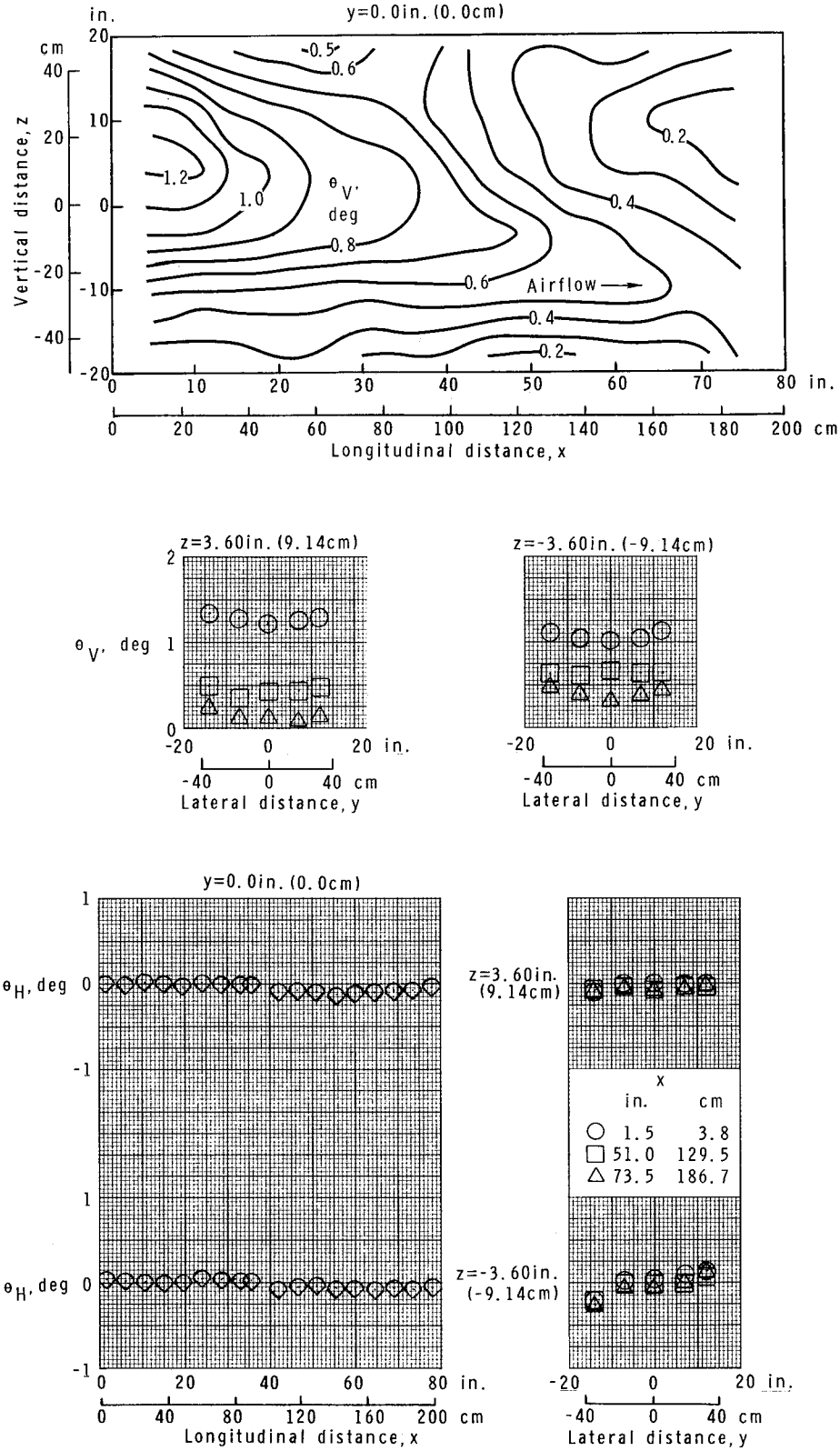

(f) M = 4.185; R = 2.61×10^6 per ft (8.56×10^6 per m).

Figure 24.- Continued.

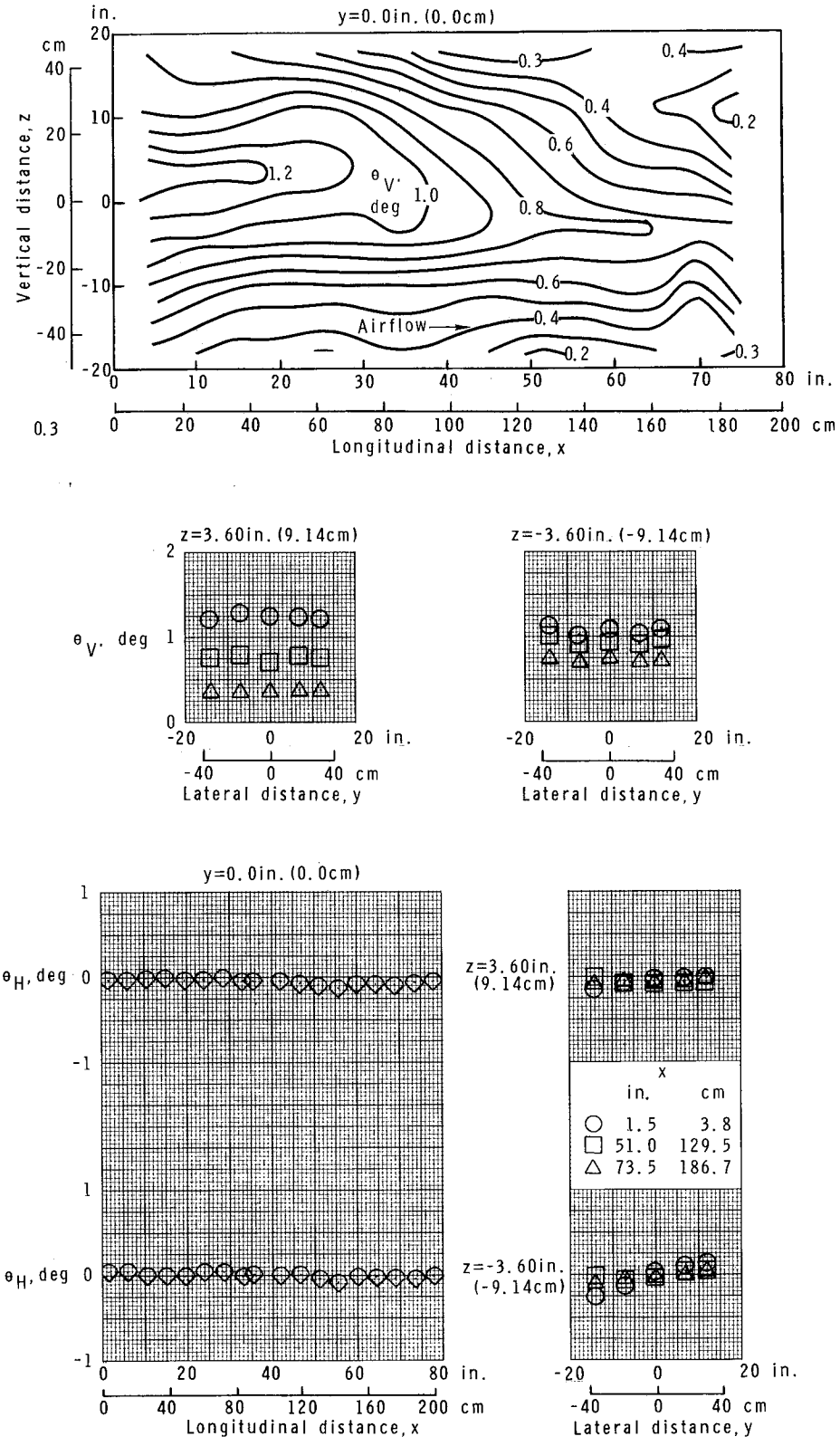

(g) M = 4.423; R = 2.86×10^6 per ft (9.38×10^6 per m).

Figure 24.- Continued.

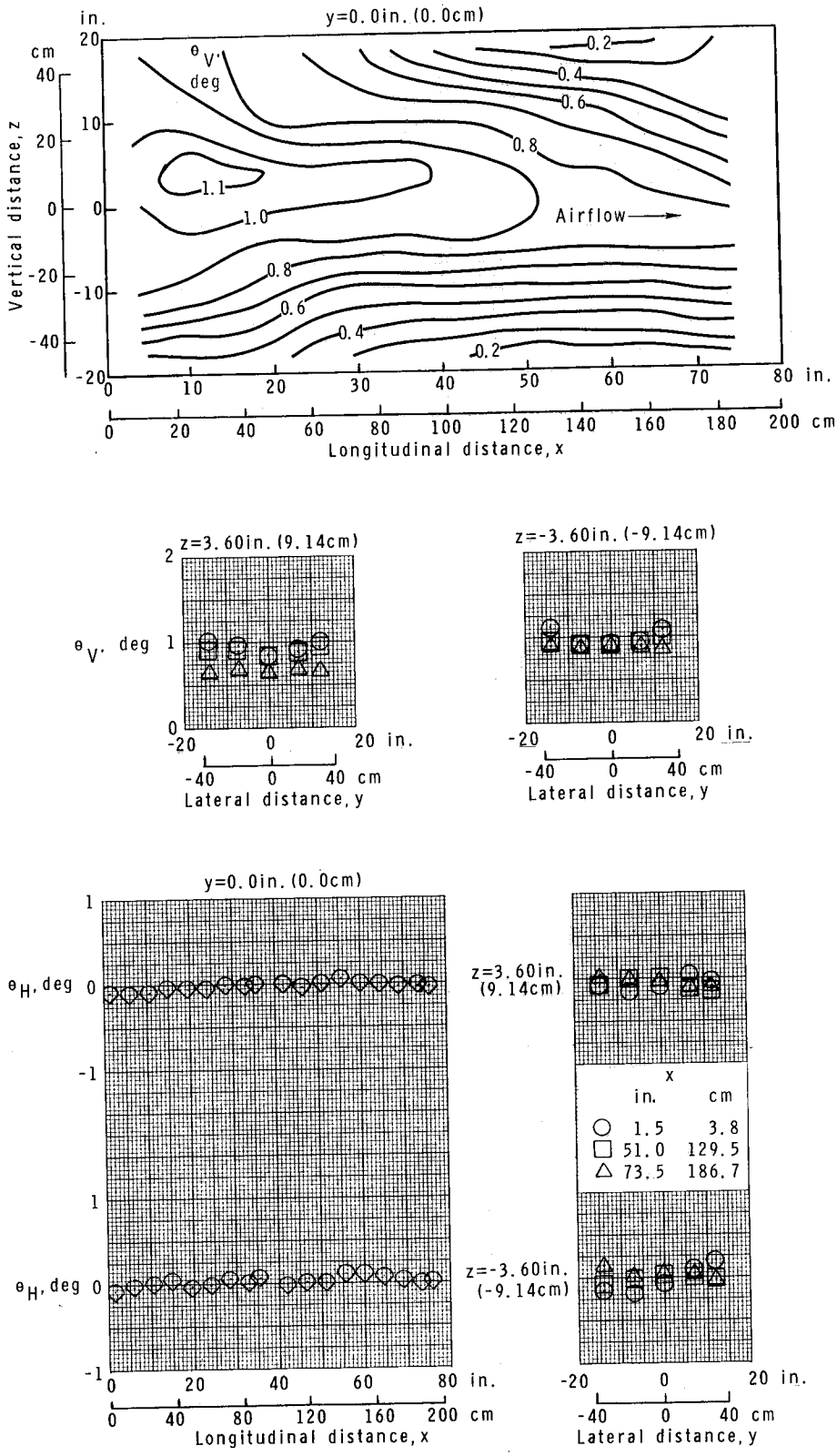

(h) M = 4.640; R = 2.99 × 10^6 per ft (9.81 × 10^6 per m).

Figure 24.- Concluded.

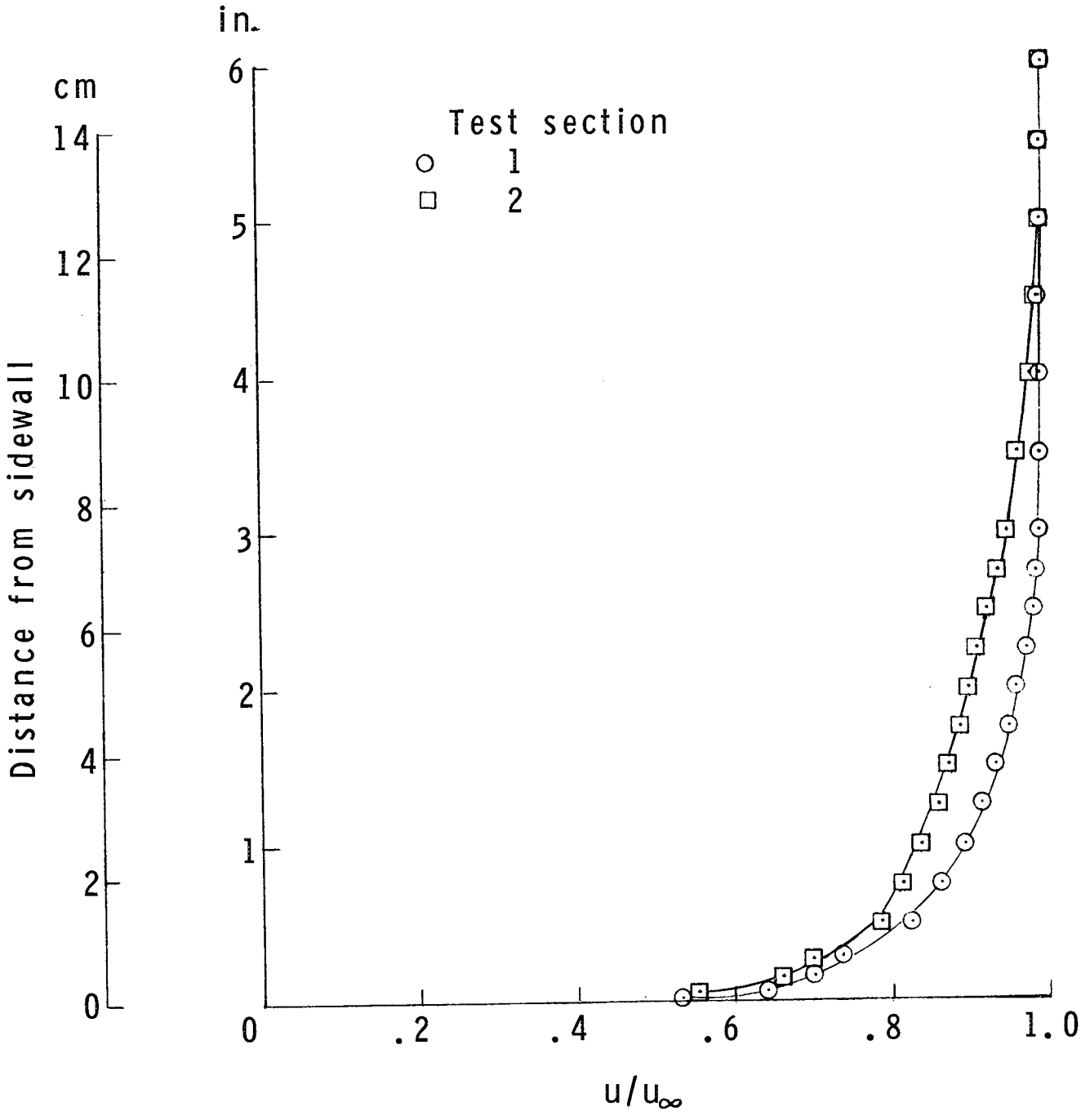

Figure 25.- Typical boundary-layer velocity profiles measured on sidewalls of tunnel test section. M = 2.86; R = 3×10^6 per ft (9.84 per m).

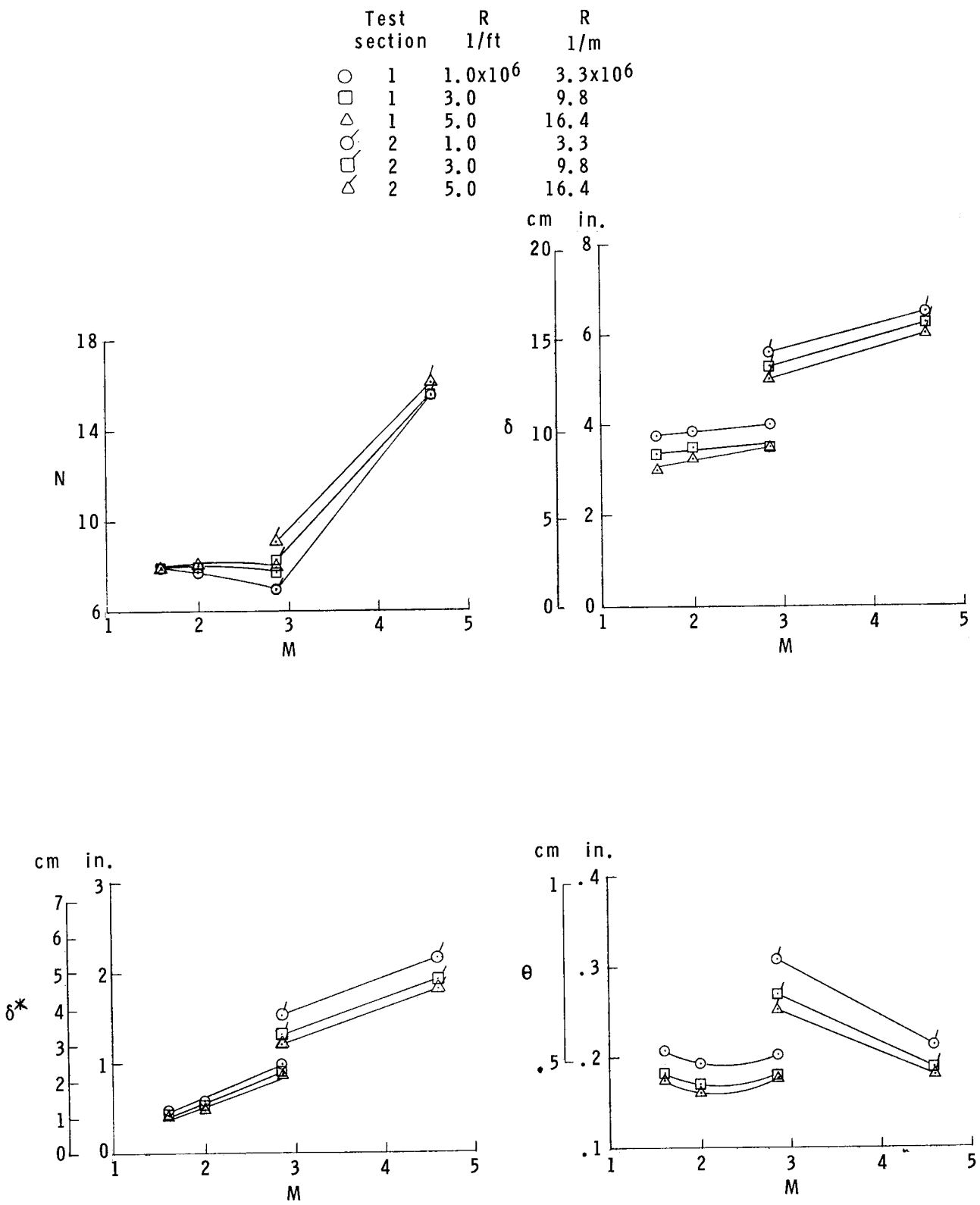

Figure 26.- Summary of boundary-layer profile characteristics on test-section sidewall.

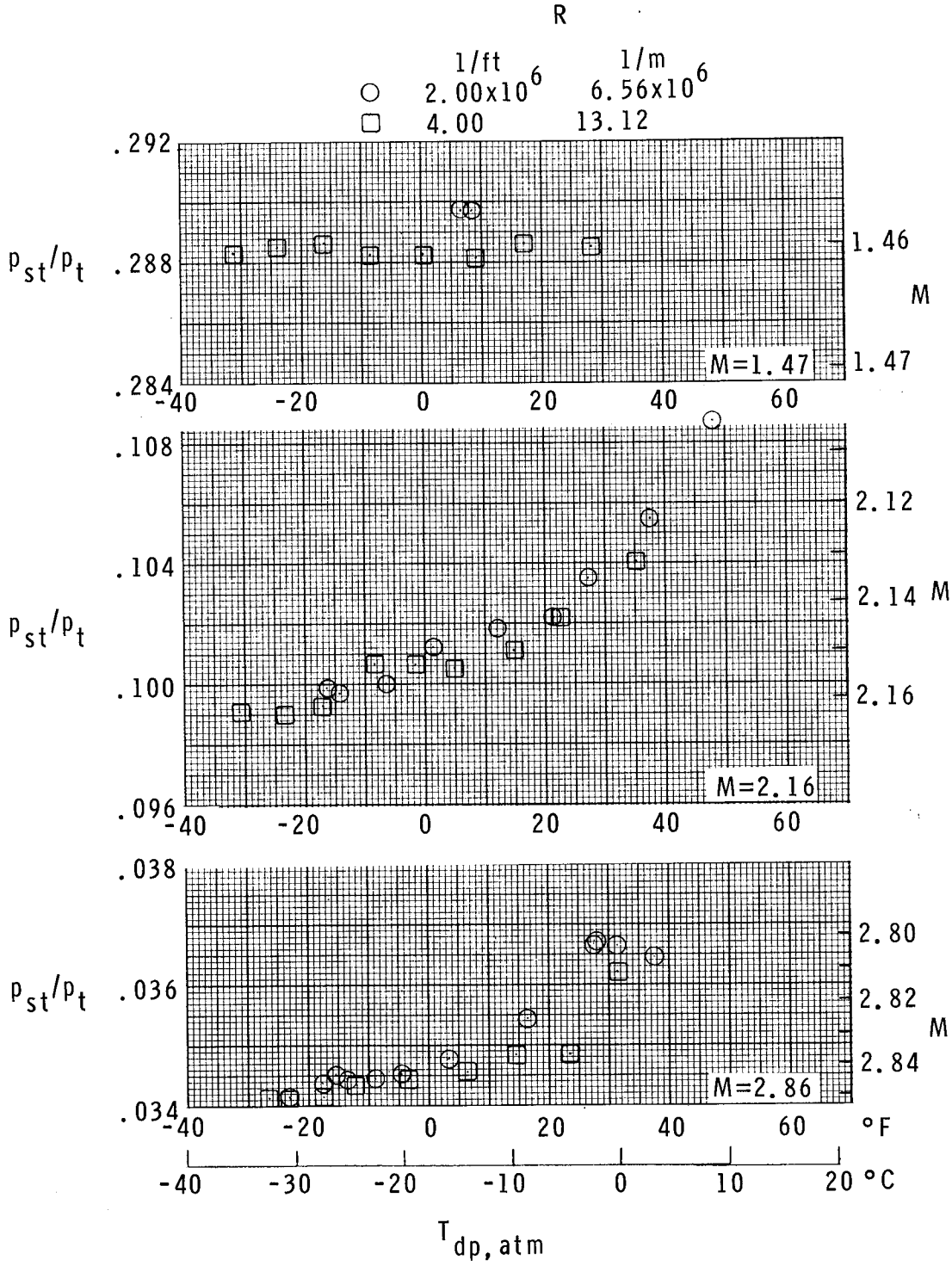

(a) Test section 1.

Figure 27.- Effect of dew point on probe static pressure.

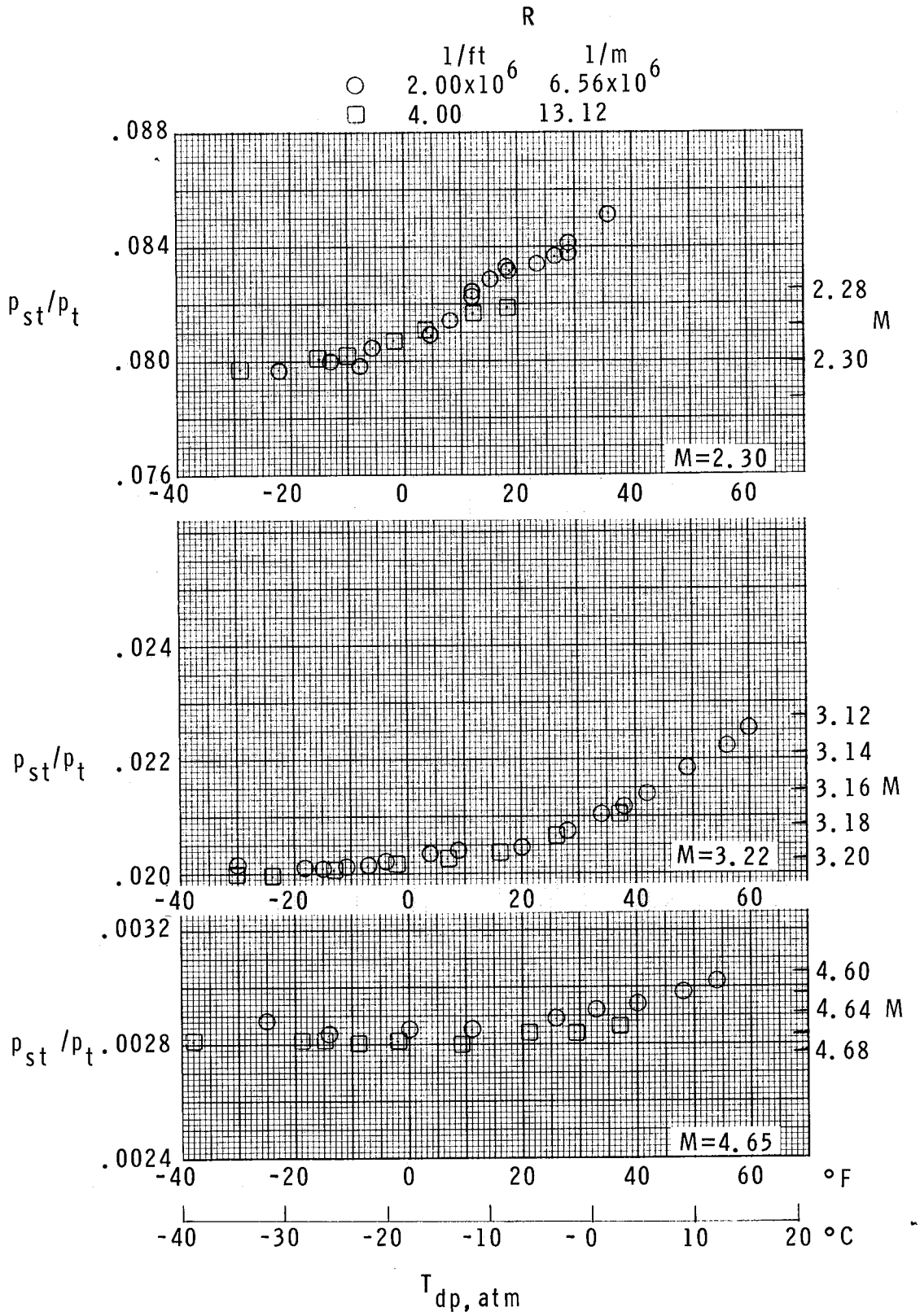

(b) Test section 2.

Figure 27.- Concluded.

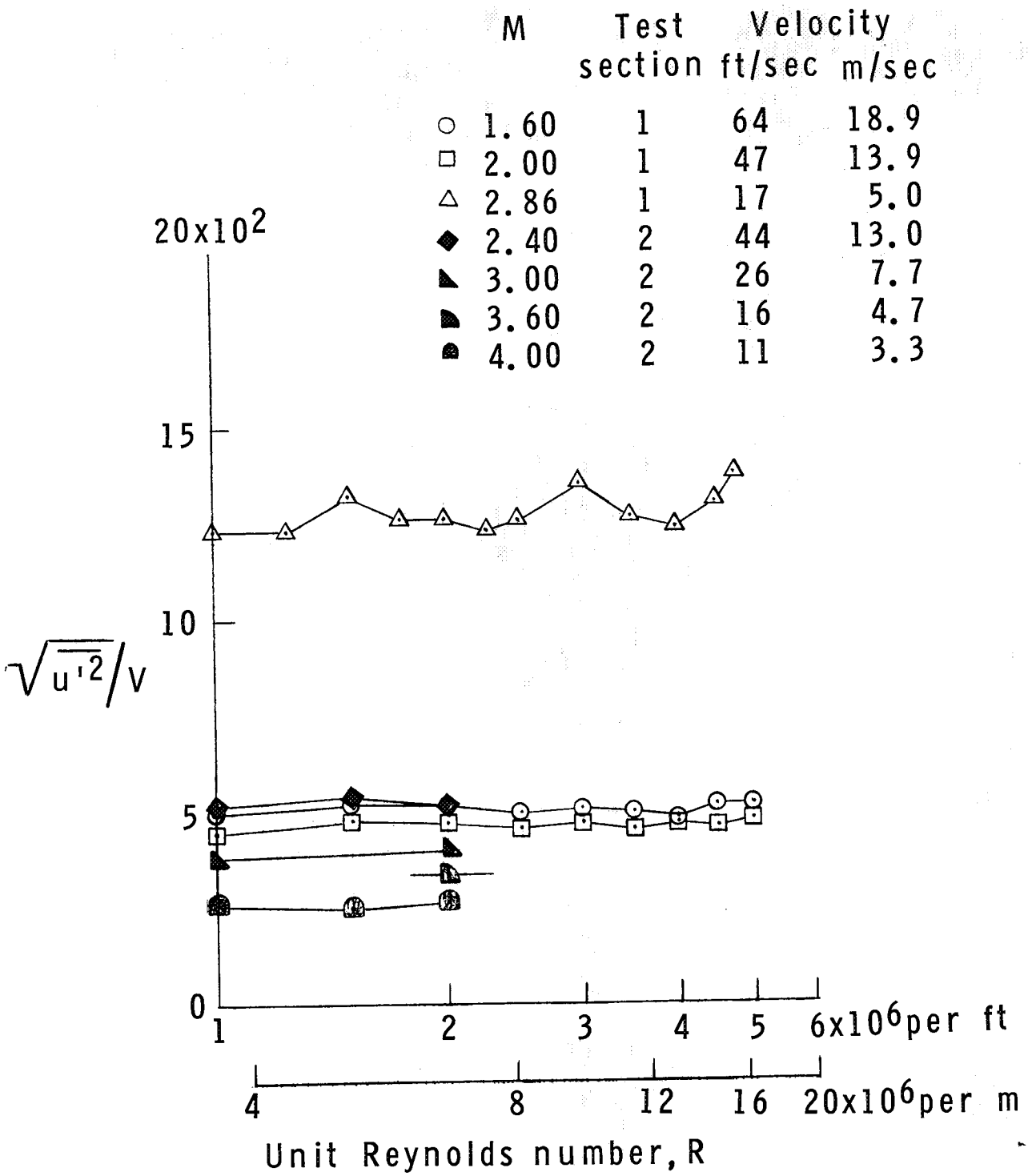

Figure 28.- Measurements of settling-chamber velocities and fluctuation velocities.

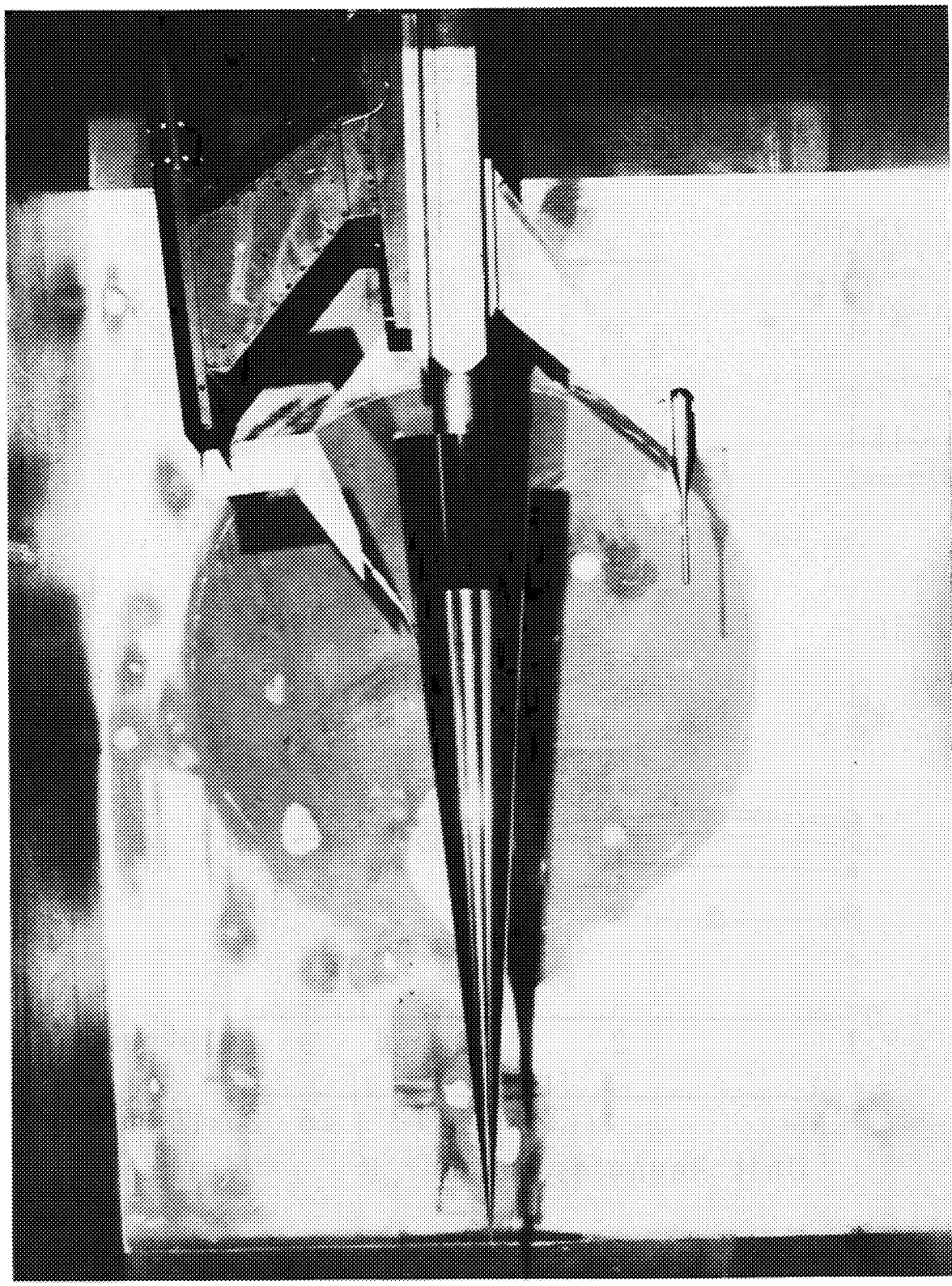

L-79-7924

Figure 29.- Photograph of 10^{o} transition cone from reference 9.

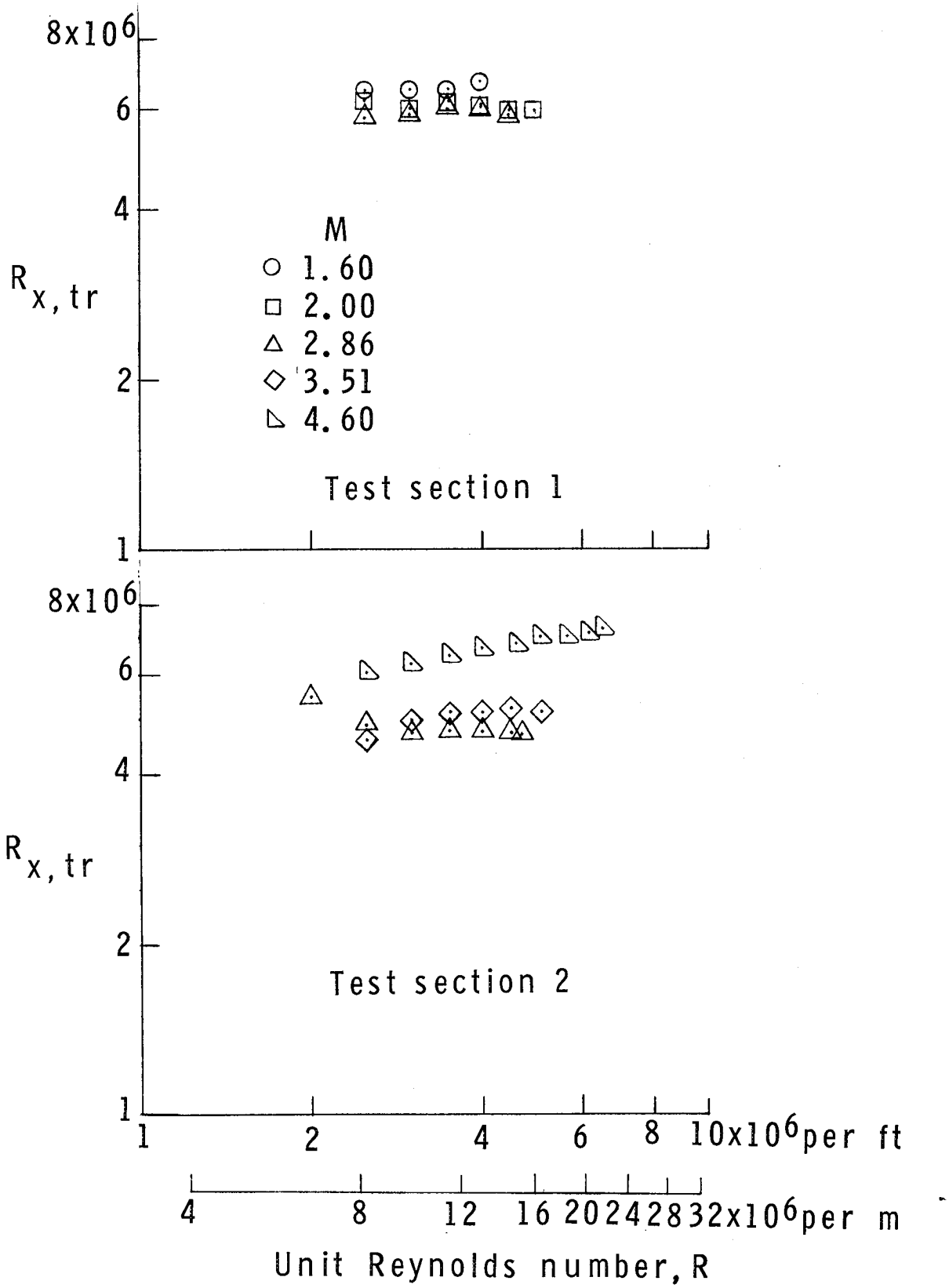

Figure 30.- Effect of unit Reynolds number on transition Reynolds number measured on an AEDC 10° cone.

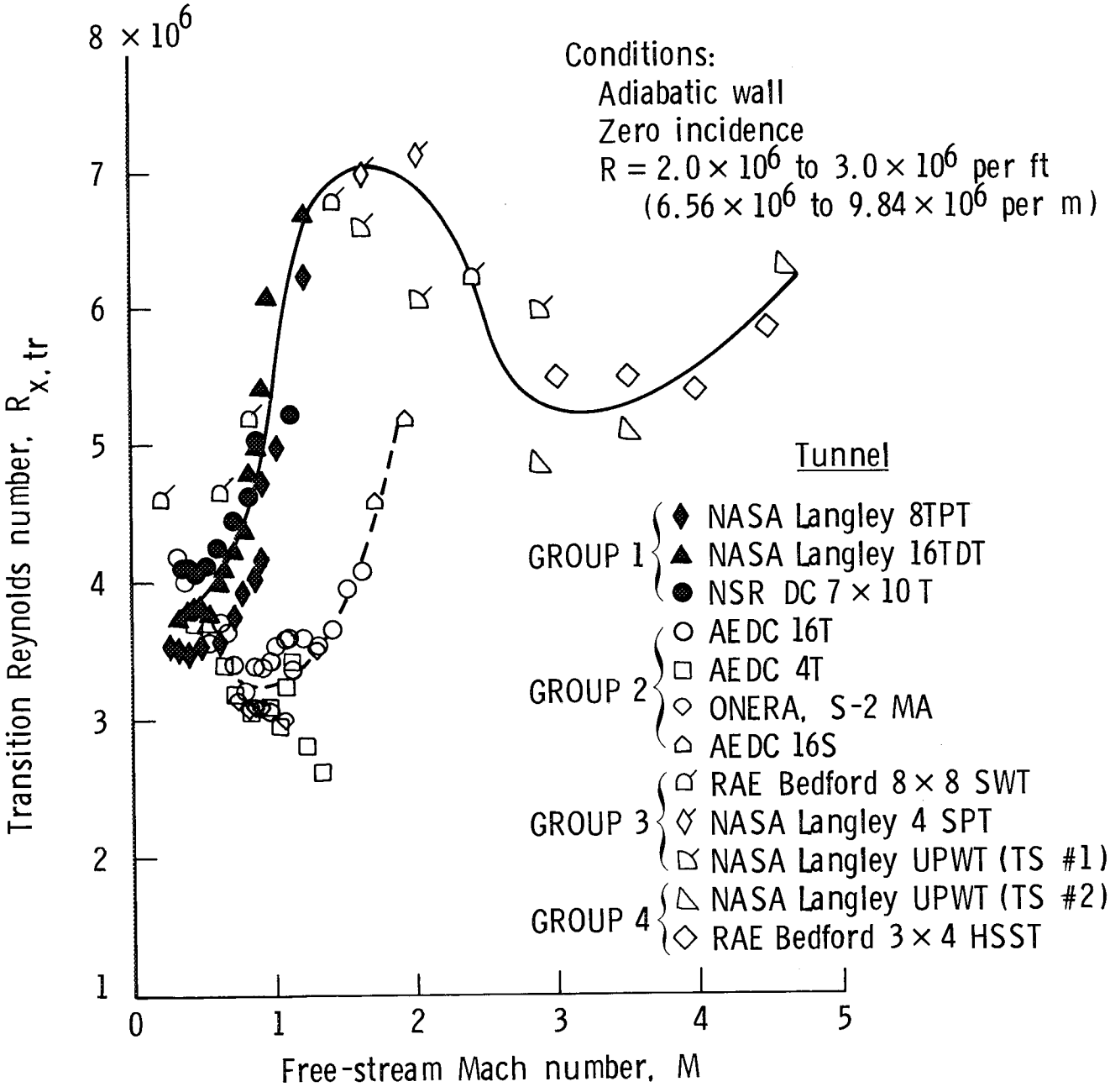

Figure 31.- General trends of the variation of cone transition Reynolds number with Mach number. Data are from reference 9. Wind-tunnel designations not previously defined: NSR DC (Naval Ship Research and Development Center); ONERA, S-2 MA (supersonic tunnel no. 2 at National Bureau of Aerospace Research at Modane-Avrieux, France); RAE Bedford (Royal Aircraft Establishment at Bedford, England).

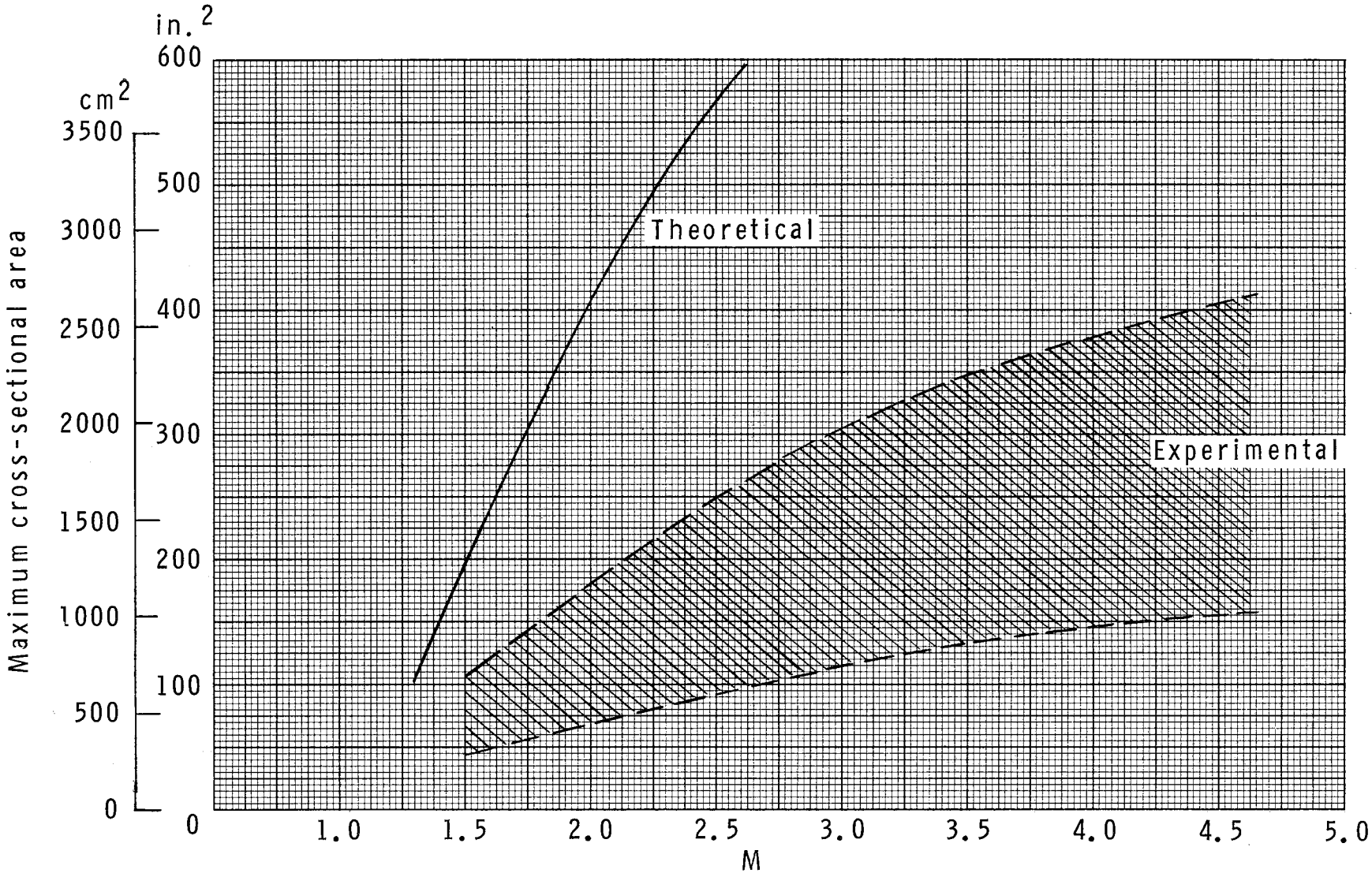

Figure 32.- Maximum model cross-sectional area for starting and maintaining supersonic flow in the Langley Unitary Plan Wind Tunnel.

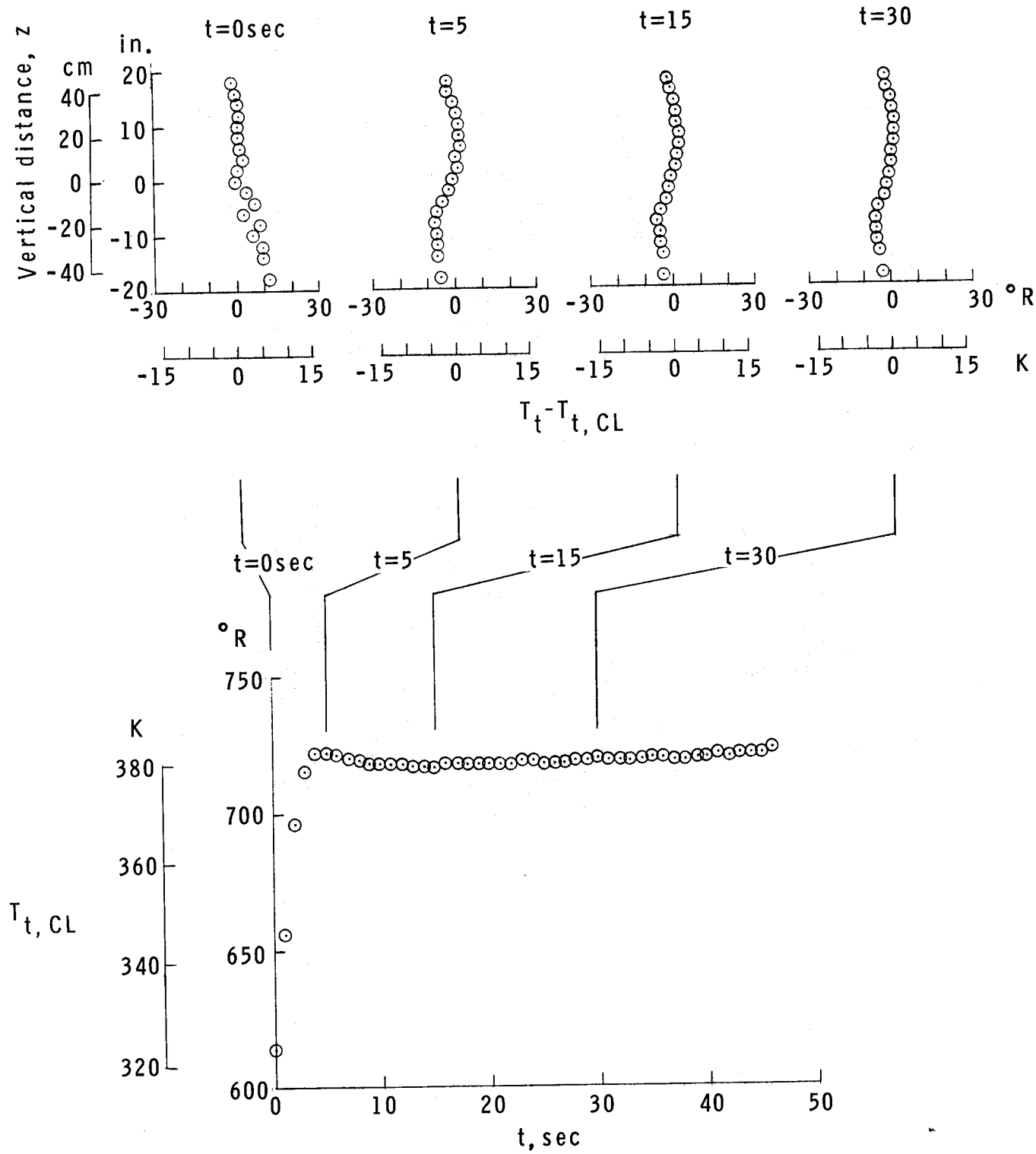

(a) M = 2.49.

Figure 33.- Total-temperature variation across test section 2. R = 3 × 10^6 per ft (9.84 × 10^6 per m).

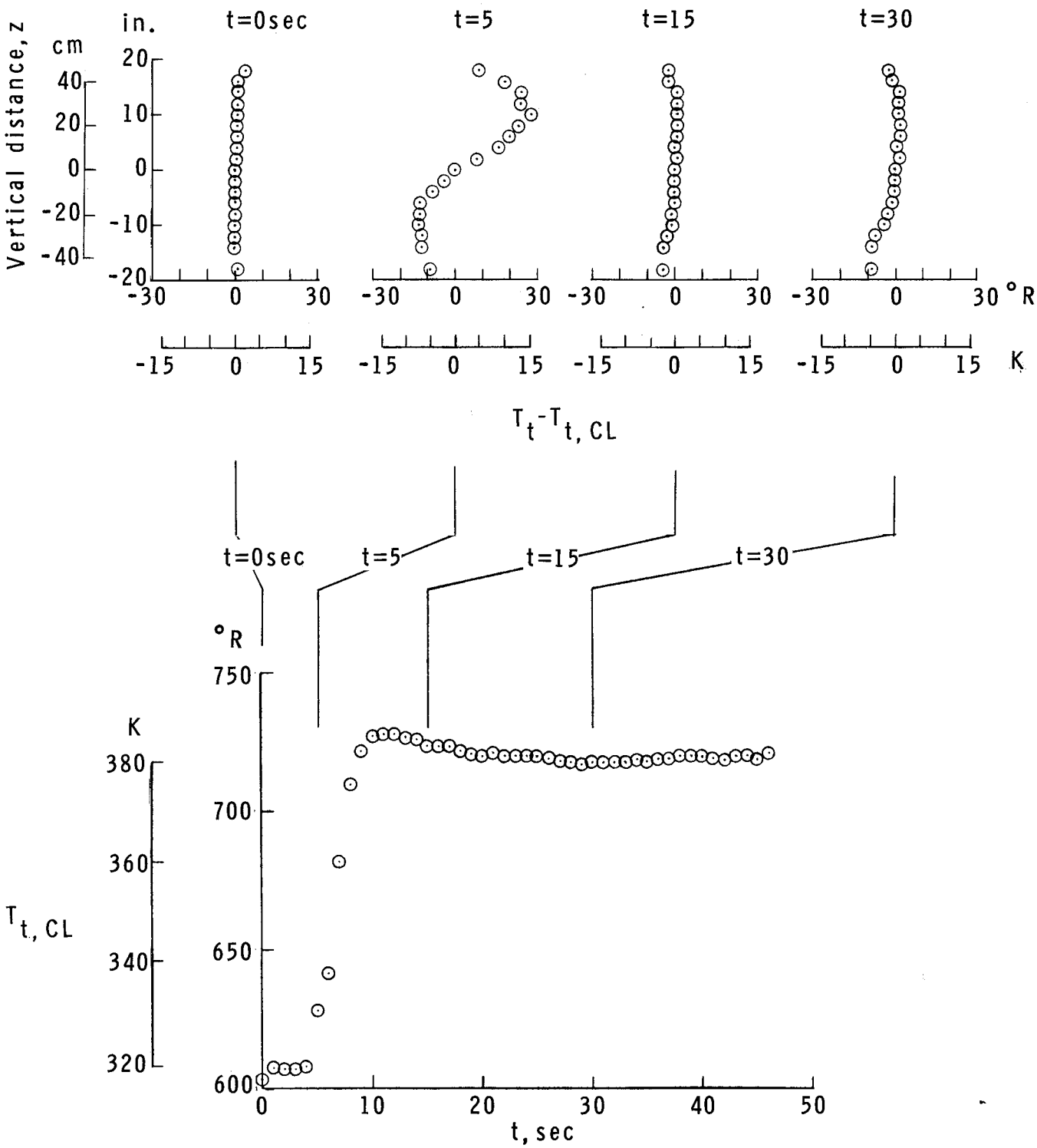

(b) M = 3.51.

Figure 33.- Continued.

C-2

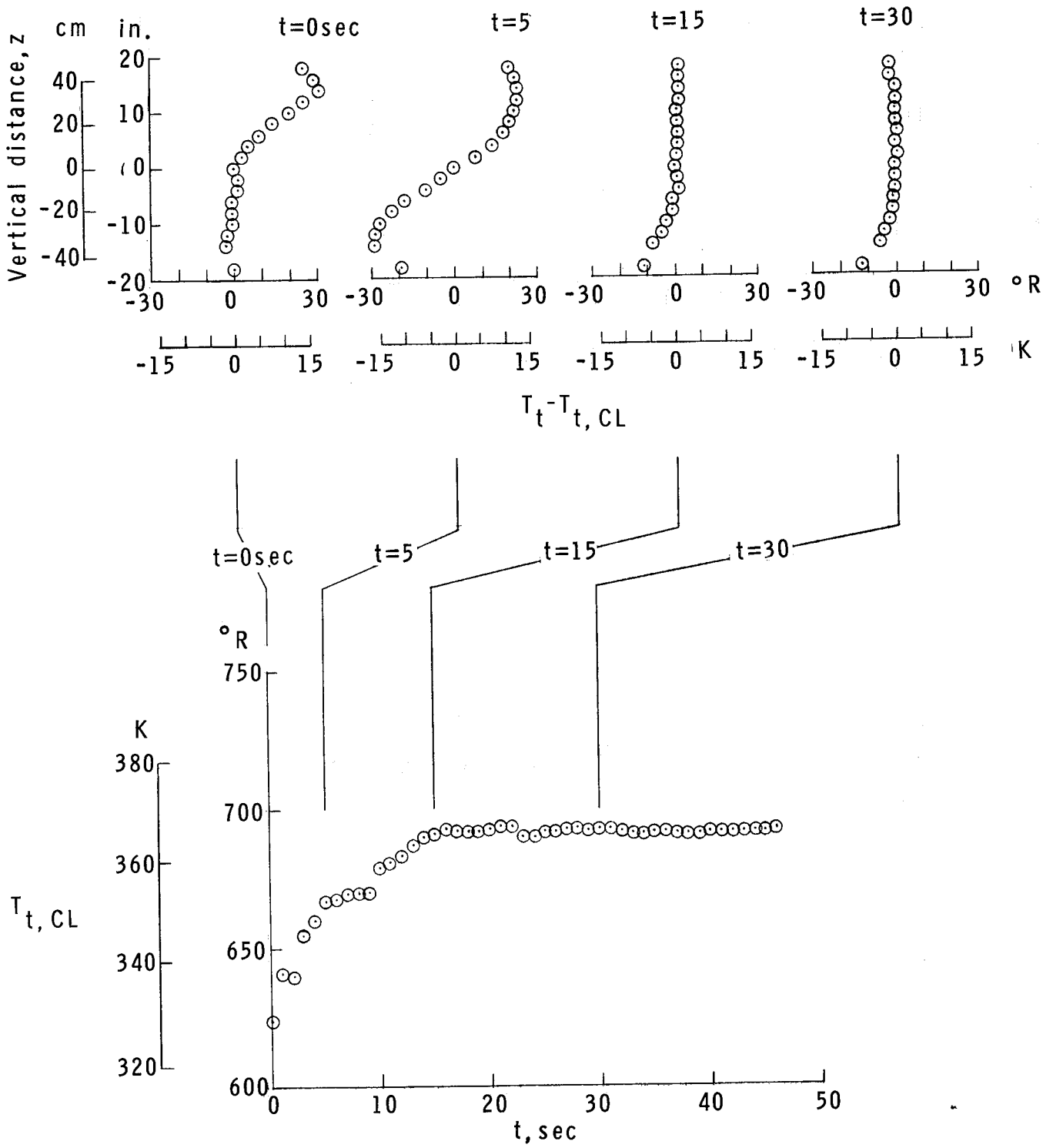

(c) M = 4.44.

Figure 33.- Concluded.

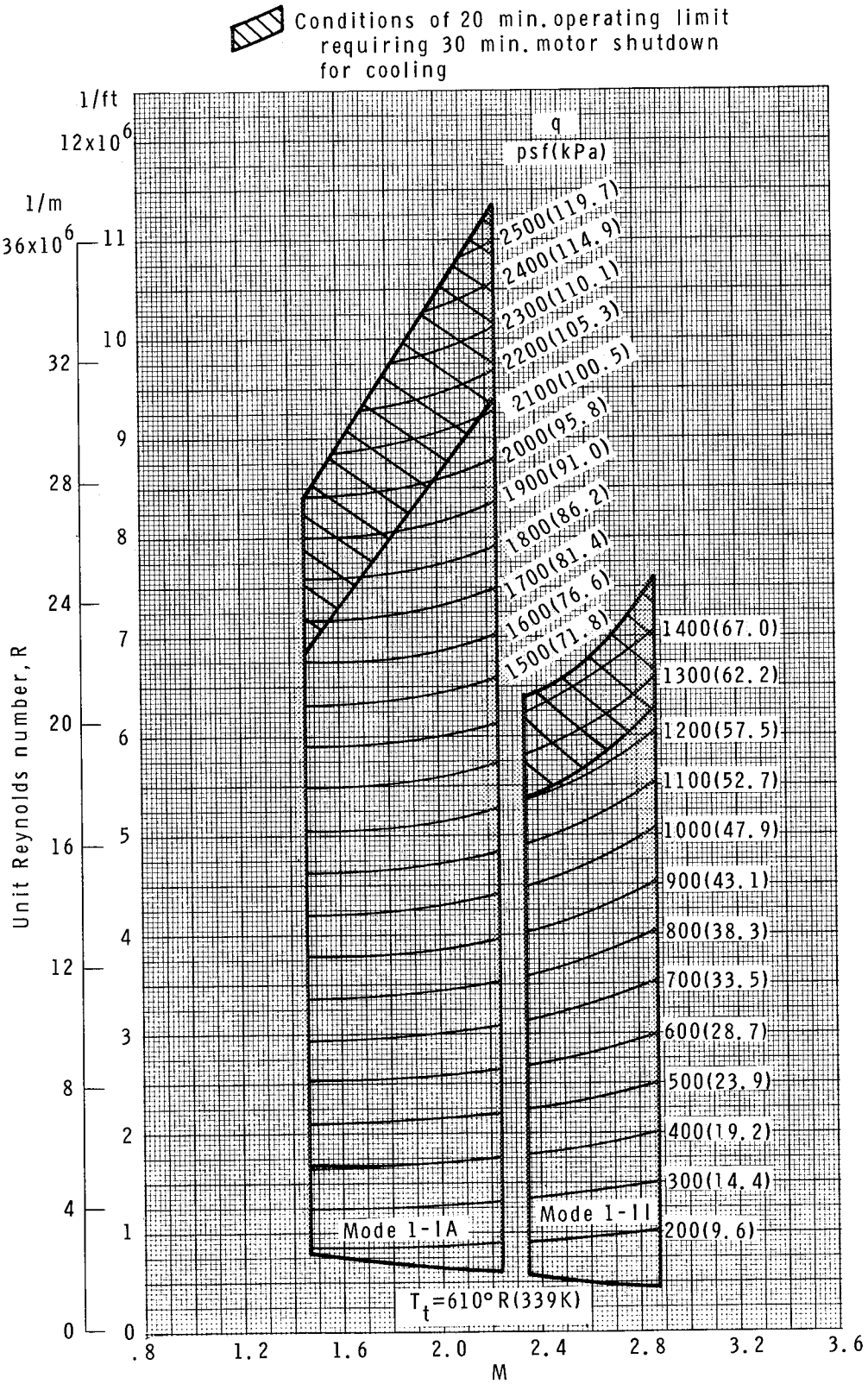

(a) Test section 1.

Figure 34.- Operating characteristics of the Langley Unitary Plan Wind Tunnel.

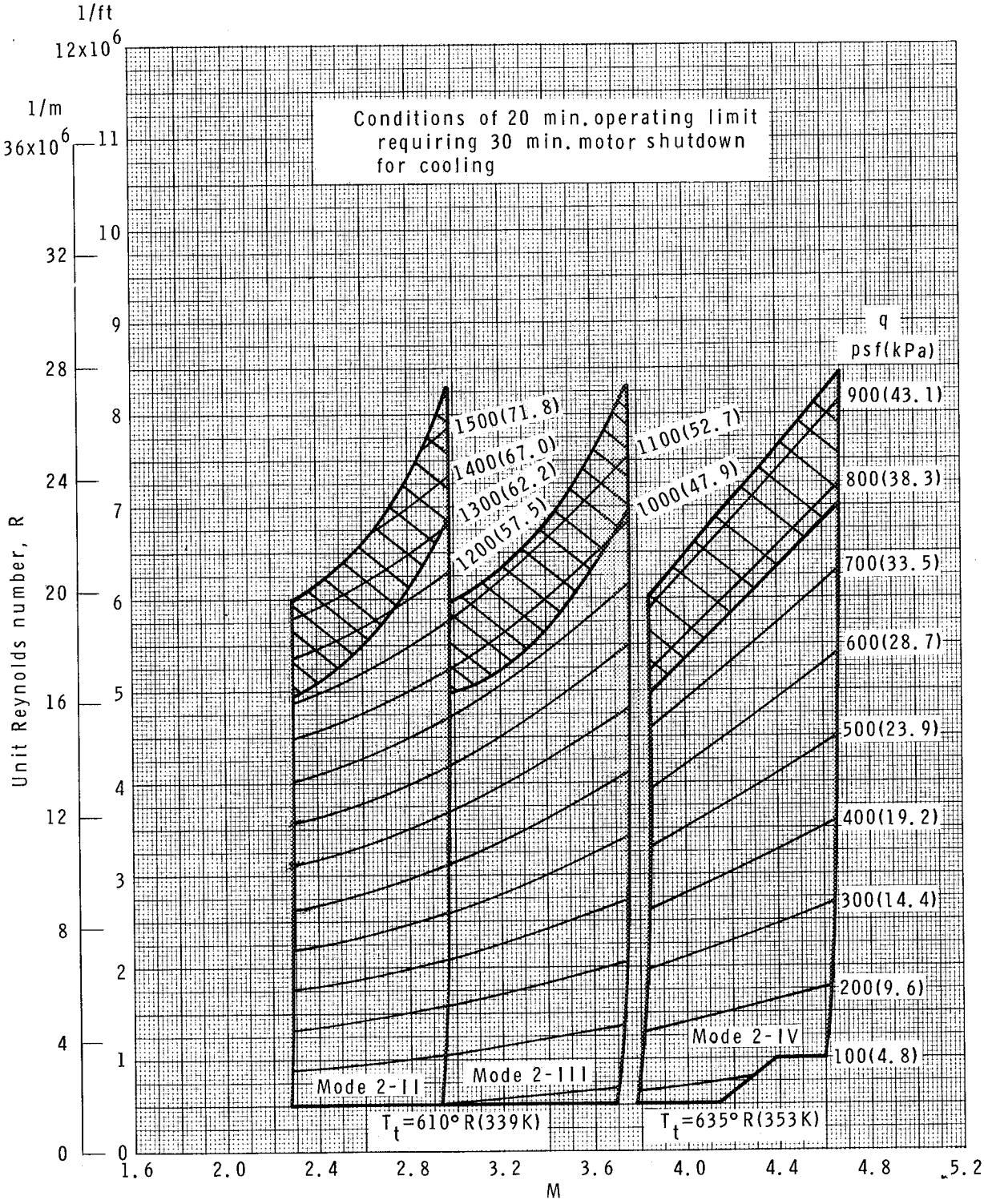

(b) Test section 2.

Figure 34.- Concluded.

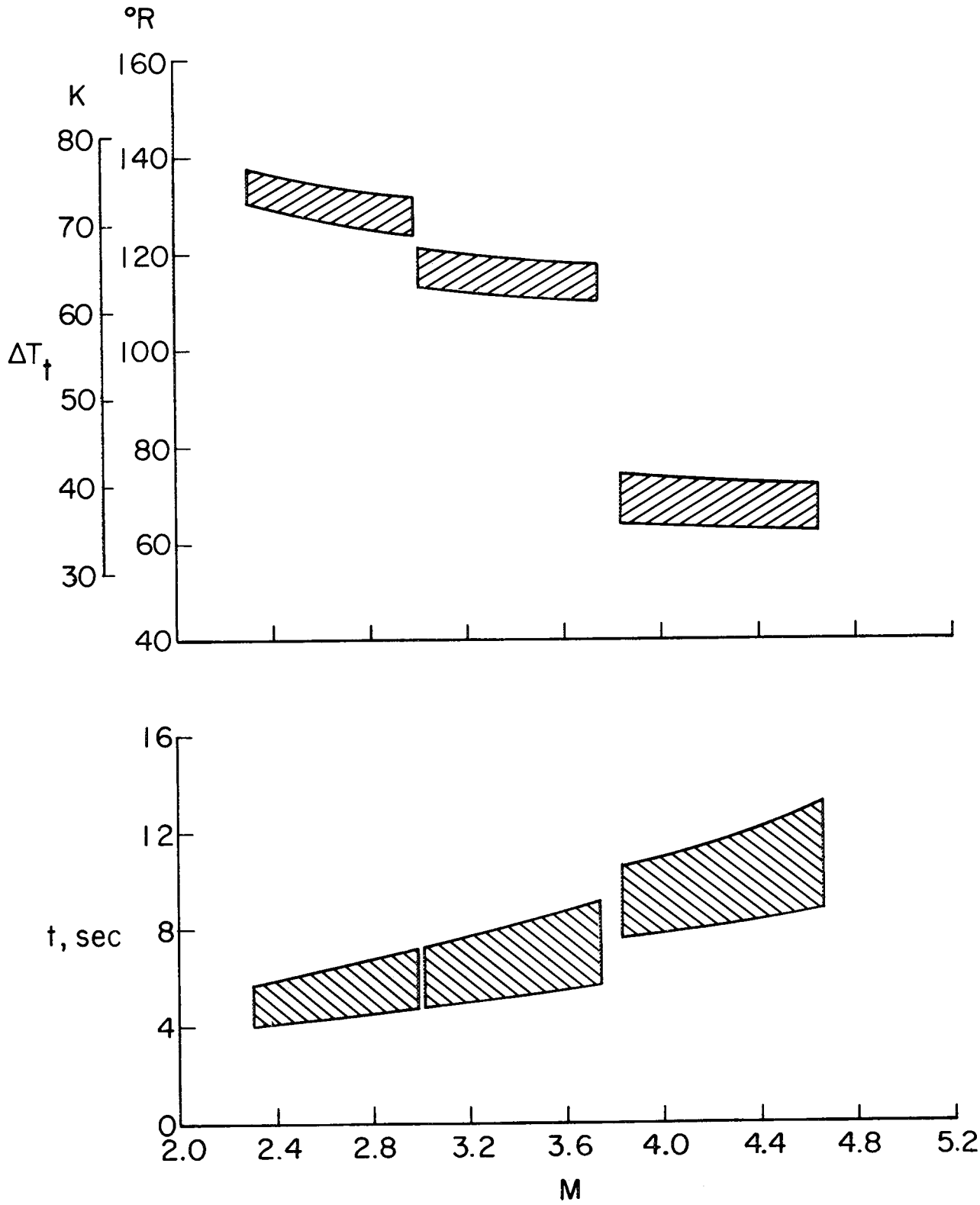

Figure 35.- Heat-pulse characteristics and time to stabilize for heat-transfer tests in test section 2 of the Langley Unitary Plan Wind Tunnel.

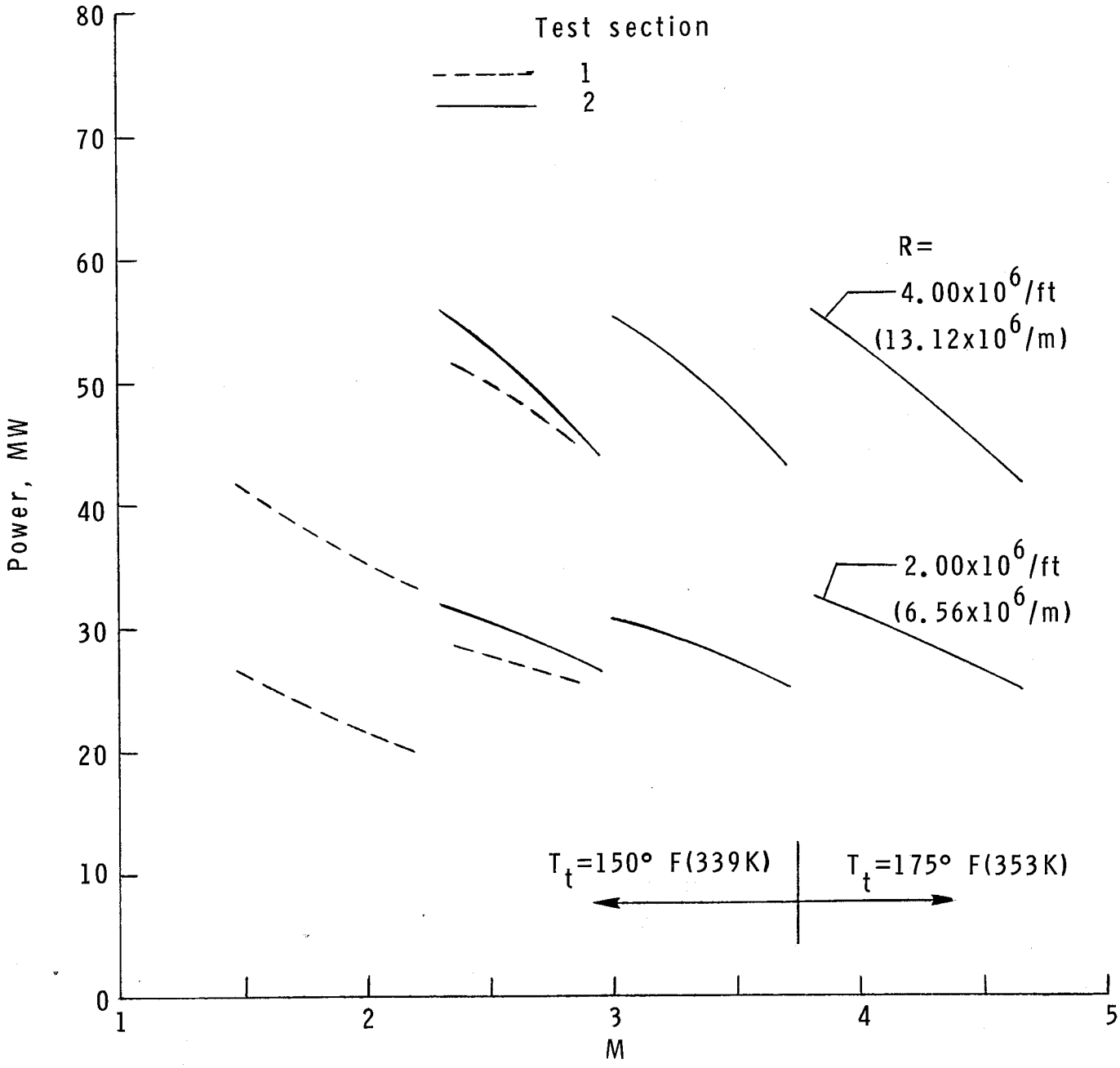

Figure 36.- Total operating power requirements for the Langley Unitary Plan Wind Tunnel.

1. Report No.	2. Government Accession No.	3. Recipient's Catalog No.
NASA TP-1905		

4. Title and Subtitle	5. Report Date
DESCRIPTION AND CALIBRATION OF THE LANGLEY UNITARY PLAN WIND TUNNEL	November 1981
	6. Performing Organization Code 505-42-23-02
7. Author(s) Charlie M. Jackson, Jr., William A. Corlett, and William J. Monta	8. Performing Organization Report No. L-14024
	10. Work Unit No.
9. Performing Organization Name and Address NASA Langley Research Center Hampton, VA 23665	11. Contract or Grant No.
	13. Type of Report and Period Covered Technical Paper
12. Sponsoring Agency Name and Address National Aeronautics and Space Administration Washington, DC 20546	14. Sponsoring Agency Code

15. Supplementary Notes

16. Abstract

The two test sections of the Langley Unitary Plan Wind Tunnel have been calibrated over the operating Mach number range from 1.47 to 4.63. The results of the calibration are presented along with a description of the facility and its operational capability. The calibrations include Mach number and flow-angularity distributions in both test sections at selected Mach numbers and tunnel stagnation pressures. Calibration data are also presented on turbulence, test-section boundary-layer characteristics, moisture effects, blockage, and stagnation-temperature distributions. The facility is described in detail including dimensions and capacities where appropriate, and examples of special test capabilities are presented. The operating parameters are fully defined and the power-consumption characteristics are discussed.

17. Key Words (Suggested by Author(s))	18. Distribution Statement
Wind-tunnel description Wind-tunnel calibration Supersonic wind tunnel	Unclassified - Unlimited Subject Category 02

19. Security Classif. (of this report)	20. Security Classif. (of this page)	21. No. of Pages	22. Price
Unclassified	Unclassified	103	A06

For sale by the National Technical Information Service, Springfield, Virginia 22161

NASA-Langley, 1981